Development of high-throughput screening assays to identify small molecule inhibitors of *Plasmodium falciparum* Hsp70-1

A dissertation submitted in fulfillment of the requirements for the degree of

Master of Science in Biochemistry and Microbiology

School of Mathematical and Natural Sciences

Department of Biochemistry and Microbiology

University of Venda

By

Hloniphani Rachel Ncube

21005834

Supervisor: Prof. A. Shonhai

February 2024

ABSTRACT

Plasmodium falciparum causes the most lethal form of malaria infection. Identification and development of novel antimalarial drugs is limited by the shortage of simple, cost-effective screening assays. Heat shock proteins (Hsps) are a special class of molecular chaperones essential for parasite survival and development within the human host. Hsps are also implicated in drug resistance. Hsp70 forms an integral part of the molecular chaperone system, participating in essential processes such as protein refolding, preventing aggregation and aiding degradation of misfolded proteins. The molecular chaperone PfHsp70-1 is essential for cell survival during stress and it is expressed throughout all the blood stages of the parasite. Thus, Hsp70(s) are essential for functionality in the cell and their function has been demonstrated using the complementation assay. The *E. coli dnaK*756 mutant strain can grow between 30- 37 ℃ but its viability diminishes at temperatures >40 ℃. In addition, the strain produces non-functional Hsp70. As such, this strain is suitable for studying Hsp70 function using the complementation assay. A high-throughput complementation assay was optimized and developed to screen potential inhibitors of Hsp70. Cells heterogously expressing DnaK were the positive control, while those expressing KPf-V436F were the negative control and the cells heterologously expressing KPf were the test cells. KPf contains a substrate binding domain (SBD) from PfHsp70-1. Protein expression was confirmed by sodium dodecyl sulfate-polyacyrlyamide and Western blot analysis. Cells grown with DMSO managed to grow normally under stress, showing that DnaK and KPf conferred cytoprotection to *E. coli dnaK*756 cells. Those heterologously expressing the negative control could not withstand the thermal stress. However, treatment with inhibitors colistin sulfate and pifithrin μ hindered the growth of cells heterologously expressing DnaK and KPf under non-permissive temperatures by 50-fold. Interestingly, the inhibitors seemed not to have any effect on the cells heterologously expressing the mutant protein KPf-V436F. The cells grown with DMSO seemed to die at the same rate as those treated with inhibitors. The colistin sulfate IC_{50} values were 0.22 μM for DnaK and 0.07 μM for KPf, whilst pifithrin μ IC_{50} values were found to be 14.48 μM and 10.41 μM for DnaK and KPf respectively. Statical analysis using Two-way ANOVA utilizing multiple comparison analysis proved the validity of this assay. Solubility studies were conducted to check the solubility status of *E. coli dnaK*756 proteome in the presence of the inhibitors. Findings from this study show that the inhibition interrupted the interaction of DnaK/KPf with some of its client proteins consequently leading to aggregation. This was a confirmation of the compromised function of DnaK/KPf due to the presence of the inhibitor. Tryptophan fluorescence studies were done to validate the findings of the complementation assay, the results show that pifithrin μ and colistin sulfate perturb the tertiary conformation of DnaK, KPf and PfHsp70-1. Since a protein's tertiary conformation is crucial for its function, perturbations in its conformation might have altered the protein functional activity. These findings further validated the complementation assay results which show cell growth defects in the presence of inhibitors. Hence, the current study demonstrated the potential of using the complementation assay as a screening assay to identify potential inhibitors of *P. falciparum* Hsp70-1.

Keywords: *Plasmodium falciparum*, PfHsp70-1, KPf, DnaK, high-throughput, inhibitor, heat shock proteins, ADP, ATP

DECLARATION

I, Hloniphani Rachel Ncube hereby declare that this thesis of Master of Science in Biochemistry and Microbiology at the University of Venda, hereby submitted, is my original work and has not been submitted for any degree at any other University or Institution. This thesis does not contain any other person's writings unless specifically acknowledged or referenced accordingly.

Signature NCUBE HR HRncube **Date:** 15/02/2024

DEDICATION

This thesis is dedicated to my late grandmother Colleta Thabeleni Nkomo-Ndlovu, she would have been proud.

I want to express my appreciation to my sisters Gloria Ncube and Wendy Ncube for their support. Thank you for being my greatest supporters. To Snqobile Ndlovu, thank you for your emotional support and encouragement. I would also like to appreciate Lungile for being my constant source of encouragement and for believing in me, I am truly grateful for your support.

ACKNOWLEDGEMENTS

I would like to thank God for guiding me throughout my MSc journey, it wasn't an easy ride, but His grace sustained me. I also would like to express my sincere gratitude to my amazing supervisor Prof Shonhai for his guidance, patience, and support throughout this journey. This section wouldn't be complete without acknowledging Prof Madala and Dr Graham Chakafana for their encouragement. There were times I felt like giving up but, they held my hand and encouraged me, I will always be grateful to them.

I also would like to acknowledge the National Research Council (NRF South Africa) for funding this project. Lastly, I would like to extend my gratitude to Thendo, Munei, Thabo and all Protein Biochemistry and Malaria Research team members (ProBioM). To the staff members of the Department of Biochemistry and Microbiology, thank you for your support.

Contents

List of figures

List of tables

List of outputs

Ncube, H.R., Dongola, T.H., Dali, U., Shonhai, A. (2024). *E. coli*-based complementation assay to study the chaperone function. Journal of Visualized Experiments (JOVE). Article published.

List of Symbols and Abbreviations

OD_{600}	Absorbance at 600 nm, OD= optical density
Bp	Base pair
kDa	Kilodalton
Hsps	Heat shock proteins
µL	Microlitre
µM	Micromolar
Nm	Nanometers
°C	Degrees Celsius
mL	Millilitre
L	Litres
µg	Microgram
Ng	Nanogram
G	Gram
A	Alpha
B	Beta
DMSO	Dimethyl sulphoxide
ER	Endoplasmic reticulum
HPD	Histidine-proline-aspartic acid
IPTG	Isopropyl-β-D-1-thiogalactopyranoside
NEF	Nucleotide exchange factor
PMSF	Phenylmethylsulphonyl fluoride
SBD	Substrate binding domain
SDS-PAGE	Sodium dodecyl sulphate polyacrylamide gel electrophoresis
NN	No nucleotide
ADP	Adenosine diphosphate
ATP	Adenosine triphosphate
ANOVA	Analysis of variance
CS	Colistin sulfate
JDPs	J domain proteins
PMB	Polymyxin B
PES	Pifithrin µ
NBD	Nucleotide binding domain
RESA	Ring infected surface antigen
NEF	Nucleotide exchange factor

Chapter 1

1.1 Malaria as a global health concern

Malaria is an infectious disease caused by protozoan members of the genus *Plasmodium.* The five identified species responsible for inflicting malaria in humans are *P. falciparum*, *P. ovale, P. vivax, P. malariae,* and *P. knowlesi*. Of these, *P. falciparum* infection is the most lethal. Children under the age of five and pregnant women are the most vulnerable (McGready *et al*., 2012; WHO, 2023). According to the World Health Organization (WHO) report, in 2022 an estimated 249 million cases and 608 000 deaths were recorded (WHO, 2023). The Sub-Saharan region has the most concerning trend, accounting for 94 % of these cases, clearly indicating that it bears the brunt of the disease (WHO, 2023). Despite efforts made in the previous years to combat malaria, the recent report indicates that there was a distressing 10 % increase in malaria related deaths in 2021 (WHO, 2022). This upsurge in mortality is attributed to disruptions in essential malaria services in the course of the COVID-19 pandemic (Velavan *et al*., 2021; WHO, 2023). Furthermore, malaria remains a threat to public health even in South Africa. Regions such as Limpopo, Mpumalanga, and Kwazulu Natal are endemic, with 10 % of the population at risk of contracting the disease (NICD, 2023). Moreover, malaria has also become a major impediment to socio-economic development in Sub-Saharan Africa, draining as much as 2 % of the gross domestic product of these countries (WHO, 2023).

1.2 The multifaceted lifecycle of the *P. falciparum* lifecycle

The *P. falciparum* lifecycle is complex, alternating between a cold-blooded mosquito vector (*Anopheles*) and warm-blooded human host. The asexual cycle begins when an infected female *Anopheles* mosquito injects sporozoites into a human host during a blood meal (Figure 1.1; Vaughan *et al*., 2008; Chora *et al*., 2022). These sporozoites migrate to the liver, invading hepatocytes where they multiply to form invasive merozoites (Amino *et al*., 2006; Cowman *et al*., 2016). These merozoites are deposited into the bloodstream, invading erythrocytes (Figure 1.1; Bannister and Sherman, 2009). Within the erythrocyte, the parasite feeds on its haemoglobin, proliferating to form more merozoites (schizont) which exit and invade more erythrocytes. This cycle is repeated several times (Figure 1.1; Bannister and Sherman, 2009). The synchronous release of merozoites from infected erythrocytes coincides with the

occurrence of fever peaks every two days. Furthermore, the blood-stage parasites are responsible for severe malaria associated pathologies (Haldar *et al*., 2007; Milner *et al*., 2015).

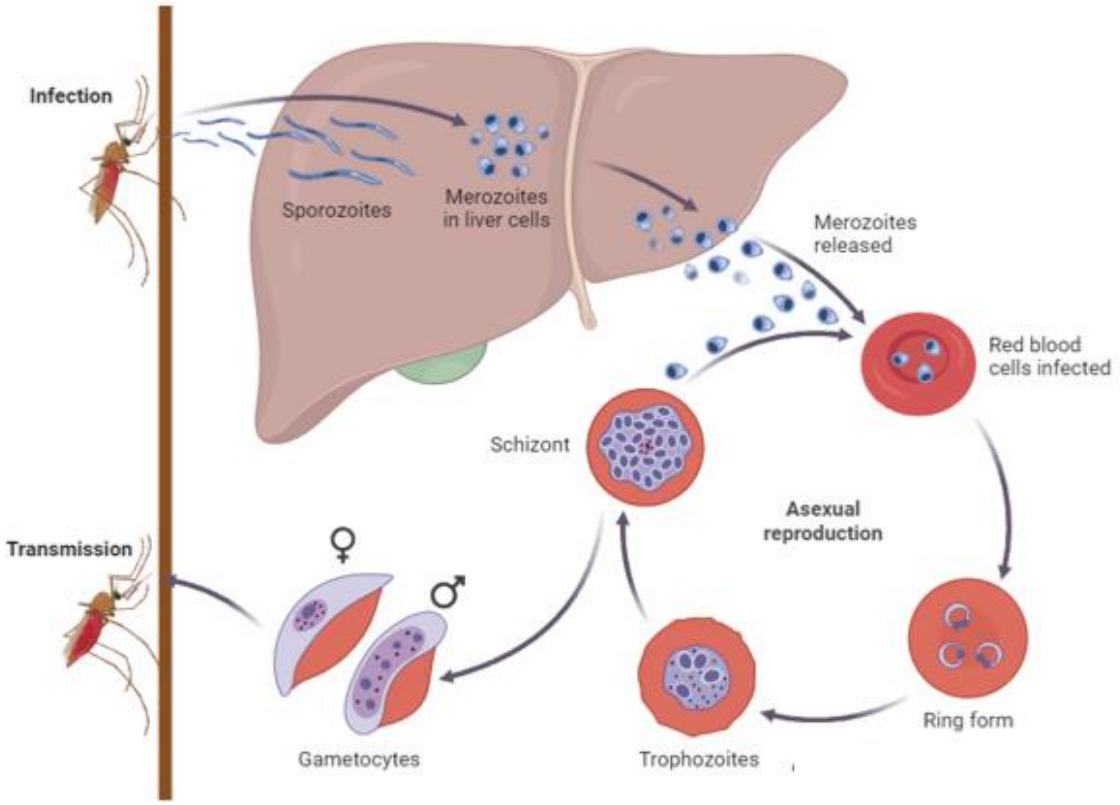

Figure 1.1. The multifaceted life cycle of *P. falciparum*. The asexual (blood) stage occurs in the erythrocytes of the host whilst the sexual stage occurs in the mosquito vector. Adapted from Seraphim *et al*., 2019.

Invaded erythrocytes rupture leading to the loss of more erythrocytes subsequently leading to anaemia and other complications. In addition, the infected erythrocytes accumulate in vital organs, leading to blockage of blood vessels causing organ dysfunction (Haldar *et al*., 2007; Milner *et al*., 2015). As an alternative to the asexual stage, the parasite also undergoes development into the sexual stage. During which some merozoites differentiate into female and male gametocytes (Cowman *et al*., 2016; CDC, 2023). In order to continue the *P. falciparum* lifecycle, the mosquito takes up gametocytes into its gut during a blood meal (Billker *et al*., 1998). The gametocytes escape from their surrounding erythrocyte membrane, in a process triggered by temperature and chemicals in the vector (Billker *et al*., 1998). The male gametocytes undergo division, producing several gametes. These gametes sprout long motile flagella, a process known as exflagellation. This enables male gametes to identify female gametocytes and fertilize them (Figure 1.1). Fertilization leads to the formation of a zygote

which then develops into an oocyst, in which sporozoites are formed. The mature oocysts rupture releasing sporozoites, which are stored in the mosquito's salivary glands, in readiness for the next transmission step (Figure 1.1; Chora *et al*., 2022).

1.3 Need for identification of alternative antimalarial drug targets

Several initiatives have been launched towards the elimination of malaria disease, encompassing control of mosquito vectors, therapeutic interventions, and endeavours to develop towards an effective vaccine (Curtis *et al*., 2006; Greenwood *et al*., 2008). Currently used antimalarial drugs are natural based, synthetic and semi-synthetic based. The antimalarial drugs which are safe for use are broadly categorized into three types including quinolone derivatives, antifolates and artemisinin derivatives (Leite *et al*., 2013; Kumar *et al*., 2018).

Quinine (QN) was discovered by Jersuit missionaries who chewed the bark of *Cinchona cordifolia* tree to combat fever associated with malaria. Following its discovery, quinine was used as first treatment for malaria from the 17th to the 19th century (Meshnick and Dobson, 2001). The active ingredients from the tree were found to be quinine and quinidine and this explained its antimalarial activity. Quinine is an alkaloid belonging to aryl amino group of drugs. This drug kills the parasite by accumulating in the digestive vacuole of the parasite and blocking haem detoxification (Fitch, 2004; Antony and Parija, 2016). Reduced efficacy of quinine against *P. falciparum* was reported in 1910 (Achan *et al*., 2011). Quinine resistance was associated with *pfmdr1* gene which encodes multidrug resistance like proteins, such as P-glycoprotein homologue 1 residing in parasite vacuole. Polymorphisms within *pfmdr1* impact sensitivity to quinine (Cowman *et al*., 1994; Sidhu *et al*., 2005). Pharmacokinetic characteristics of the drug as well as therapeutic effects differ according to age, severity of the infection, immunity and pregnancy (White, 1992; Dagen, 2020). Nonetheless, quinine is still used for less severe malarial infections and in combination with therapy with a fast-acting drug which has less side effects (Achan *et al*., 2011).

In the 1940s, chloroquine emerged as standard treatment for malaria. Chloroquine is a derived from quinine as 4-aminoquinoline. This drug had rapid action, enhanced tolerability, simplified dosage and decreased toxicity as compared to quinine (Djimde *et al*., 2003; Teixeira *et al*., 2014). *P. falciparum* unfortunately developed resistance to the drug, and it was first reported in 1979 in East Africa (Wellems and Plowe, 2001). Chloroquine resistance is linked to mutation

of the *pfmdf1* and *pfcrt* mutation (Fidock *et al*., 2000; Ecker *et al*., 2012). These mutations lead to altered drug sensitivity and modify resistance phenotypes (Veiga *et al*., 2016; Dhingra *et al*., 2019). The increase in cases of *P. falciparum* resistance to quinolones necessitated the development of new derivatives with minimal modifications, such as amodiaquine and 4-phenyl-amino-quinoline (Teixeira *et al*., 2014; Kumar *et al*., 2018).

Piperaquine, a bis-4-aminoquinoline was shown to be effective against chloroquine resistant parasites (Kiaco *et al*., 2015). The resistance was attributed to mutation in chloroquine resistance transporter gene (*pfcrt*) (Dhingra *et al*., 2017). A food vacuole membrane protein predicted to be a member of drug/metabolite transport family is encoded by the *pfrcrt* gene (Martin and Kirk, 2004; Tran and Sair, 2004). Since the structure of piperaquine share similarity with chloroquine, it is suggested to inhibit the transporter mediated drug efflux pathway and shield other drugs against chloroquine resistance (Cunico *et al*., 2008).

Quinolones derivatives such as pyronaridine and mefloquine were also developed for malaria treatment and prevention. Pyronaridine was discovered in China in 1979 (Zheng *et al*., 1979) and this compound was found to be more effective than chloroquine. Pyronaridine is thought to modulate haemoglobin metabolism, blocking β-haematin polymerization (Bailly, 2021). Mefloquine was used to combat chloroquine resistance (Cunico *et al*., 2008).

Antifolates, were used to treat malaria and as a replacement of chloroquine especially in African countries (Kublin *et al*., 2003). Antifolates are classified according to their mechanism of action as class I and II. Type I consists of sulfadoxin and type II includes pyrimethamine and proguanil. Sulfadoxin and pyrimethamine are still used for preventive treatment in pregnant women throughout Africa (Kayentao *et al*., 2013). Sulfadoxine functions by inhibiting the dihydropteroate synthetase enzymes. It used to treat severe *P. falciparum* infections in combination with pyrimethamine (Antony and Parija, 2016). The type II antifolates, pyrimethamine and proguanil inhibit dihydrofate reductase activity and also inhibit folate biosynthesis (Antony and Parija, 2016). The efficacy of antifolate drugs was limited by the emergence of drug resistance and its low tolerance in humans (Conrad *et al*., 2019). Resistance to antifolates is driven by mutations in *pfdhps* and *pfdhfr* genes encoding dihydropteroate synthase and dihydrofolate reductase enzymes respectively. These mutations lead to decreased drug sensitivity (Conrad and Rosenthal, 2019).

The third class of antimalarial drugs, artemisinin was isolated from sweet wormwood plant *Artemisia annua* by a Chinese scientist (Tu *et al*., 2015). Artemisinin and its derivatives (dihydroartemisinic, artesunate and artemether) have been used as first line treatment for malaria in artemisinin combination therapies. Furthermore, the WHO recommends the use of fast acting drug artemisinin in combination with a partner drug for treatment of uncomplicated malaria (Kumar *et al*., 2018; WHO, 2022). Artemisinin targets the early stages of parasite development. Sadly, artemisinin drugs developed resistance which is associated with mutation in *kelch13* gene of the parasite. The resistance leads to delayed clearance of parasites after artemisinin exposure. However, delayed clearance of artemisinin does not frequently lead to failure in combination therapies. Furthermore, activity loss by partner drugs such as mefloquine has regrettably led to failure of artemisinin combination therapies for *P. falciparum* treatment in Southeast Asia (Conrad and Rosenthal, 2019). Recent studies show that triple artemisinin therapy which combines artemisinin derivatives with two partner drugs is effective at delaying multidrug resistance (Nguyen *et al*., 2023). Nonetheless, it is encouraging to note that since 2021, WHO approved the broad use of a recombinant based RTS,SAS01 malaria vaccine in children infected by *P. falciparum*. Reports show that the vaccine significantly reduces malaria related deaths in children (WHO, 2021). A second protein based R21/Matrix-M vaccine has also been recommended by WHO (WHO, 2023).

The ability of *P. falciparum* to withstand drug induced stress is facilitated by molecular chaperones which aid proper folding of proteins (Akide-Njuge *et al*., 2009). *P. falciparum* harbours functional evolution involving upregulation of stress proteins which facilitate refolding of denatured *Plasmodium* proteins (hormetic response) (Pallavi *et al*., 2010a; Daniyan *et al*., 2019). In addition, the *P. falciparum* employs the hormetic response adapt to change in environments. One of the mechanisms involves the hormetic response involving transcriptional factors, presiding expression of vitagenes such as heat shock proteins (Calabrese *et al*., 2010; Calabrese *et al*., 2011). Vitagenes are crucial for maintaining cellular proteostasis and redox balance during pathogenesis of infections, thus coordinating mechanisms of stress resistance (Calabrese *et al*., 2010, Siracusa *et al*., 2020). Moreover, the parasite possesses a genome that is "eroded", some of these "erosions" result in inaccurate translation of the genetic code consequently leading to production of mutated proteins (Melnikov *et al*., 2018). Hence, this leads change in protein structure, function, and quality (Kumar *et al*., 2006), posing a hurdle in the efficacy of antimalarial drugs. Since molecular chaperones are involved in drug

resistance and parasite survival, there is a need for development of therapeutic interventions tailored to target these chaperones. (Shonhai, 2010; Belete, 2020).

1.4 Molecular chaperones

Molecular chaperones are ubiquitously expressed and play an important role in protein homeostasis within the cell (Edkins and Boshoff, 2021; Macosek *et al*., 2021). Molecular chaperones facilitate correctly folding other proteins ensuring they attain their functionally active conformation (Hartl, 1996; Hartl and Hayer-Hartly, 2009). In addition, molecular chaperones are responsible for preventing aggregation and facilitating protein assembly (Edkins and Boshoff, 2021). Furthermore, molecular chaperones play an important role in maintaining protein quality control and directing damaged proteins for proteolytic degradation (Hartl and Hayer-Hartyl, 2002). Some molecular chaperones are constitutively expressed (Craig *et al*., 1983; Hayes, 1996), whilst some are induced by stress (Baker *et al*., 1984). A special class of molecular chaperones known as heat shock proteins (Hsp, section 1.5) is known to be upregulated during stress (Hartl *et al*., 2011). Hsps promote parasite survival and development within the human host and targeting them for therapeutic purposes has been shown to disrupt parasite growth (Pallavi *et al*., 2010a).

1.5 Heat shock proteins as molecular chaperones

The capability of heat shock proteins (Hsps) to cope with stress was first described by Ritosa (Ritosa, 1963). He observed that heat shock exposure produced chromosomal puffs in the salivary glands of fruit flies (*Drosophilia*) (Ritosa, 1963). In the following years, similar chromosomal puffs were observed in organisms exposed to stress such as hypoxia and reactive oxygen species (Ritossa, 1964). Heat shock proteins have since been used to study stress response in organisms (Clark and Perk, 2009) and have been presented as desirable drug targets in diseases such as cancer and malaria (Charttajee and Walker, 2017; Daniyan and Blatch, 2017; Shonhai, 2021). Heat shock proteins are conserved and ubiquitous, involved in similar roles across organisms from plants and bacteria to humans (Garrido *et al*., 2001). Furthermore, heat shock proteins are known to be involved in biological processes such transcription, translation and posttranslational modifications (Acharya *et al*., 2007; De Maio *et al*., 2012).

1.5.1 Major heat shock protein groups of *P. falciparum*

Hsps are classified into various families which perform diverse functions (Table 1.1; Hu *et al*., 2022). Hsps are classified according to their molecular weight in kilodaltons (kDa) (Table 1.1; Hu *et al*., 2022).

Table 1.1 Heat shock protein families in *P. falciparum* and their functions

Protein Family	M.W kDa	Cellular localization	Function	References
Hsp110	100- 150	ER, cytoplasm	Involved as a NEF for Hsp70, suppressing protein aggregation	Mulidharan, 2012; Zininga *et al*., 2016; Kudyba *et al*., 2019
Hsp100	80-110	cytosol nucleus parasitophorous vacuole chloroplast apicoplast	Protein folding and degradation	Mogk *et al*., 1999 Mogk *et al*., 2015; Johnston *et al*., 2017
Hsp90	82- 96	nucleus cytosol ER mitochondria apicoplast	Protein folding, signal transduction, maturation of steroid of steroid hormone receptors and kinases	Shonhai *et al*., 2011 Buchner and Li, 2013 Seraphim *et al*., 2019;
Hsp70	66-78	cytosol nucleus mitochondria, ER	Confer cytoprotection, protein folding and refolding,	Shonhai *et al*., 2007; Hartl and Hayer-Hartyl, 2009; Shonhai, 2021
Hsp60	58- 65	mitochondria	Protein folding and assembly	Sato and Wilson, 2005; Padma *et al*., 2015
Hsp40	40-100	cytosol	Recruiting substrate for Hsp70, regulates Hsp70 activity	Botha *et al*., 2007; Njuge *et al*., 2013; Kampiga *et al*., 2019
sHsps	15- 30	Cytosol nucleus	Prevent protein aggregation	Veinger *et al*., 1998; Gusev *et al*, 2002; Haslbeck and Veirling, 2015

Table legend: MW-molecular weight, ER-endoplasmic reticulum

1.5.2 The J domain proteins (Hsp40s)

Hsp40s are also known as J domain proteins (JDPs) because they contain a characteristic feature known as the J domain (Kampiga *et al*., 2019). The J domain is made up of 70 amino acid residues and is highly conserved (Wall *et al*., 1994). J domain proteins are similar to the *E. coli* Hsp40, DnaJ (Walsh *et al*., 2004). There are 44 Hsp40 genes encoded in humans and 49 *P. falciparum* (Kampiga and Craig, 2010; Njuge *et al*., 2013). The J domain proteins are categorized into four types (type I, II, III and IV) based on their domain structure and function (Botha *et al*., 2011). A variety of J domain proteins are present across species where they are involved in specialized roles (Kampiga and Craig, 2010).

The *P. falciparum* J domain family (PfJDP) is classified into four subclasses; type I, type II, type III and type IV. Type I contain the J domain (with HPD), glycine/phenylalanine rich region (G/F), a cysteine rich zinc binding region (CRR) and a conserved C-terminal domain (Figure 1.2). Type II are similar to type I, but instead of CRR region, they contain glycine/methionine rich region (Figure 1.2). Type I and type II use the J (with HPD) domain to bind non-native proteins and direct them to Hsp70, stimulating its ATPase activity (Liberek *et al*., 1991; Walsh *et al*., 2004). Mutation in the HPD motif prevents proper interaction between J domain protein and Hsp70 (Mayer *et al*., 1999; Hennessy *et al*., 2005; Genevaux *et al*., 2001). Type III lack GF and CRR region but contain the typical J domain. Type IV share similarity with type III, but instead possess a non-conserved J domain without HPD motif and lacks C terminal domain (Figure 1.3; Botha *et al*., 2007).

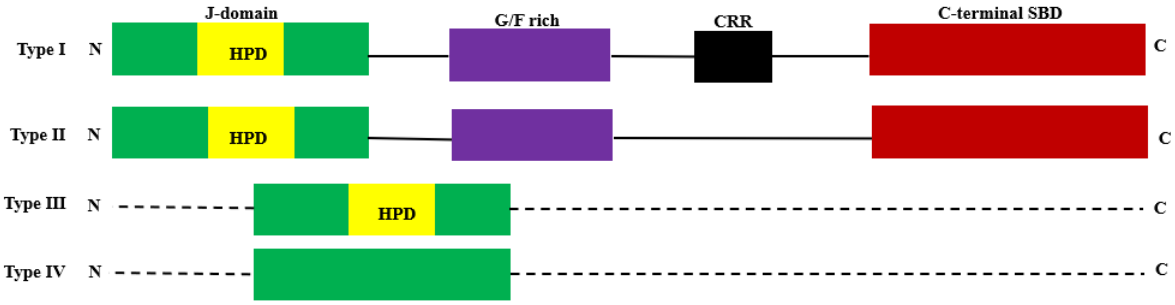

Figure 1.2. Classification of J domain proteins according to their domain organization. The various subdomains shown as follows; the J domain with conserved HPD (His-Pro-Asp motif, glycine/phenylalanine G/F rich region, CRR region and C-terminal SBD. The N-terminus is shown as 'N'. Adapted from Botha *et al*., 2007.

JDPs function as co-chaperones of Hsp70 (Figure 1.3). JDPs recognize substrates with exposed hydrophobic region and bind them (Figure1.3; Fan *et al*., 2004). Their J domain interacts with the NBD domain of Hsp70, stimulating its ATPase activity thus, ATP hydrolysis (Botha *et al*., 2007; Botha *et al*., 2011). JDP then transfers the substrate to Hsp70 for subsequent folding (Figure 1.3; Summers *et al*., 2009a). The JDP-Hsp70 folding pathway is initiated when JDP recruits a non-native protein client and directs it to ATP bound Hsp70 with low affinity for substrate (Figure1.4; Mayer and Gierasch, 2020). Upon hydrolysis of ATP to ADP, inducing Hsp70 conformation resulting in Hsp70-ADP complex. TheHsp70-ADP complex has increased affinity for substrates (Figure 1.3; Cyr *et al*., 2015). A nucleotide exchange factor (NEF) then binds to Hsp70 resulting in the dissociation of ADP and release of substrate (Figure 1.3; Mayer and Gierasch, 2020).

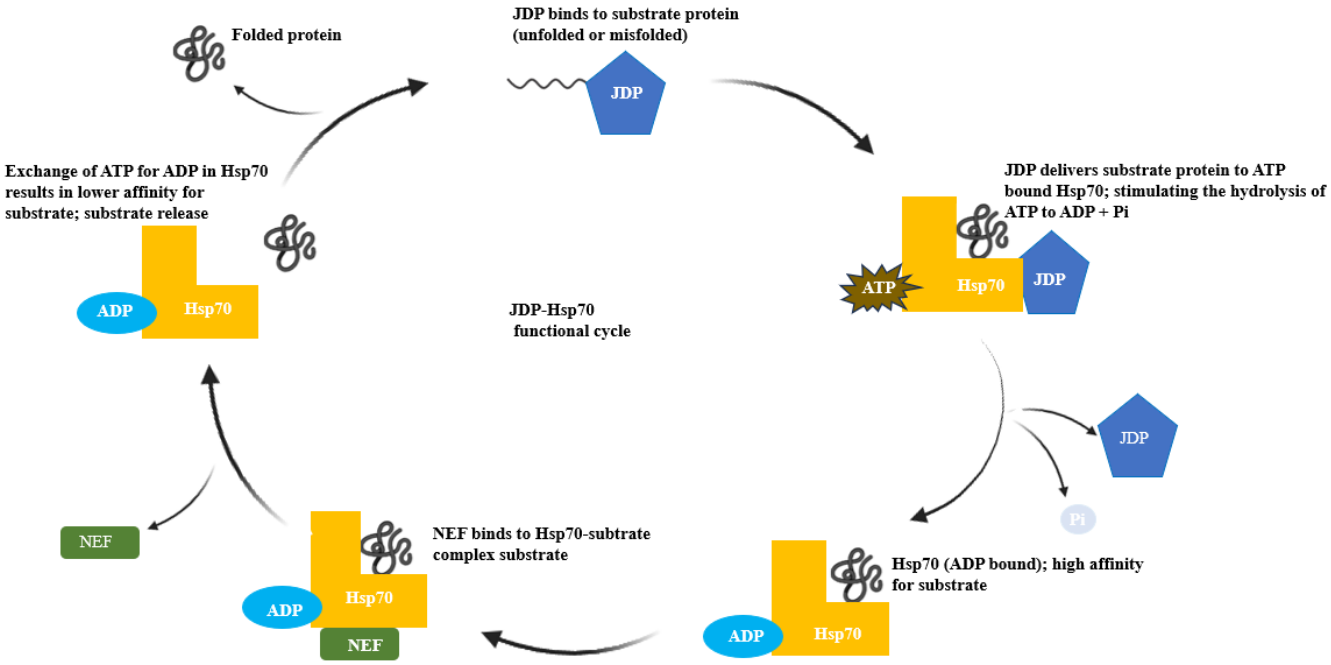

Figure 1.3. The JDP-Hsp70 folding pathway. Initially, the substrate (unfolded protein), that is bound to the JDP, forms a complex with the ATP bound Hsp70. ATP hydrolysis leads the subsequent transfer of the substrate to the substrate binding pocket of Hsp70. The substrate is transferred, JDP dissociates from the complex and this is followed by recruitment of the nucleotide exchange factor (NEF) to the Hsp70-substrate complex, promoting the ADP-ATP exchange in HSP70. Binding of ATP to Hsp70 induces a conformational change that subsequently leads to the release of both NEF and substrate. Adapted from Hennesy *et al*., 2005; Mayer and Gierasch, 2020.

P. falciparum JDPs (PfJDPs) localize all compartments of the infected erythrocyte, with exported proteins being the largest number of the family (Sagearnt *et.al*, 2006; Dutta *et al*., 2021a). In addition, a significant number of the exported proteins are expressed during the early stages (asexual) of the malaria parasite life cycle (Bozdech *et al*., 2003). Amongst exported

JDPs, type IV JDP (PFA0110w) known as 'ring infected erythrocyte surface antigen protein (RESA) has been shown to reinforce parasite development and pathogenesis (Silver *et al*., 2005; Njuge *et al*., 2013, Zhang *et al*., 2018). In a study by (Silva *et al*., 2005), cells with disrupted RESA gene had increased susceptibility to heat shock, vesiculation and were severely damaged. Proving that indeed RESA is important for parasite development (Silva *et al*., 2005). Additionally, type IV PfJDPs are unique to the parasite, they do not have human homologues, hence they are a promising group of potential drug targets (Botha *et al*., 2011).

Type I and type II function as co-chaperones of Hsp70, facilitating the transport of client proteins and ensure that they are kept in transport competent state (Dutta *et al*., 2021a, b). *P. falciparum* has two type I PfJDPs, PFD37_1437900 and PFD0462w. Complementation studies in *E. coli* (OD259) heterologously expressing the JDP PFD0462w showed that the PfJDP functionally interact with *E. coli* Hsp70 (DnaK) *in vivo* (Nicoll *et al*., 2007). Moreover, PFD0462w also stimulated the *in vitro* protein refolding activity of PfHsp70-1 (Misra and Ramachandran, 2009). In addition, studies by (Botha *et al.,* 2007, Botha *et al*., 2011) showed that type I JDP, PF3D7_1437900 forms a functional complex with PfHsp70-1 stimulating its ATPase activity. Furthermore, type I and type II JDPs are thought to function independently as chaperones, preventing aggregation (holdase) (Langer *et al*., 1992; Bao *et al*., 2002). Type II PfJDP, PFA0660w has been demonstrated to be essential for parasite survival *in vitro* (Maier *et al*., 2008). Type III PfJDPs are thought to be involved in the assembly of complexes and recruiting Hsp70s to fold their substrates (Botha *et al*., 2007).

Findings by (Botha *et al*., 2011) revealed that pyrimidinone inhibitor selectively inhibits JDP-PfHsp70-1 partnership, without targeting the humanJDP-Hsp70 system. In addition, Cockburn and colleagues (2011) reported that melangenone A, B and C and lapachol inhibited the capability of JDP to stimulate the ATPase activity of PfHsp70-1. These findings have established foundation for targeting JDP-Hsp70 partnerships, as well as provide insights into identification of novel antimalarials (Zininga and Shonhai, 2019; Shonhai, 2021).

1.5.3 Hsp70 family

The 70 kDa (Hsp70) proteins are ubiquitous, highly conserved and represented in all domains of life (Daugaard *et al*., 2007). Hsp70s are divided into two subfamilies, DnaK-like (canonical Hsp70s) and Hsp110 (the non-canonical Hsp70s) (Easton *et al*., 2000; Chakafana *et al*., 2019b). DnaK/canonical Hsp70s are capable of refolding misfolded proteins and suppressing protein aggregation (Shonhai, 2010; Kumar *et al*.,, 2011). Hsp110 members have an extended lid segment and they function to suppress protein aggregation. In addition, the latter also function as nucleotide exchange factors for canonical Hsp70s (Chakafana *et al*., 2019b). Both groups are critical for maintaining protein homeostasis as well as maintaining quality control in the cell (Mayer and Bukau, 2005; Kohler and Andreason, 2020). Furthermore, Hsp70s are involved membrane translocation of organellar and secretory proteins, as well as control of the activity of regulatory proteins. The above-mentioned functions are based on the ability of Hsp70 to interact with hydrophobic peptide segments of proteins in an ATP controlled fashion (Mayer and Bukau, 2005; Mayer and Gierasch, 2020). Hsp70s functionality is enhanced by its interaction with co-chaperones such as JDP, Hsp60, Hsp90 and Hsp100 (Mogk *et al*., 2015; Chakafana *et al*., 2019b).

1.5.4 The structural features of Hsp70s

Generally, the Hsp70 domain organization consists of an N-terminal ATPase domain (44 kDa) known as the nucleotide binding domain (NBD) which hydrolyzes ATP. On the C-terminal there is the substrate binding domain (SBD) of 28 kDa (Figure1.4; Mayer and Bukau, 2005). The substrate binding domain is further subdivided into a β-sandwich subdomain of 15-18 kDa, followed by an α-helical subdomain lid segment of 10 kDa (Figure1.4; Mayer, 2013; Mayer and Kityk, 2015). The SBDβ binds extended polypeptides (Flaherty *et al*., 1990; Lee-Youn *et al*., 1995), whilst the SBDα serves as a flexible lid enclosing the Hsp70 SBDβ (Hatherley *et al*., 2014). The two domains are connected by a highly conserved short linker segment, which plays a crucial role in allosteric communication (Figure1.4; Chakafana *et al*., 2019a; Mayer *et al*., 2021). Hence, Hsp70 function requires coordinated action of all domains (Zhu *et al*., 1996). Superseding the SBDα, there is the EEVD motif which takes part in binding co-chaperones and other heat shock proteins such as Hsp90 (Hartl, 1996; Zininga and Shonhai, 2019).

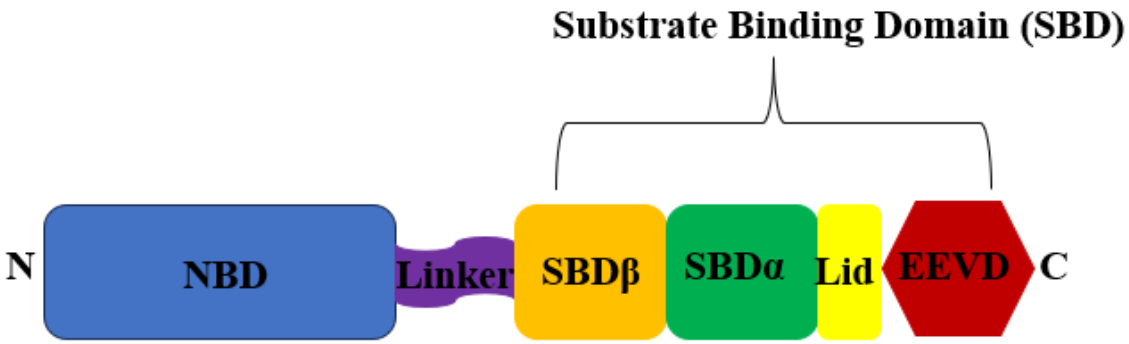

Figure 1.4. Domain architecture of Hsp70. The N-terminal ATPase domain (45 kDa) and a C-terminal substrate binding domain (SBD) of 25 kDa. Cytosolic Hsp70s harbour a highly conserved EEVD motif. Adapted from Sharma and Massison (2009).

Hsp70s exert their chaperone function through ATP hydrolysis. The nucleotide binding status determines the affinity of the C-terminal SBD. In the ATP bound state, Hsp70s have weak affinity for substrate (section1.5.2). The substrate binding affinity increases when ATP is hydrolyzed to ADP (Mayer and Kityk, 2015). In the event where a co-chaperone and substrate are absent, the rate of ATP hydrolysis is limiting hence Hsp70s display low ATPase activity. Hsp70 functionality is enhanced by cooperating with co-chaperones such as JDPs and nucleotide exchange factors (NEF) (section 1.5.2). The latter bind the Hsp70 NBD facilitating the binding and release of substrates (Figure 1.3; Henessy *et al*., 2005). This functional interplay between Hsp70s and JDPs is essential for successful substrate refolding (Figure 1.3).

1.5.5. *P. falciparum* Hsp70s

P. falciparum encodes six Hsp70 proteins localizing different cellular organelles of the parasite as summarized in the table below (Table 1.2; Shonhai *et al*., 2007, 2021).

Table 1.2: Hsp70 members of *P. falciparum*.

Name	Molecular weight (kDa)	Localisation	Functions	References
PfHsp70-1 (PF3D7_0818900)	74	nucleus and cytosol	protein folding and aggregation	Shonhai *et al.*, 2007; Pesce *et al.*, 2008
PfHsp70-x (PF3D7_0917900)	76	exported to infected RBC	parasite protein export and refolding in host red blood cell	Kulzer *et al.*, 2012; Cobb *et al.*, 2017; Charrnaud *et al.*, 2017
PfHsp70-2 (PF3D7_1134000)	73	ER	import of *P. falciparum* protein to the ER, protein folding and quality control in the ER	Njuge *et al.*, 2013 Chen *et al.*, 2013
PfHsp70-3 (PF3D7_0831700)	73	Mitochondrion	import of proteins into mitochondrial matrix	Shonhai *et al.*, 2007 Njuge *et al.*, 2013 Nyakudi *et al.*, 2016
PfHsp70-y (PF3D7_1344200)	108	ER	NEF for PfHsp70-2	Shonhai *et al.*, 2007 Njuge *et al.*, 2013 Kudyba *et al.*, 2019
PfHsp70-z (PF3D7_0708800)	100	Cytoplasm	NEF for PfHsp70-1, suppresses protein aggregation	Muralidharan *et al.*, 2012; Zininga *et al.*, 2015a; Zininga *et al.*, 2016

Table legend. NEF, nucleotide exchange factor; ER, endoplasmic reticulum; RBC, red blood cell

1.5.6 PfHsp70-1

PfHsp70-1 is a prominent cytosolic chaperone in the erythrolyic stages of the parasite (Shonhai *et al*., 2007; Anas *et al*., 2020). PfHsp70-1 has been found to be prevalent in the asexual stages at 37 ℃ as well as induced and exported to the nucleus upon heat shock at 41 ℃ (Shonhai *et al*., 2007). Thus, the protein combines both housekeeping and stress response roles (Przybroski *et al*., 2015). Moreover, PfHsp70-1 stress inducibility, is important for cytoprotection and pathogenicity of the malaria parasite (Zininga *et al*., 2015a). The molecular chaperone properties of PfHsp70-1 have been demonstrated *in vitro* (Matambo *et al*., 2004; Shonhai *et al*., 2008) and *in vivo* heterologous assays (Shonhai *et al*., 2005; Makhoba *et al*., 2016; Lebepe *et al*., 2020). PfHsp70-1 displayed chaperone activity when heterologously expressed in *E. coli* and yeast cells with compromised endogenous Hsp70 function (Shonhai *et al*., 2005; Bell *et al*., 2011). Furthermore, a recombinant form of this protein suppressed the aggregation of aggregation prone protein *in vitro* (Shonhai *et al*., 2008; Lebepe *et al*., 2020). PfHsp70-1 also partners with the proteome degradation pathway facilitating the transfer of misfolded proteins for degradation by the proteosome. PfHsp70-1 is expressed in response to antimalarial drug stress (Akide-Nduge *et al*., 2009; Mok *et al*., 2015). Presence of antimalarial drugs causes parasite to undergo oxidative stress, to counter this, PfHsp70-1 expression is upregulated to reverse the damage (Bell *et al*., 2011).

It goes without saying that PfHsp70-1 is a desirable drug target (Shonhai, 2010; Shonhai, 2021). However, selectively targeting *P. falciparum* is challenging due to the high sequence conservation with their human homologs. For example, the cytosolic PfHsp70- 1 and the human HSP1A share over 72 % sequence similarity (Acharya *et al*., 2007). Interestingly, despite the sequence similarity to its human homologue, PfHsp70-1 was found to display a much higher ATPase activity than the human Hsp70 (Matambo *et al*., 2004; Anas *et al*., 2020). Additional findings showed that PfHsp70-1 is more efficient in refolding misfolded proteins than human Hsp70 (Anas *et al*., 2020), further proving that PfHsp70-1 possesses distinct structure-function features compared to its huma homologue (Chakafana *et al*., 2019a). Due to these structural and functional variations, between PfHsp70-1 and its human homologue, PfHsp70-1 has been suggested as a potential antimalarial drug target (Shonhai, 2010; Chakafana *et al*., 2019a; Lebepe *et al*., 2020). Inhibitors with antimalarial properties targeting PfHsp70-1 have been described (Cockburn *et al*., 2011; Cockburn *et al*., 2014; Zininga *et al*.,

2017a, b). Potential antiplasmodial inhibitors have been reported to inhibit the function of parasite Hsp70 whilst exhibiting minimal effects on the human Hsp70 (Cockburn *et al*., 2011; Daniyan and Blatch, 2017).

1.5.7 DnaK, KPf and KPf-V436F

DnaK is a major *E. coli* Hsp70, structurally constituting a canonical Hsp70 (Bukau and Walker, 1989). It is made up of a conserved NBD and SBD interconnected by a highly conserved linker motif (Bertelson *et al*., 2009). Studies have shown that DnaK is not essential at intermediate temperatures, but it becomes essential for viability at elevated temperatures (Bukau and Walker, 1989). The protein plays a critical role in repairing denatured proteins and this relies on DnaK ability to suppress aggregation of misfolded proteins, allowing their refolding (Mogk *et al*., 1999). Also, DnaK cooperates with co-chaperone DnaJ and regulator GrpE to refold misfolded proteins (Shonhai *et al*., 2007).

DnaK (Hsp70) function has extensively been studied *in vivo* using the complementation assay in *E. coli dnaK*756 cells (Shonhai *et al*., 2005; Makhoba *et al*., 2016; Lebepe *et al*., 2020). Previous studies have demonstrated DnaK and KPf capacity to protect *E. coli dnaK*756 cells with functionally compromised DnaK against heat stress (Makhoba *et al*., 2016; Lebepe *et al*., 2020). KPf is an Hsp70 chimeric protein constituting ATPase domain of DnaK and substrate binding domain of PfHsp70-1 (Figure 1.5). On the other hand, a variant of KPf, KPf-V43F harbours a mutation in the hydrophobic residue (*V43F*) (Figure1.5) in the substrate binding cavity, fails to protect the *E. coli* thermosensitive phenotype against heat stress (Makhoba *et al*., 2016; Lebepe *et al*., 2020). The same study by (Makhoba *et al*., 2016; Lebebe *et al*., 2020) demonstrated enhanced production of recombinant forms of *P. falciparu*m S-adenosylmethionine decarboxylase in *E. coli dnaK*756 cells co-expressing PfHsp70-1 and KPf. This suggests that PfHsp70-1 and KPf (Figure1.5) are adapted to facilitate folding of plasmodial proteins and their functional specificity is influenced by the SBD (Lebepe *et al*., 2020).

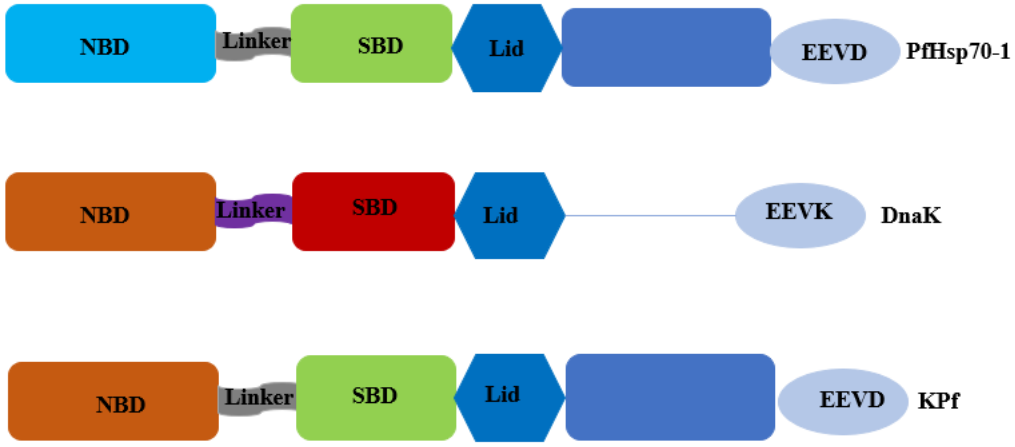

Figure 1.5. Structural organization of DnaK, PfHsp70-1 and KPf. All the proteins harbour NBD (light blue for PfHsp70-1, orange for DnaK and KPf). PfHsp70-1 and KPf both harbour the same SBD (light green) and red for DnaK. A flexible linker interconnecting the SBD and NBD exists, (grey for PfHsp70-1 and KPf) and (purple for DnaK). At the C-terminus, PfHsp70-1 possess the GGMP residues (blue) towards the EEVD motif (light blue). The DnaK C-terminus lacks GGMP residues. KPf is a chimeric product of NBD from DnaK and the SBD of PfHsp70-1. NBD: nucleotide binding domain, SBD: substrate binding domain. Adapted from Dongola 2022.

1.6.1 Hsp70s as drug targets

Although there is high sequence conservation among Hsp70 members, there is sufficient structural and functional variations in Hsp70s of different species allowing their selective inhibition (Shonhai, 2010; Chakafana *et al*., 2019a). The ATPase, substrate binding and linker domain have been identified as drug targets aimed at disrupting the parasite protein functionality. Chakafana *et al*., (2019a) noted the specific motifs namely, Magic, Tedywlee, GGMP and EKEK, present in malarial parasites. These motifs distinguish parasite Hsp70s from their human counterparts (Chakafana *et al*., 2019a). Moreover, PfHsp70-1 has been shown to exhibit unique structure-function features (section 1.5.4; Lebepe *et al*., 2020). Hence, it is not surprising that Hsp70s have received attention as antimalarial drug targets (Shonhai *et al*., 2021).

Numerous inhibitors of Hsp70 have been identified (section 1.6.2; Cockburn *et al*., 2011; Cockburn *et al*., 2014; Zininga *et al*., 2017 a,b,c). There are various features which make Hsp70s desirable drug candidates, including the fact that their role is regulated by nucleotides, the structural-functional distinctions across species and the formation of multiprotein complex with co-chaperones such as PfHsp90-PfHsp70, and PfHsp70-JDP-PfHsp60. Hence, it has been

suggested that inhibiting these complexes could potentially disrupt the function of *P. falciparum* Hsp70 (Zininga and Shonhai., 2019; Dutta *et al*., 2021a).

1.6.2 Small molecule inhibitors targeting *P. falciparum* Hsp70

Several potential Hsp70 inhibitors have been identified, these include adenosine analogues, fatty acids, malongenones, pyrimidines, and peptides (Table 3). Some of the inhibitors are cancer drugs repurposed as antimalarials (Zininga and Shonhai, 2019).

Table 1.3: Hsp70 inhibitors and their antimalarial effects

Name of inhibitor	Target protein	Antimalarial effect	References
Malonganenone derivatives (A, B, C)	PfHsp70-1 and PfHsp70-x	Selectively inhibited the ATPase activity for both PfHsp70-1 and PfHsp70-x	Cockburn *et al*., 2011; Cockburn *et al*., 2014
Lapachol (1,4 naphthoquinone)	PfHsp70-1 and PfHsp70-x	Selectively inhibited the ATPase activity for both PfHsp70-1 and PfHsp70-x	Cockburn *et al*., 2011
EGCG	PfHsp70-1 and PfHsp70-z	Binds the NBD of PfHsp70-1. Additionally, EGCG inhibited the chaperone and ATPase activities of PfHsp70-1 and PfHsp70-z, and also EGCG inhibited parasite growth IC_{50} = 2.9 µM.	Zininga *et al*., 2017b
PMB	PfHsp70-1 and PfHsp70-z	Inhibited the chaperone and ATPase activity for both PfHsp70-1 and PfHsp70-z	Zininga *et al*., 2017a
Apoptozole, MKT-077, VER-15008 (repurposed anticancer inhibitors)	PfHsp70-2	Bind to PfHsp70-2, in addition they exhibited some antiplasmodial activities to *P. falciparum* 3D7 and W2 strains.	Chen *et al*., 2018

Table legend: EGCG-Epigallocatechin-3-galate, PMB- Polymyxin B, NBD- Nucleotide binding domain

This study sought to repurpose two known inhibitors of Hsp70 (colistin sulfate and pifithrin μ), towards their use in targeting malarial proteins. Colistin sulfate is amongst different compounds of polymyxins (A-E), is also known as polymyxin E. Its molecularformula is $C_5H_{10}N_{16}O_{17}S$ (Falagas and Kasiakou, 2005; Minagawa *et al*., 2011). The discovery of colistin sulfate dates back to 1949 (Komura and Kurahashi, 1979). Colistin sulfate was synthesized from *Bacillas polymyxa*, subspecies *colistinus Koyama* (Komura and Kurahashi, 1979). Colistin sulfate acts by targeting bacterial cell membrane through binding to anionic lipopolysaccharide molecules and altering bacterial outer membrane permeability. Thereby leading to cell content release hence bacterial death (Falagas and Kasiakou, 2005; Minagawa *et al*., 2011).

In addition, colistin sulfate has been widely used in the treatment of multidrug-resistance Gram-negative bacteria (Nation and Li, 2009). Previously, colistin sulfate was used in cancer to target Hsp90. It was shown to bind the N-terminal of Hsp90 thus inhibiting its chaperone function (Bergen *et al*., 2006; Nation and Li, 2009; Minagawa *et al*., 2011). Furthermore, the derivative of colistin sulfate, PMB,has been shown to bind to Hsp70 and modulate its function (Zininga *et al*., 2017a). Interestingly, colistin sulfate and PMB share similar mechanism of action, which makes colistin sulfate a desirable compound to target Hsp70.

A

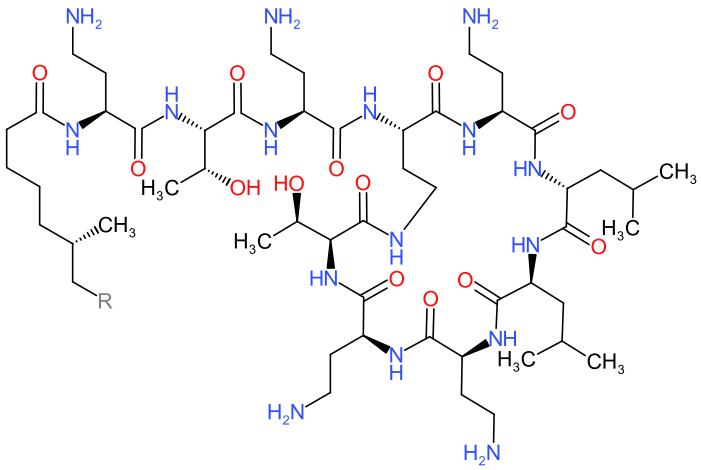

B

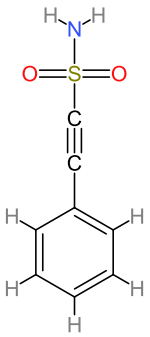

Figure 1.6. Chemical structures of colistin sulfate (A) and pifithrin μ (B). Chem4Word version 3.1 was used to generate the structures.

1.7 Commonly used methods to screen and identify Hsp70 inhibitors

1.7.1 Surface plasmon resonance analysis

Small molecule inhibitors have been shown to interrupt the function as well as conformations of Hsp70 (Zininga *et al*., 2017a; Muthelo *et al*., 2022). Various *in vivo* and *in vitro* assays have previously been employed to identify small molecule inhibitors of Hsp70. Surface plasmon resonance (SPR) is a real-time optical technique used to study protein-protein interactions and protein-drug target interactions (Zininga *et al*., 2015a). In a study conducted by (Zininga *et al*., 2017a), SPR was used to investigate the interaction of polymyxin B which targets both PfHsp70-1 and PfHsp70-z. Additional data from circular dichroism spectrometric analysis and tryptophan fluorescence spectroscopy showed that polymyxin B modulates the secondary and tertiary structure of Hsp70. Moreover, PMB also inhibited the basal ATPase as well as chaperone function of PfHsp70-1 and PfHsp70-z. Just like any other assay, SPR has its limitations. SPR instruments are expensive, research labs with less resources might not be able to access them. In addition, another con of this assay is that it is low-throughput. Though SPR offers information on binding affinity, it does not offer insight on the binding mechanism, or the specific protein residues involved in interaction (Gupta and Sharma, 2005).

1.7.2 Aggregation suppression assay

The aggregation suppression assay is used to study the chaperone activity (holdase) of a protein (Zininga *et al*., 2017a; Muthelo *et al*., 2022). The technique typically involves exposing malate dehydrogenase (MDH) to high temperatures leading to protein aggregation (Zininga *et al*., 2017a). Hsp70 is added to the mixture to function as a chaperone preventing MDH aggregation. The assay can be used to identify inhibitors that interrupt Hsp70 function to prevent MDH aggregation. Previously MDH assay was used to screen small molecule inhibitors of Hsp70. Various small molecule inhibitors were found to have effects on the aggregation suppression activity of PfHsp70-1 (Cockburn *et al*., 2011; Cockburn *et al*., 2014). These small molecule inhibitors are namely, malonganenone A-C, lapachol and bromo β-lapachol. In addition, a study done by (Muthelo *et al*., 2022) also employed the MDH technique to demonstrate inhibition of PfHsp70-1 activity. PfHsp70-1 and PfHsp70-x function to suppress the heat induced aggregation of malate dehydrogenase (Cockburn *et al*., 2011; Cockburn *et al*., 2014). In another study by (Zininga *et al*., 2017) PMB was reported to inhibit PfHsp70-1 function to suppress

MDH aggregation. The disadvantage of this assay is that it is low-throughput and it does not offer cellular insights, since the protein is taken out of the cell and the study done *in vitro*.

1.7.3 ATPase assay

Since PfHsp70-1 is an ATPase, its activity depends on the hydrolysis of ATP to carry out its activities, including protein folding and trafficking (Rule *et al*., 2016). ATPases hydrolyze ATP to ADP and an inorganic phosphate, ATPase activity is determined by quantitating the inorganic phosphate released *in vitro* (Brune *et al*., 1984; Rule *et al*., 2016; Mabate *et al*., 2018). The assay was previously utilized to demonstrate PMB inhibited the ATPase activity of PfHsp70-1 (Zininga *et al*., 2017a). The amount of inorganic phosphate released in the presence of PfHsp70-1, Hsp40 and PMB, showed that PfHsp70-1 ATPase activity was inhibited. Additional studies by (Cockburn *et al*., 2014) utilized the ATPase technique to screen inhibitors affecting ATPase activity of PfHsp70-1. This assay is low-throughput.

1.8 *E. coli* based complementation assay as a tool for identifying Hsp70 inhibitors

Hsp70s are an integral part of the chaperone system that safeguards proteostasis within the cell. Hsp70s are involved in all the stages of protein cycle from biosynthesis to degradation, involving facilitating protein folding, preventing aggregation and facilitating degradation of misfolded proteins (Mogk *et al*., 1999; Edkins and Boshoff, 2021). In addition, Hsp70s promote cell survival during stress (Bukau *et al*., 2000). Thus, Hsp70s are essential for functionality in a cellular context and its function is well demonstrated by a complementation assay (Makumire *et al*., 2021). As such, a complementation assay can be used to screen inhibitors targeting Hsp70 function. Furthermore, unlike biochemical assays, which remove the protein from its native cellular environment, potentially altering some of its characteristics. Complementation assay offers the advantage of monitoring Hsp70 function and its interactions with its co-chaperones, whilst causing minimal disruptions to the cellular environment (Blaszack *et al*., 2021). In addition, *in cellulo* complementation assays offer alternatives to *in vitro* assays for analysing protein function (Slabaugh *et al*., 2014b).

This study makes use of *E. coli dnaK*756 strain (Figure 1.7), characterized by resistance to bacteriophage λ DNA, sensitivity to temperatures above 40 °C, and expression of DnaK variant with three glycine to aspartate substitutions at position 32, 455 and 468, resulting in truncated non-functional DnaK, due to the mutation on its *dnaK* gene. Of these mutations, one reduces affinity for GrpE, whilst the other two substitutions elevate the basal ATPase activity of DnaK (Buchburger *et al*., 1999). As such, this strain serves as a desirable model to investigate the activity of heterologously expressed Hsp70 *in cellulo*, particularly at elevated temperatures. *E. coli* is an extensively studied microorganism which offers several advantages for investigating Hsp70 chaperone function. It is amenable to genetic manipulation, exhibits rapid growth, and facilitates cost-effective experimentation (Taj *et al*., 2014; Tungekar *et al*., 2021).

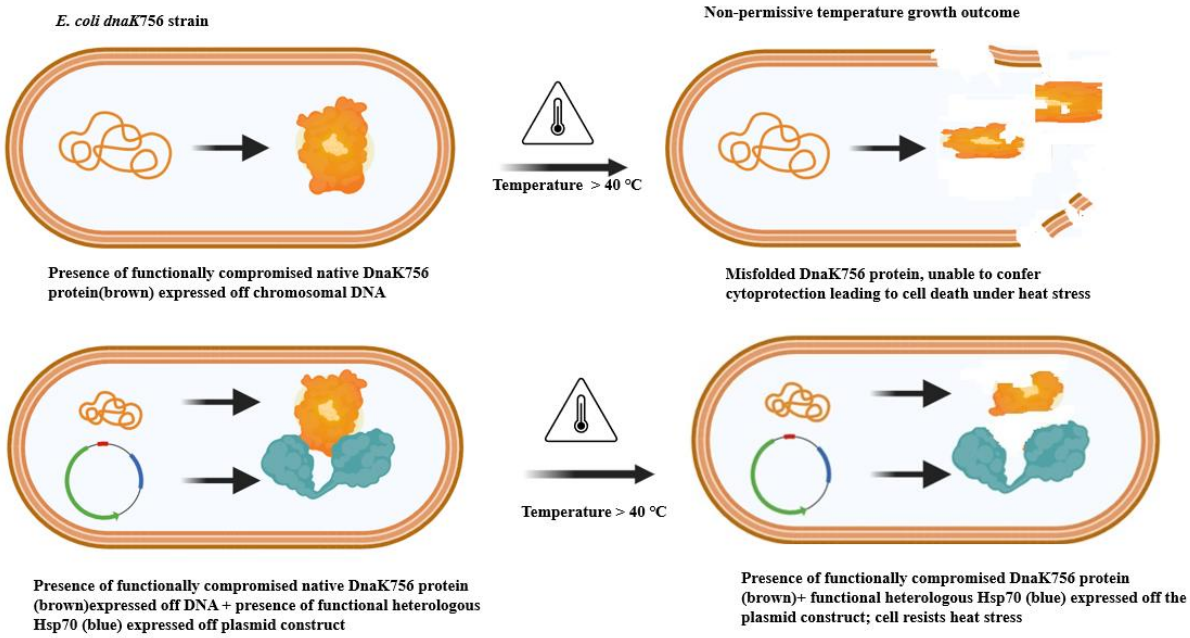

Figure 1.7. *E. coli dnaK*756 as a model for drug screening. Illustrating the essential role played by DnaK and KPf in conferring cytoprotection to the thermosensitive phenotype of *E. coli dnaK*756 cells, particularly at elevated temperatures. At temperatures above 40 °C, *E. coli dnaK*756 cells die. However, when the cells heterologously express DnaK and KPf, they survive under stress (above 40 °C). Introducing inhibitors compromise the capability of DnaK and KPf to protect *E. coli dnaK*756 cells leading to growth defects. Adapted from Ncube *et al*., 2024.

Here, an *E. coli* based complementation assay was developed to screen potential inhibitors targeting DnaK and KPf function to confer cytoprotection to *E. coli dnaK*756 cells. Previously, complementation assays using *E. coli dnaK*756 cells were done to demonstrate the cytoprotective role played by PfHsp70-1, DnaK and KPf at elevated temperatures (Makhoba *et al*., 2016; Lebepe *et al*., 2020; Makumire *et al*., 2021). Thus, the cytoprotective function of

these proteins was leveraged to screen potential inhibitors of DnaK and KPf. What makes this assay desirable is the fact that it is liquid based, making it high-throughput hence the 96-well microplate was used. This allowed for identification of various inhibitors and facilitating the titration of different inhibitors concentrations at the same time. Moreover, this study allowed evaluation of cellular response to various inhibitor concentrations.

1.9 Problem statement

Malaria remains as one of the most severe public health concerns worldwide. It is a leading cause of mortality in Sub-Saharan Africa, where pregnant women and young children are the most affected. WHO estimated 249 million malaria cases in 2022, and 608 000 deaths (WHO, 2023). *P. falciparum* is the main causative agent of malaria disease. The burden of malaria is further complicated by the emergence of drug resistance to existing antimalarial drugs (Akide-Njuge, 2009). In addition, the progress made in the previous years to fight off the disease has levelled off, as shown by a resurgence in malarial infections in 2022 (Monroe *et al*., 2022; WHO, 2023). This therefore necessitates an urgent need for novel approaches to tackle this disease (Zininga *et al*., 2015a).

The malaria parasite depends on molecular chaperones such as PfHsp70-1 for survival inside the host cell. Futhermore, PfHsp70-1 has been demonstrated to be expressed throughout the parasite's erythrocytic cycle, playing a significant role in maintaining protein quality control (Shonhai, 2007; Zininga and Shonhai 2014). Furthermore, PfHsp70-1 has been implicated in helping malarial proteins to resist drug pressure. As such, there is a need screen for novel small molecule inhibitors specifically targeting PfHsp70-1. However, developing and identification of potential inhibitors of *P. falciparum* is complicated by the requirement of costly models. This necessitates the development of simple and cost-effective high-throughput experimental systems. Previous studies have explored identification small molecule inhibitors targeting to PfHsp70-1 using techniques such as ATPase assay and surface plasmon resonance (Zininga *et al*., 2017a; Kayamba *et al*., 2021, Salomane, Pooe and Simelane, 2021). However, these small molecule inhibitors of PfHsp70-1 are limited hence there is need to screen for more. Therefore, this study seeks to develop high-throughput screening assays to identify small molecule inhibitors targeting PfHsp70-1, which will help broaden the search of antimalarials.

1.10 Hypothesis

A complementation assay can be used as a high-throughput screening assay to identify small molecule inhibitors of PfHsp70-1.

1.11 Aim

This study seeks to develop high-throughput screening assays to identify small molecule inhibitors of PfHsp70-1

1.12 Specific objectives

- To heterologously express PfHsp70-1, DnaK and KPf in *E. coli* XL1 Blue cells and purify the recombinant proteins using immobilized metal affinity chromatography.
- Optimize fluorescence assay to screen small molecule inhibitors modulating the tertiary conformation of PfHsp70-1, DnaK and KPf.
- Optimize and develop a complementation assay to identify inhibitors of DnaK and KPf
- Investigate the effects of colistin sulfate and pifithrin μ on the solubility of *E. coli dnaK*756 proteome.

Chapter 2: Materials and methodology

2.1 Materials

The plasmids listed in Table 2.2 were used in this study. The pQE30/KPf and pQE60/KPf plasmid constructs were utilized to express the recombinant KPf protein (Shonhai *et al*., 2005; Makhoba *et al*., 2016; Table 2.2). On the other hand, pQE60/KPf-V436F plasmid was used to express KPf-V436F mutant recombinant protein (Shonhai *et al*., 2005; Table 2.2). Plasmids in pQE30 vector express His-tagged proteins whilst those in pQE60 are untagged and they were used for the complementation assay. Plasmids, pQE30/DnaK (Shonhai *et al*., 2005; Table 2.2) and pQE60/DnaK (Burkholder *et al*., 1994; Table 2.2) were used to express DnaK recombinant protein. PfHsp70-1 (PF3D7_0818900) recombinant protein was expressed from pQE30/PfHsp70-1 plasmid (Shonhai *et al*., 2005; Table 2.2). The following antibodies were used to verify recombinant proteins: rabbit raised α-PfHsp70-1 (Shonhai *et al*., 2008), mouse raised α-DnaK (Zininga *et al*., 2016) and α-His-horseradish peroxidase conjugated antibody produced in rabbit from Thermo Scientific (USA). *E. coli* strains used for recombinant production and complementation assay are listed in Table 2.1. The rest of the reagents are listed in Appendix A.

E. coli JM109 DE3 competent cells were transformed with the following constructs: pQE30/DnaK (Makumire *et al*., 2021), pQE60/DnaK (Burkholder *et al*., 1994, Dongola, 2022), pQE30/KPf (Makhoba *et al*., 2016, Dongola 2022), pQE60/KPf (Shonhai *et al*., 2005, Dongola, 2022), pQE60/KPf-V436F (Shonhai *et al*., 2005; Makumire *et al*., 2021), pQE30/PfHsp70-1 (Shonhai *et al*., 2005; Mudau, 2021). The plasmids were then purified using a Zippy ^{TM} mini prep kit following the manufacturer's instructions (Thermo Scientific, USA). Thereafter, the purified DNA was analyzed with restriction digest for integrity confirmation. Restriction enzymes *Bam*HI and *Hind*III (Thermo Scientific, USA), were used for pQE30/PfHsp70-1, pQE30/DnaK, pQE30/KPf verification. To confirm the integrity of pQE60/KPf and pQE60/KPf-V436F restriction enzymes *Bam*HI and *Hind*III (Thermo Scientific, USA) were employed. For pQE60/DnaK validation, *Nco*I and *Hind*III ((Thermo Scientific, USA), restriction enzymes were utilized. The products were then visualized in 0.8 % agarose gel.

Table 2.1 Features of *E. coli* strains

Cell lines	Description	Supplier/reference
E. coli dnaK756 (BB2362, *E. coli dnaK756* recA::TcR pDMI,1))	DnaK expressed by this strain has 3 amino acid substitutions at residues 32, 455 and 468. Resulting in strain with low GrpE affinity.	Buchberger *et al*., 1999; Shonhai *et al*., 2005
E. coli JM109	e14-(McrA-) recA1 endA1 gyrA96 thi-1 hsdR17 (rK-mK+) A1 Δ(lac-proAB) (F' traD36 proAB lacIqZΔM15)	Thermo Fisher Scientific
E. coli XL1 Blue	recA1 endA1 gyrA96 thi1 hsdR17 supE44 relA1 lac (F' proAB laclqZM15 Tn10 (Tetr)	Bullock *et al*., 1987

Table 2.2 Plasmid constructs description

Plasmids	Protein encoded for	Antibiotic resistance	His-tag	References
pQE30/KPf	KPf	Amp^R	✓	Makhoba *et al*., 2016
pQE60/KPf	KPf	Amp^R	X	Shonhai *et al*., 2005
pQE30/PfHsp70-1	PfHsp70-1	Amp^R	✓	Shonhai *et al*., 2005
pQE30/DnaK	*E. coli* Hsp70 (DnaK)	Amp^R	✓	Makumire *et al*., 2021
pQE60/DnaK	*E. coli* Hsp70 (DnaK)	Amp^R	X	Burkholder *et al*., 1994
pQE60/KPf-V436F	KPf-V436F	Amp^R	X	Makhoba *et al*., 2016

Amp^R: ampicillin resistant, ✓: presence of his-tag, x: absence of a His-tag

2.2 Expression of PfHsp70-1, KPf and DnaK in *E. coli* XL1 Blue cells

E. coli XL1 Blue chemically competent cells were transformed with the following plasmid constructs: pQE30/PfHsp70-1, pQE30/DnaK and pQE30/KPf in 2 x YT media

[1.6 % tryptone (w/v), 1 % yeast extract (w/v), 0.5 % NaCl (w/v), 1.5 % agar (w/v)] containing 100 µg/mL ampicillin. The expression was done following a previously described protocol by (Zininga *et al.*, 2015a). A single colony from the transformants was inoculated into 50 mL 2x YT broth [1.6 % tryptone (w/v), 1 % yeast extract (w/v), 0.5 % NaCl (w/v)] containing 100 µg/mL ampicillin and incubated overnight at 37 °C, shaking at 250 rpm using the FMH 200 (FMH Electronics, RSA). The overnight culture was then transferred into 450 mL 2x YT broth supplemented with 100 µg/mL ampicillin. Growth of the culture was monitored until mid-log phase at OD_{600} and then induced with 1 mM of isopropyl-β-D-1-thiogalactopyranoside (IPTG). Upon induction with IPTG, recombinant proteins PfHsp70-1, DnaK and KPf were expressed for 6 hours. Hourly expression samples were collected and analyzed by 12 % sodium dodecyl sulfate-polyacrylamide gel electrophoresis (SDS-PAGE) and visualized using Coomassie Brilliant blue. The remnant culture was harvested by centrifugation at 5000 x g for 20 minutes at 4℃, the supernatant was discarded, and the remaining pellets were resuspended in 10 ml lysis buffer (10 mM Tris-HCl, pH 7.5, 300 mM NaCl and 10 mM Imidazole). Thereafter, the cell lysates were incubated at room temperature while shaking for 30 minutes and then they were stored at -80 ℃ freezer for future use. The expression of recombinant proteins was confirmed by Western blot analysis using α-PfHsp70-1, α-DnaK and α-His antibodies.

2.3 Recombinant protein purification

The recombinant proteins were purified using Sepharose nickel affinity chromatography as previously described (Zininga *et al.*, 2015). Cell lysates were centrifuged for 20 minutes at 4 ℃ at 5000 x g (Shonhai *et al.*, 2008). Soluble extract was added to HisPur Nickel-charged nitrilotriacetic (Ni-NTA) (Thermo Scientific, USA) immobilized affinity chromatography column and incubated for 1 hour to facilitate binding of recombinant protein. Two-bed volume of wash buffer I (100 mM Tris-HCl pH 7.5; 300 mM NaCl; 25 mM imidazole; 1mM PMSF) was used to wash unbound proteins. Wash buffer II (100 mM Tris-HCl pH 7.5; 300 mM NaCl; 80 mM imidazole; 1mM PMSF). Proteins bound to the beads were eluted with elution buffer I (100 mM Tris-HCl pH 7.5; 300 mM NaCl; 250 mM imidazole; 1mM PMSF) and elution buffer II (100 mM Tris-HCl pH 7.5; 300 mM NaCl; 500 mM imidazole; 1mM PMSF, lysozyme 1mg/mL). Purification samples wash and elution samples were prepared for analysis by 12 % SDS-PAGE and Western blot.

2.4 Fluorescence spectroscopy

Inhibitor dependent conformational modulation of PfHsp70-1, KPf and DnaK was investigated by tryptophan fluorescence as previously described by (Zininga *et al*., 2016). PfHsp70-1 has three tryptophan residues W32, W101 and W593 whilst KPf possesses W102 and W578. On the other hand, DnaK possesses a single W91 residue. Tryptophan is known to emit fluoresce (Ghisaidoobe and Chung, 2014) and this forms the rationale of this assay. This assay is used to monitor protein conformational changes, ligand binding and interactions (Teale and Webber, 1957).

An aliquot of 1 µM of recombinant protein(s) (PfHsp70-1, KPf and DnaK) was allowed to equilibrate with phosphate buffered saline buffer (PBS) (137 mM NaCl, 27 mM KCl, 4.3 mM Na_2HPO_4, 1.4 mM KH_2PO_4, 10 % glycerol, 1mM PMSF pH 7.5), at 25 ℃ for 15 minutes. The respective protein(s) emission spectra were monitored between 320 nm and 400 nm, following excitation at 295nm, using a JASCO FP-6300 spectrofluorometer (JASCO FP, Tokyo Japan). The recombinant proteins were incubated with 5 mM of ATP/ADP in PBS buffer under similar conditions. Next, the effects of inhibitors on the tertiary conformation of the proteins were determined. The recombinant protein(s) (PfHsp70-1, DnaK, KPf) at 1 µM were incubated with increasing concentrations: 0.4 µM, 0.6 µM and 0.8 µM of colistin sulfate and 5 µM, 10 µM, 15 µM in PBS buffer for 15 minutes at 25 ℃.

Table 2.3: Tryptophan fluorescence experimental controls

Control type	Treatment
Protein	Protein (1 µM) equilibrated with PBS buffer for 15 mins at 25 ℃
Nucleotide	ATP/ADP (5mM) incubated in PBS, for 15 minutes at 25 ℃
Buffer	PBS emission monitored at 320- 400 nm
Buffer + inhibitor	Varying concentrations of colistin sulfate and pifithrin µ incubated in PBS buffer, emission spectra observed.

All the control emission spectra were read at 320- 400nm, following excitation at 295 nm.

Control buffer titrations were run in parallel with the experiment. The emission spectra of PBS buffer alone was taken under similar conditions, this was done to account for background signal caused by the buffer itself. The PBS was also allowed to equilibrate with nucleotides

(ADP/ATP) and inhibitors (colistin sulfate and pifithrin μ), in the absence of the respective proteins. Afterward, their emission spectra were monitored under similar conditions. This was done to ascertain that the change in the emission spectra was induced by ligand binding to the respective proteins (Table 2.3).

2.5 Complementation assay

In cellulo complementation assay was conducted to screen inhibitors targeting DnaK and KPf function to protect thermosensitive *E. coli dnaK*756, BB2362, (*dnaK*756 *recA::Tc*^{R} *1 pDMI,1)* cells, whose endogenous Hsp70 is functionally compromised (Georgopoulos *et al*., 1979; Makumire *et al*., 2015). The capability of DnaK and KPf to confer cytoprotection to the *E. coli dnaK*756 cells at elevated temperatures, and in the presence of inhibitors was explored. Complementation assay typically employs *E. coli* cells that are either deficient of DnaK or express non-functional native DnaK (Bukau and Walker, 1989; Makumire *et al*., 2015). DnaK is not essential for *E. coli* growth under normal conditions but becomes essential for *E. coli* growth under stressful conditions such as elevated temperatures or other forms of stress (Bukau and Walker, 1989).

The *E. coli dnaK756* cells grow transiently at 30 °C- 37°C but die in temperatures above 40 °C. The strain expresses a mutant truncated or non-functional DnaK characterized by resistance bacteriophage λ (Georgopoulos, 1979), three glycine to aspartate substitutions at positions 32, 455 and 468. Of these mutations, one reduces affinity for GrpE, whilst the other two substitutions elevate the basal ATPase activity of DnaK (Buchberger *et al*., 1999). Furthermore, the strain possesses enough DnaJ levels to meet physiological requirements (Spence *et al*., 1990; Suppini *et al*., 2004). As such, this DnaK mutant strain serves as a desirable model for screening inhibitors targeting the chaperone activity of Hsp70.

Chemically competent *E. coli dnaK756,* BB2362, (*dnaK756 recA::Tc*^{R} *1 pDMI,1)* cells were transformed with the following constructs: pQE60/DnaK, pQE60/KPf and pQE60/KPf-V436F plasmid constructs prior to growing them (Table 2.2). A colony from transformants was inoculated into 10 mL 2 x YT [1.6 % tryptone (w/v), 1 % yeast extract (w/v), 0.5 % NaCl (w/v)] broth, containing 10 μg/mL tetracycline, 50 μg/mL kanamycin for the respective strain and 100 μg/mL ampicillin for plasmid selection. The culture was grown overnight (17 hours) at 35 °C while shaking at 150 rpm using the FMH 200 (FMH Electronics, RSA) in a shaking incubator.

The protein KPf-V436F was heterologously expressed as the negative control since its mutation on the hydrophobic pocket essentially blocks it from interacting with substrates thus abrogating its chaperone activity (Makhoba *et al*., 2016). The positive control was represented by cells heterologously expressing DnaK. On the other hand, cells heterologously expressing KPf were the test cells since KPf (ATPase from DnaK fused with substrate binding domain from PfHsp70-1) contains a substrate binding domain from PfHsp70-1 (section 1.8; Figure 1.7).

Followed by overnight growth, the overnight inoculum was standardized with fresh 2x YT broth, to a cell density of $OD_{600=}$ 0.2. NB: The benchtop was swabbed with 70 % ethanol to ensure aseptic conditions were maintained. Thereafter, the necessary antibiotics were added as well as 1mM IPTG to induce recombinant protein production. A culture volume of 250 µL was transferred into a sterile 96-well microplate and growth was monitored at a permissive temperature of 35 ℃ and non-permissive temperature of 42 ℃.

Pifithrin µ was initially identified as a small molecule inhibitor acting against p53 in mitochondria and has been reported to interact with Hsp70 SBD in cancer research (Figure 1.5; Strom *et al*., 2006; Leu *et al*., 2009). Pifithrin µ was also reported to bind *Plasmodial* Hsp70 (Muthelo *et al*., 2022). Colistin sulphate is a polycationic peptide antimicrobial belonging to the polymyxin family of antibiotics (Falagas *et al*., 2005; Gallardo-Godoy *et al*., 2016). Colistin sulphate has been reported to bind the N-terminus of Hsp90 thus inhibiting its chaperone function (Bergen *et al*., 2006; Minagawa *et al*., 2011). Furthermore, previous studies have shown that colistin sulfate derivative polymyxin B binds Hsp70 and modulate its function (Zininga *et al*., 2017a). Interestingly, colistin sulphate and polymyxin B possess similar mechanism of action making it a desirable small molecule inhibitor against Hsp70. Hence, the current study sought to assess the effects of colistin sulphate and pifithrin µ on cells heterologously expressing DnaK and KPf to protect *E. coli dnaK*756 cells, at elevated temperatures.

Colistin sulfate was titrated in varying concentrations of 0.2 µM, 0.4 µM, 0.6 µM, 0.8 µM and 1 µM, whilst 2.5 µM, 5µM, 10 and 15 µM concentrations were used for pifithrin µ. To investigate the effects of these inhibitors on the cells, the above-mentioned concentrations of colistin sulfate and pifithrin µ were added to different wells on the 96-well microplate. To the

other wells cells treated with 0.5 % dimethyl sulfoxide (DMSO), were aliquoted. DMSO is a solvent in which inhibitors were dissolved in, this step is important to ascertain that DMSO does not interfere with the growth of cells. The cells grown with DMSO are the experimental baseline. A plate blank consisting of freshly prepared 2 x YT broth supplemented with IPTG and the respective antibiotics was also added into the wells of the 96-well microplate. The blank was used to negate any background absorbance present in the 2 x YT broth. The 96-well microplate was taken into SpectraMax ID3 (Molecular Devices, USA) and cell growth was assessed by taking optical density readings at OD_{600} at a permissive temperature of 35 ℃ for 12 hours. The same protocol was followed to assess the growth of the cells at a non-permissive of 42 ℃, in the presence of varying concentrations of colistin sulfate and pifithrin μ. Afterward, cell growth comparison was done as follows: analysis of cells treated with 0.5 % DMSO against those that received colistin sulfate and pifithrin μ treatment. The data generated was analyzed using GraphPad Prism10 software (San Diego, USA). The experiment was performed three times independently.

It was important to ascertain that *E. coli dnaK*756 cells indeed heterologously expressed DnaK, KPf and KPf-V436F. This confirmed the production of the proteins and excluded the possibility that the lack of protein function might be due to failed expression in *E. coli dnaK*756 cells. Protein expression associated with DnaK, KPf and KPf-V436F was monitored. This was done by inoculating the remaining colonies on the agar plate used for the growth assay and growing the culture. IPTG (1mM) was added to induce recombinant protein production. Cells were harvested by centrifuging at 5000 x g for 4 minutes at 4 ℃ and the pellet fraction suspended in lysis buffer (100 mM Tris-HCl, pH 7.4, 300 mM NaCl, 10 mM imidazole, 1 mM EDTA, 1mM PMSF and 1 mg/mL lysozyme). The proteins expressed were analyzed by SDS-PAGE analysis and confirmed by a Western blot.

2.6 Protein solubility studies

Molecular chaperones play a critical role in protein solubility and preventing aggregation (Edkins and Boshoff, 2021; Christensen *et al*., 2022). Inhibition of molecular chaperones tends to lead to protein aggregation, particularly during stress. Hence solubility studies were done to evaluate the solubility profiles of *E. coli dnaK*756 cells proteome after exposure to inhibitors thought to target Hsp70 function to confirm the aggregation fate of Hsp70 substrates. The following plasmids: pQE60/DnaK, pQE60/KPf and pQE60/KPf-V436F were transformed with

E. coli dnaK756, BB2362, (*dnaK756 recA::Tc*^{R} *1 pDMI,1)* cells. A colony from the transformed cells was inoculated into 10 mL 2x YT broth, containing 10 µg/mL tetracycline, 50 µg/mL kanamycin for the respective strain and 100 µg/mL ampicillin for plasmid selection. Thereafter, the culture was grown overnight at 35 °C shaking at 150 rpm using the FMH 200 (FMH Electronics, RSA) in a shaking incubator. The overnight culture was transferred into 90 mL 2 x YT broth supplemented with the necessary antibiotics. IPTG (1 mM) was added to induce recombinant protein production. The effect of colistin sulfate and pifithrin µ on *E. coli dnK*756 proteome was determined. In this experiment, colistin (0.4 µM) and pifithrin µ (5 µM) were used. The control consisted of cells grown with 0.5 % DMSO (solvent in which the inhibitors were dissolved in). Protein expression in the presence and absence of inhibitors was allowed for 12 hours at 42 ℃, while shaking at 150 rpm using FMH 200 (FMH Electronics, RSA) shaking incubtor. Afterwards, the cell culture was harvested by centrifuging at 5000 x g for 20 mins and the supernatant was discarded. The resultant pellet was resuspended in 5 mL lysis buffer (10 mM Tris-HCl, pH 7.5, 300 mM NaCl, 10 mM Imidazole, 1 mM PMSF and 1 mg/mL lysozyme). The recombinant proteins were resolved by 12 % SDS-PAGE analysis, followed by Western blot using α-PfHsp70-1 which detects the PfHsp70-1 epitope in KPf and KPf-V436F. On the other hand, α-DnaK antibodies were used to confirm DnaK protein.

Chapter 3: Results and discussion

3.1 Confirmation of plasmid DNA integrity

3.1.1 Confirmation of pQE30/PfHsp70-1

The integrity of the pQE30/PfHsp70-1 plasmid (Makumire *et al*., 2021) was confirmed by restriction digest analysis using restriction enzymes *Bam*HI and *Hind*III (Figure 3.1.1). The four bands on the lane representing uncut DNA show the various conformations of the plasmid DNA, which are relaxed circular, linear and supercoiled (Figure 3.1 B). A linearized plasmid of 5459 bp (Figure 3.1.1 B) resulted from restriction with either *Bam*HI or *Hind*III. Double restriction digest of pQE30/PfHsp70-1 with *Bam*HI and *Hind*III produced two distinct linear bands, a 2035 bp PfHsp70-1 insert and the plasmid vector at 3424 bp (Figure 3.1.1 B).

A **B**

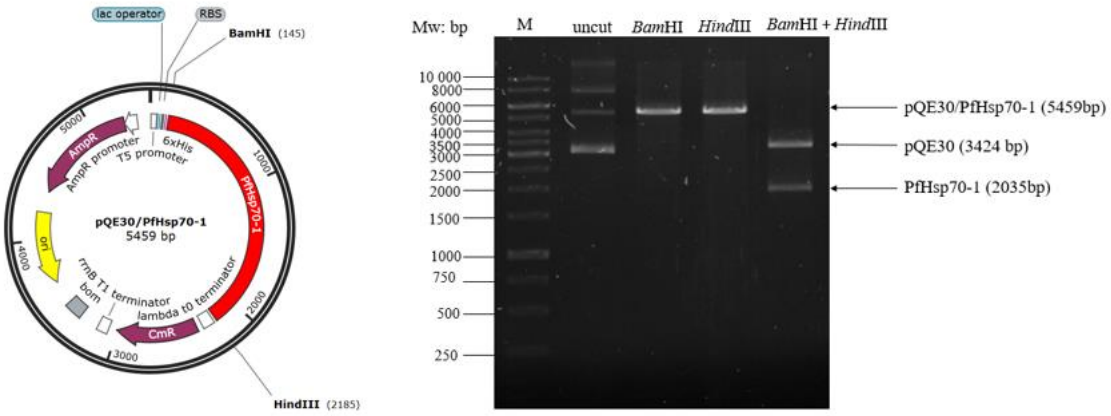

Figure 3.1.1. Restriction analysis of pQE30/PfHsp70-1.

(A) Restriction map of pQE30/PfHsp70-1 showing *Bam*HI; *Hind*III restriction sites. **(B)** Agarose gel electrophoresis of pQE30/PfHsp70-1, various lanes representing plasmid DNA, uncut and treated enzymatically are shown as follows; lane M, DNA molecular marker in bp; lane 1, uncut plasmid; lane 2, restricted with *Bam*HI; lane 3, restricted with *Hind*III; lane 4, restricted with *Bam*HI and *Hind*III.

3.1.2 Confirmation of pQE30/DnaK

Restriction digestion of pQE30/DnaK (Makumire *et al*., 2021) was carried out to verify integrity of the plasmid using *Bam*HI and *Hind*III (Figure 3.1.2). Three bands were observed in the lane where uncut DNA was loaded, representing various conformations of the plasmid which are supercoiled, relaxed circular and linear. Single restriction digest with either *Bam*HI or *Hind*III produced a linearized plasmid of 5342 bp (Figure 3.1.2 B). On the other hand, the

plasmid digested with both *Bam*HI and *Hind*III resulted in two separate bands, representing the plasmid vector (3424 bp) and the insert (1918 bp).

A **B**

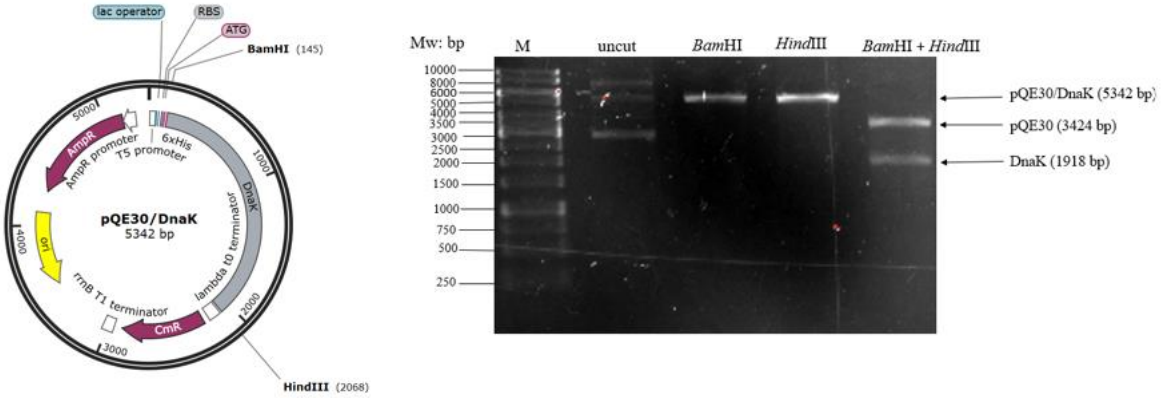

Figure 3.1.2. Restriction analysis of pQE30/DnaK plasmid DNA.

(A) Restriction map of pQE30/DnaK showing the *Bam*HI and *Hind*III restriction sites. **(B)** Agarose gel electrophoresis of pQE30/DnaK, various lanes representing plasmid DNA, uncut and treated enzymatically are shown as follows; M, DNA molecular weight marker in bp; lane1, uncut plasmid; lane2, restricted with *Bam*HI; lane3, restricted with *Hind*III; lane 4, double restriction with both *Bam*HI and *Hind*III.

3.1.3 Confirmation of pQE30/KPf

The restriction enzymes *Bam*HI and *Hind*III (Figure 3.1.3) were used to verify plasmid DNA integrity of pQE30/KPf (Makhoba *et al*., 2016). The plasmid pQE30/KPf single digestion with either *Bam*HI or *Hind*III produced a linearized plasmid of 5411 bp. Whilst restriction with both *Bam*HI and *Hind*III yielded two separate bands, the plasmid 3424 bp and the insert 1987 bp respectively.

A **B**

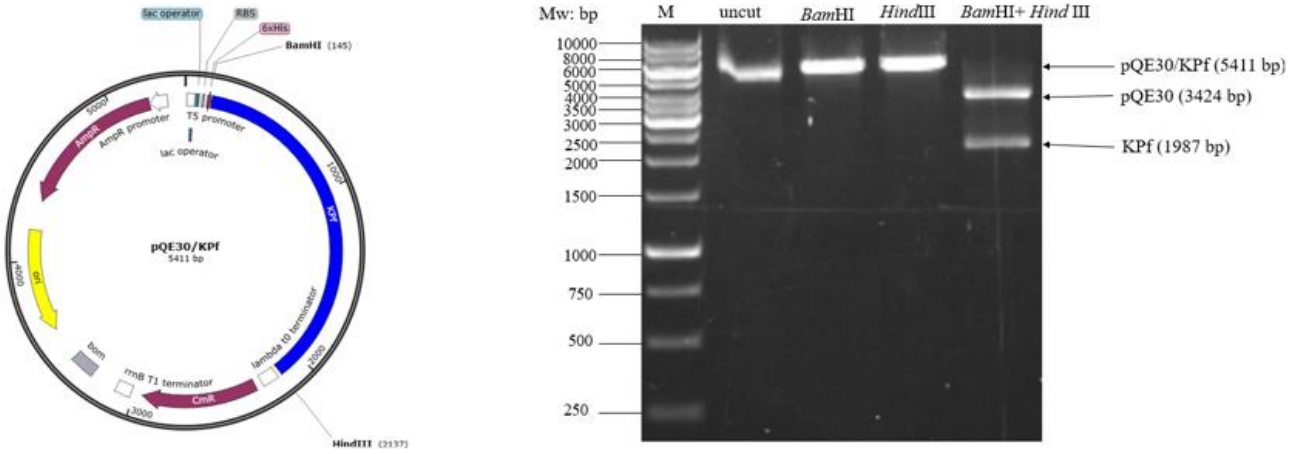

Figure 3.1.3. Restriction analysis of pQE30/KPf plasmid DNA.

(A) Restriction map of pQE30/KPf showing the *Bam*HI and *Hind*III restriction sites. **(B)** Agarose gel electrophoresis of pQE30/KPf, with various lanes representing plasmid DNA, uncut and treated enzymatically are shown as follows; lane M, molecular weight marker in bp; lane1, uncut; lane 2, restricted with *Bam*HI; lane3, restricted with *Hind*III; lane 4, double restriction with *Bam*HI and *Hind*III.

3. 2 Expression and purification of recombinant proteins

3.2.1 Expression and purification of recombinant protein PfHsp70-1

Recombinant PfHsp70-1 protein was successfully expressed in *E. coli* XL1 Blue cells transformed with the pQE30/PfHsp70-1 plasmid. The protein was analyzed using SDS-PAGE and Western blotting (Figure 3.2.1 A). The pQE30 vector plasmid was used as a negative control. As expected, no PfHsp70-1 was expressed in the control sample representing cells transformed with the pQE30 plasmid (Lane C; Figure 3.2.1 A; lower panel). Upon induction with IPTG, incremental expression of PfHsp70-1 was observed from 1- 6 hours (Figure 3.2.1 A). An N-terminal polyhis tag was present in all proteins used in this study. From 1- 6 hours, a PfHsp70-1 band was observed at 74 kDa and was confirmed by Western blot analysis using α-His and α-PfHsp70-1 antibodies (Figure 3.2.1 A; lower panel).

A **B**

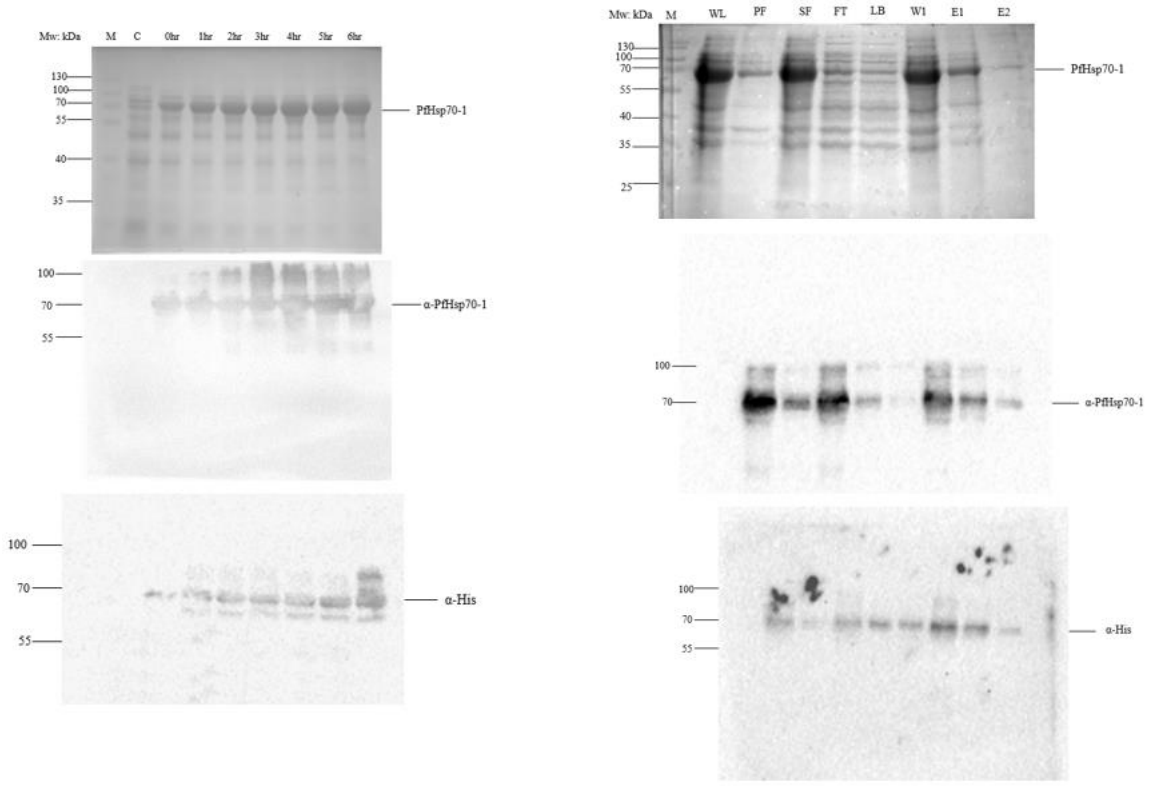

Figure 3.2.1. Expression and purification of PfHsp70-1 protein.

PfHsp70-1 was expressed in *E. coli* XL1 Blue cells transformed with pQE30/PfHsp70-1 plasmid. **(A)** SDS-PAGE analysis for the expression of PfHsp70-1. M, molecular weight marker (in kDa); C, pre-induction sample; lane 1-6, post induction with IPTG hourly samples. **(B)** Purification PfHsp70-1. WL, whole lysate sample; PF, pellet fraction; SF, supernatant; FT, flow through of non-binding proteins; W1, sample collected after washing with lysis buffer; E1- E2, protein dislodged from the beads with elution buffer. Lower panels show Western blot analysis of purification and expression using α-His and α-PfHsp70-1 antibodies.

Prior to separating the soluble fraction from the insoluble fraction, 0.1 % Triton X-100 was added to the whole lysate to maintain the recombinant protein in the soluble state. PfHsp70-1 was purified from the soluble fraction by nickel affinity chromatography. The purification was analyzed by SDS-PAGE (Figure 3.2.1 B) and confirmed by Western blot analysis using both α-His and α-PfHsp70-1 antibodies (Figure 3.2.1 B; lower panel). SDS-PAGE of PfHsp70-1 purification shows that some of the protein was lost in the flow through. However, a notable amount was successfully eluted at a yield of 7.0 mg in 1L of culture.

3.2.2 DnaK protein expression and purification

SDS-PAGE analysis reveals that the recombinant DnaK protein was successfully expressed and purified (Figure 3.2.2 A, B). DnaK was not observed in the negative control cells (pQE30) (Lane C; Figure 3.2.2 A). After inducing with IPTG, protein expression increased from 1- 6 hours (Figure 3.2.2 A). DnaK was detected as a band at approximately 70 kDa and was confirmed by Western blot using α-DnaK and α-His antibodies (Figure 3.5 A; lower band).

A **B**

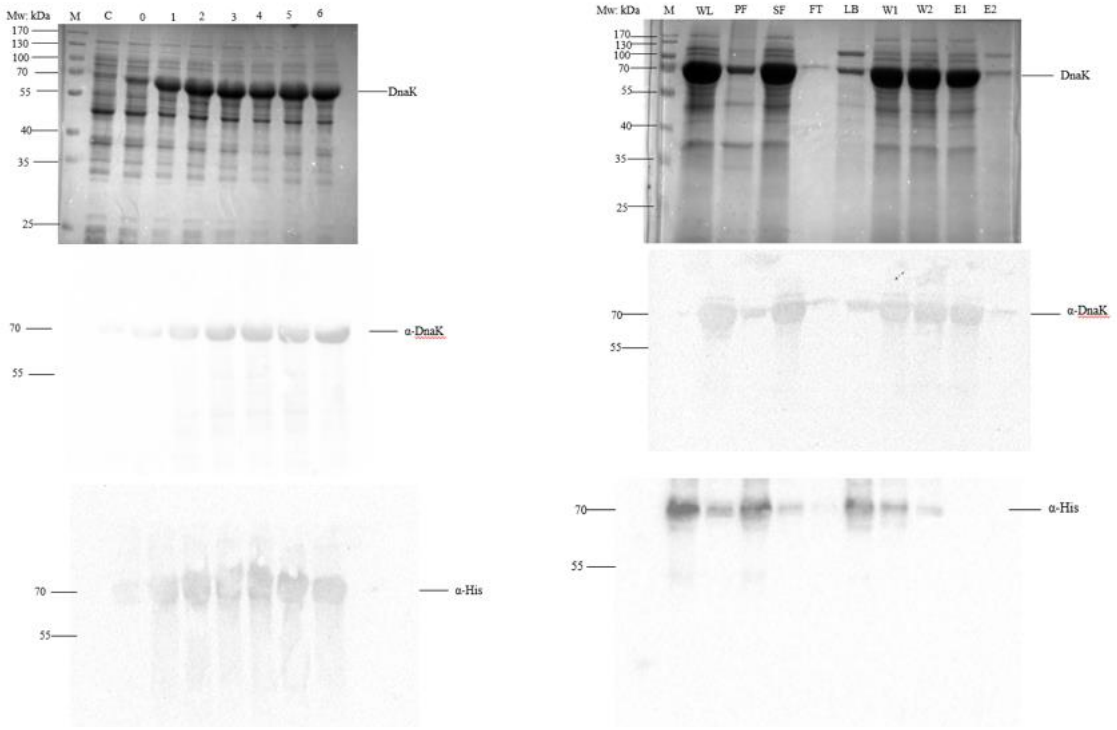

Figure 3.2.2. Analysis of the expression and purification of DnaK.
DnaK was expressed in *E. coli* XL1 Blue cells transformed with pQE30/DnaK plasmid (**A**) SDS-PAGE representing DnaK expression in *E. coli* XL1 Blue cells. Lane M, molecular weight maker (in kDa); C, pre-induction sample; lane 1-6, respective hourly samples collected after induction with IPTG. **(B)** Purification of DnaK. WL, whole lysate sample; PF, pellet fraction sample; SF, soluble fraction sample; W1-W2, wash samples; E1- E2, protein eluted with elution buffer. Lower panels, DnaK purification verified by Western blot using α-DnaK and α-His antibodies.

Purification of the protein was facilitated by the presence of an N-terminal histidine tag using nickel affinity chromatography (Figure 3.2.2 B). Prior to purification, DnaK solubility was analyzed. A prominent band was observed on the supernatant fraction compared to the pellet fraction suggesting DnaK is soluble, hence it was purified from soluble cell fraction. Notably, the protein was recovered from the elution at 9.0 mg per 1L and the yield was satisfactory

(Figure 3.2.2 B). The protein was then verified by Western blot analysis using α-DnaK and α-His antibodies (Figure 3.2.2 B; lower band).

3.2.3 Expression and purification of KPf protein

The plasmid pQE30/KPf was transformed into *E. coli* XL1 Blue cells, toward recombinant expression of the chimeric protein KPf. Protein expression was induced by 1mM IPTG at 37 ℃. The plasmid vector pQE30 was used as a negative control. As expected, the control cells transformed with pQE30 did not show KPf expression (Lane C; Figure 3.2.3 A). SDS-PAGE analysis shows a subsequent increase in KPf protein expression from 1- 6 hours, after IPTG induction (Figure 3.2.3 A). Protein expression was verified by Western blot analysis us α-PfHsp70-1 and α-His antibodies. The α-PfHsp70-1 antibody detects the PfHsp70-1 epitope in KPf, since the chimeric protein contains a substrate binding domain from PfHsp70-1. If α-DnaK antibody was used, it was going to detect endogenous DnaK in the control. Hence α-PfHsp70-1 antibody was the most suitable antibody for this experiment, as it allows differentiation between endogenous DnaK and chimeric KPf in the sample.

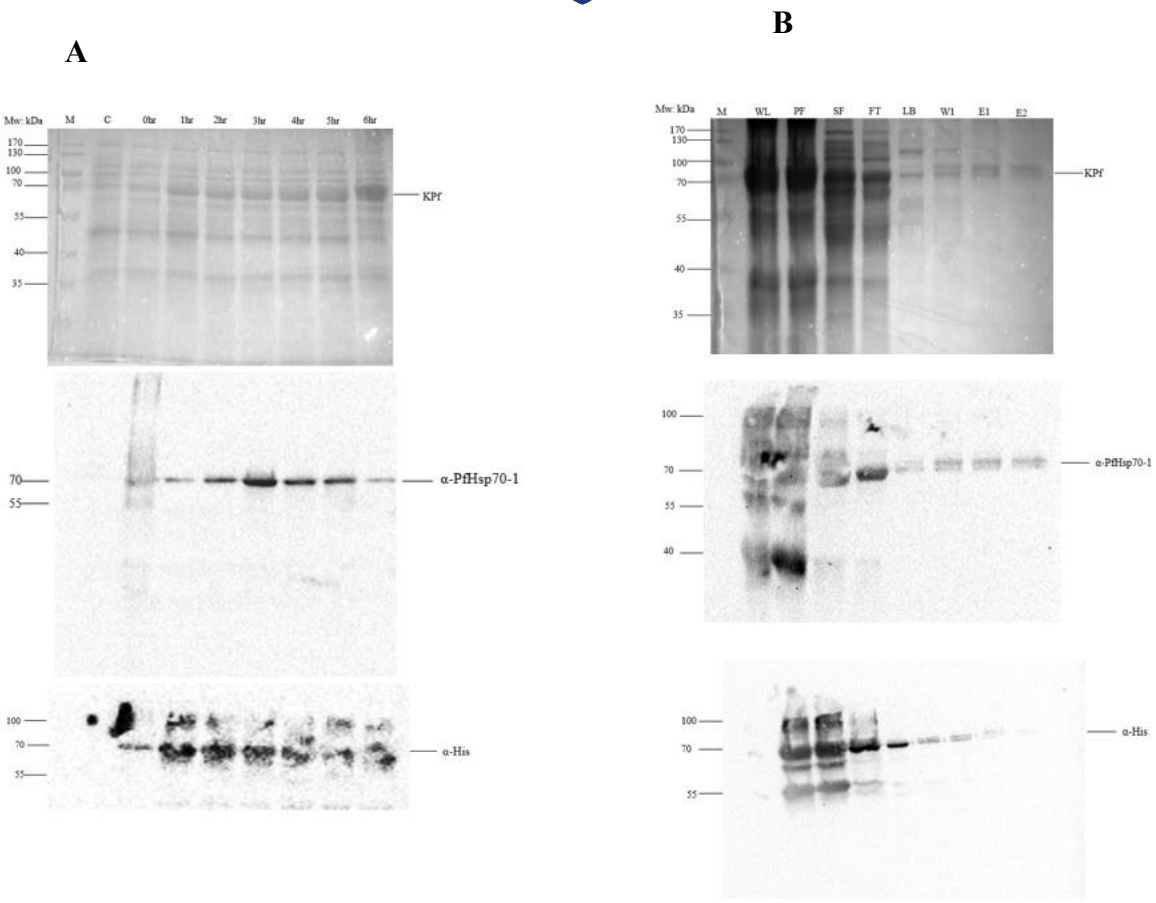

Figure 3.2.3. KPf expression and purification analysis.

KPf was expressed in *E. coli* XL1 Blue cells transformed with pQE30/KPf plasmid. **(A)** SDS-PAGE analysis of KPf expression. M, molecular weight marker (in kDa); C, pre-induction sample; 1- 6, hourly samples taken after IPTG induction. (B) KPf purification. WL, whole lysate sample; PF, pellet fraction; SF, soluble fraction; W1, wash sample; E1- E2, protein eluted from the beads with elution buffer. Lower panels, KPf expression and purification confirmation by Western blot using α-His and α-PfHsp70-1 antibodies.

Recombinant chimeric protein KPf was purified using nickel affinity chromatography (Figure 3.2.3 B) under native conditions. The resultant protein purification was assessed by SDS-PAGE (Figure 3.2.3 A). A band at approximately 70 kDa representing KPf was obtained from the elution at 3.6 mg per 1 L (Figure 3.2.3 B). A Western blot was done to validate KPf protein using α-His and α-PfHsp70-1 antibodies (Figure 3.2.3 B; lower band).

3.3 Pifithrin μ and colistin sulfate modulate the tertiary structures of PfHsp70-1, KPf and DnaK

The three-dimensional tertiary structure of Hsp70 is crucial to fulfilling its chaperone function. In addition, ligands that bind proteins tend to effect conformational changes. As such, the current study sought to investigate the effects of known chemical inhibitors (colistin sulfate and pifithrin μ) on Hsp70 (PfHsp70-1, DnaK, KPf). These conformational changes were observed as change in fluorescence emission maxima. Furthermore, they reflect on the tryptophan's intimate environment (Hellman and Scheineider, 2019). A red shift describes a phenomenon where tryptophan fluorescence emission spectrum shifts towards a longer wavelength, due to protein unfolding (Lackowicz, 2006). Whilst a blue shift refers to a shift in the tryptophan's emission spectrum to lower wavelengths, due to increased hydrophobicity of the protein (Lackowicz, 1983). PfHsp70-1 has three tryptophan residues W^{32}, W^{101} and W^{593} whilst KPf possesses W^{102} and W^{578}. On the other hand, DnaK possesses a single W^{91} residue. Tryptophan is known to emit fluoresce (Ghisaidoobe and Chung, 2014) and this forms the rationale of this assay. Previously described protocols by (Zininga *et al*., 2016; Lebepe *et al*., 2020) were used. All proteins employed in this study were standardized to a concentration of 1 μM, for comparative analysis. It should be noted that all the experiments were carried out under the following conditions: equilibrate in PBS buffer for 15 minutes at 25 ℃. The emission spectra was observed from 320- 400nm following excitation at 295 nm using the using a JASCO FP-6300 spectrofluorometer (JASCO FP, Tokyo Japan).

The tertiary structural conformation of PfHsp70-1, DnaK and KPf was determined using tryptophan fluorescence in the presence of nucleotides (5 mM ADP/ATP), inhibitors [colistin sulfate (0.4 μM, 0.6 μM, 0.8 μM) and pifithrin μ (2.5 μM, 5 μM, 10 μM)]. PfHsp70-1 and KPf both gave a maximum emission peak at 342 nm. PfHsp70-1 displayed marginal blue shifts in the presence of ADP (Figure 3.3.1 A) and slight decrease in the fluorescence intensity. In contrast, PfHsp70-1 exhibited drastic blue shift in the presence of ATP and a 50-fold decrease in the fluorescence intensity. ADP bound PfHsp70-1 gave a maximum emission peak at 340 nm and in the ATP bound state PfHsp70-1 maximum emission peak occurred at 337 nm (Figure 3.3.1 A). On the other hand, KPf bound to ADP/ATP gave drastic blue shifts with maximum emission peaks occurring at 337 nm (Figure 3.3.2 A). Introducing nucleotides led to a 50-fold increase in the tryptophan fluorescence intensity. These changes in tryptophan fluorescence emission maxima and intensity are an indication of conformational alterations to PfHsp70-1

and KPf. Although blue shifts were observed, ADP and ATP hold different effects to the proteins, when the protein is ADP bound its lid is closed and when its ATP bound, its lid is open. The effects of varying concentrations of colistin sulfate and pifithrin μ on the tertiary structure of PfHsp70-1 and KPf was investigated. The maximum tryptophan emission peak of the protein alone was the experimental control. The other control included the protein incubated with nucleotides. ADP and ATP are known to bind the nucleotide binding domain of Hsp70s subsequently inducing conformational changes, so these nucleotides were used as experimental controls to confirm conformational changes to PfHsp70-1 and KPf. When PfHsp70-1 was exposed to various concentrations of colistin sulfate, a significant blue shift in the emission peak to 336 nm from 342 nm was observed, coupled with slight changes in the fluorescence intensity. Upon exposure to pifithrin μ, PfHsp70-1 gave a maximum emission peak at 335 nm (Figure 3.3.1 B, C), coupled by a drastic 60-fold decrease in the fluorescence intensity. Following exposure to inhibitors, KPf exhibited maximum emission peak at 337 nm for colistin and 335 nm for pifithrin μ (Figure 3.3.2 B, C). Moreover, KPf displayed a 50-fold increase in the fluorescence intensity in the presence of colistin sulfate inhibitor (Figure 3.3.2 B). This suggests that pifithrin μ and colistin sulfate bind PfHsp70-1 and KPf, consequently inducing conformational changes. These observations point toward change in the local environment of tryptophan residue due to inhibitors binding to the protein, modulating its tertiary conformation, and subsequently leading to the shift in its maximum emission peak (Munishkina and Fink, 2007). In addition, pifithrin μ has been reported to bind Hsp70 (Muthelo *et al*., 2022) and colistin sulfate derivative (polymyxin B) has been reported to bind Hsp70 as well. Hence this validates the findings of this experiment. These results are consistent with those obtained by (Lebepe *et al*., 2020; Muthelo *et al*., 2022).

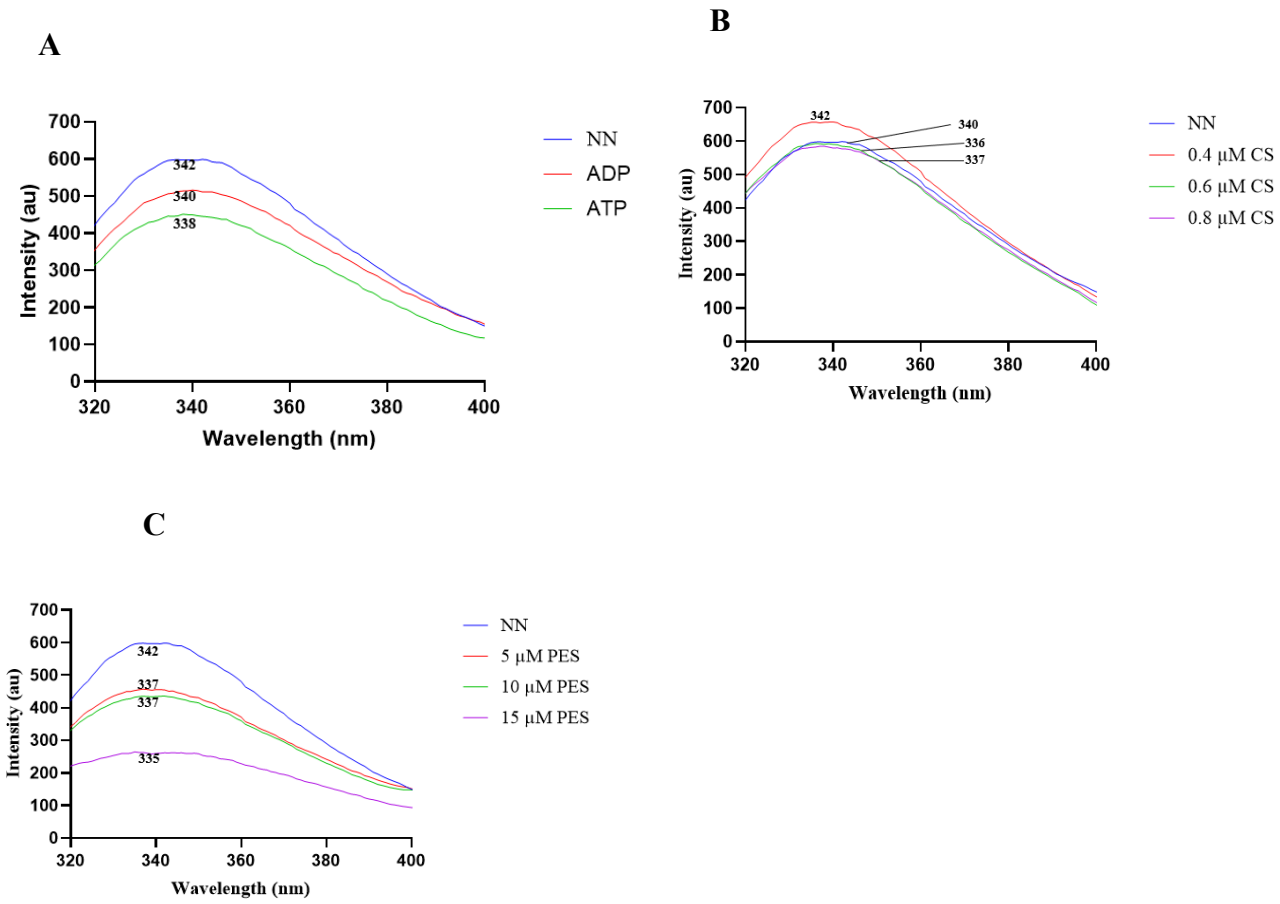

Figure 3.3.1. Analysis of the modulatory effects of colistin sulfate and pifithrin µ on the tertiary conformation of PfHsp70-1 using tryptophan fluorescence. (A) Changes in PfHsp70-1 tryptophan fluorescence emission in response to 5 mM ADP/ATP **(B)** Effects of pifithrin µ (5 µM, 10 µM, 15 µM) on PfHsp70-1 tryptophan fluorescence and **(C)** Effects of colistin sulfate (0.4 µM, 0.6 µM, 0.8 µM) on PfHsp70-1 tryptophan fluorescence. The tryptophan residues in protein were excited at 295 nm and emission was recorded between 320 nm to 400 nm.

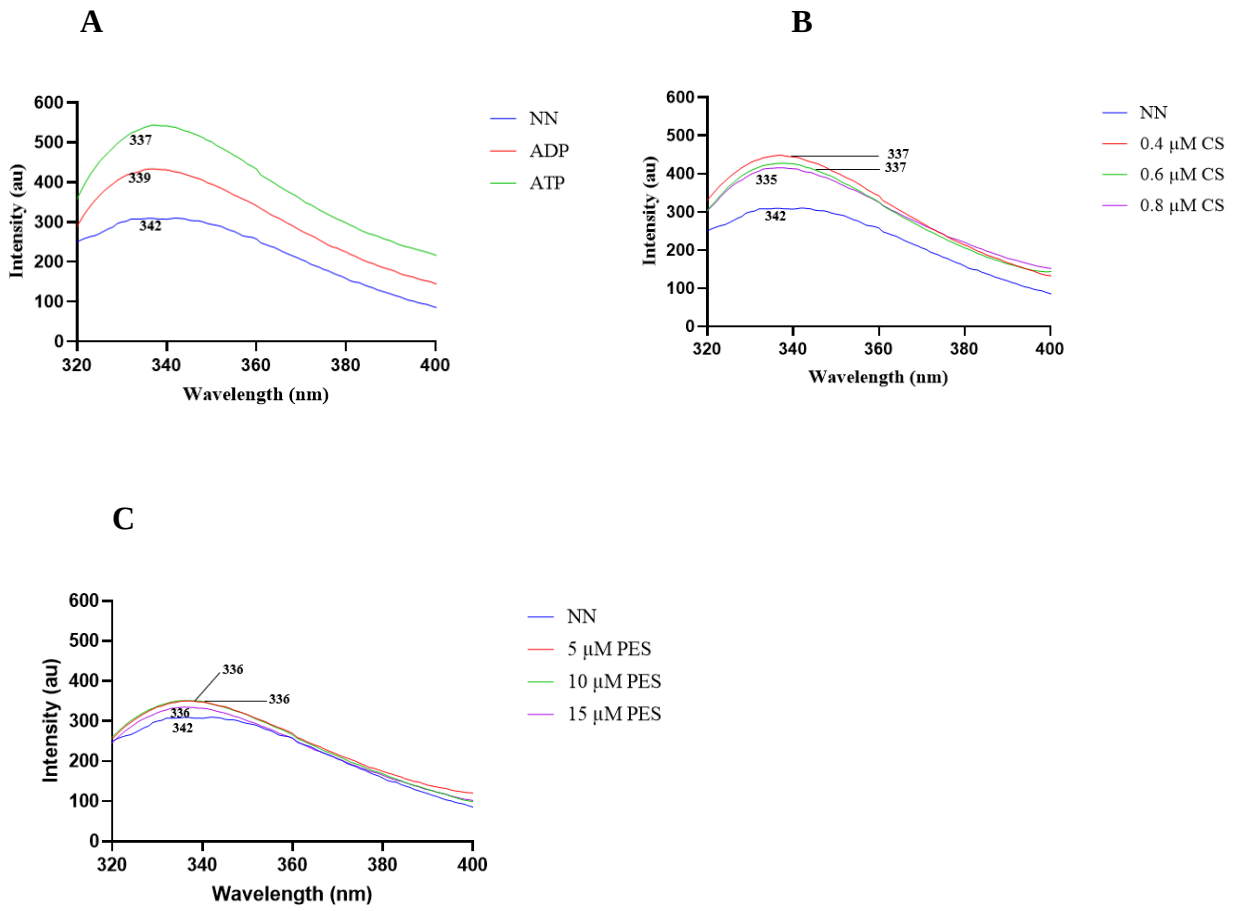

Figure 3.3.2. Assessing the tertiary conformational effects of pifithrin µ and colistin sulfate on KPf using tryptophan fluorescence (A) Changes in KPf tryptophan fluorescence emission in response to 5 mM ADP/ATP **(B)** Effects of pifithrin µ (5 µM, 10 µM, 15 µM) on KPf tryptophan fluorescence and **(C)** Effects of colistin sulfate (0.4 µM, 0.6 µM, 0.8 µM) on KPf tryptophan fluorescence. The tryptophan residues in protein were excited at 295 nm and emission was recorded between 320 nm to 400 nm.

Lastly, DnaK tryptophan fluorescence gave a maximum emission peak at 346 nm (Figure 3.3.3 A). Incubating DnaK with 5 mM ADP/ATP resulted in marginal blue shifts from 346 nm to 344 for ADP and 342 for ATP. Interestingly, a drastic 50-fold decrease in the fluorescence intensity was observed in the presence of ATP, while presence of ADP resulted in slight decrease in the fluorescence intensity as observed with PfHsp70-1. Exposing DnaK to colistin sulfate and pifithrin µ resulted in significant blue shifts at 341 nm for colistin sulfate and 344 nm for pifithrin µ (Figure 3.3.3 B, C). Likewise, DnaK gave a 50-fold decline in the fluorescence intensity in the presence of pifithrin µ, while colistin sulfate induce slight changes in the fluorescence intensity. These spectral and intensity shifts are an indication of change in the tryptophan local environment due to the inhibitors binding DnaK, inducing conformational changes. Also, the increased hydrophobicity of the protein causing blue shifts, might have led to the decrease in the fluorescence intensity of DnaK (Figure 3.3.3). Lastly, when comparing

the 3 proteins, PfHsp70-1 gave the highest fluorescence intensity as compared to KPf and DnaK. This could be attributed to the number of tryptophan residues contained by the proteins, PfHsp70-1 has the highest number which is 3. Since a protein's tertiary conformation is important for its function, inhibiting its tertiary structure could impact the protein's activity. These findings further validated the complementation assay results.

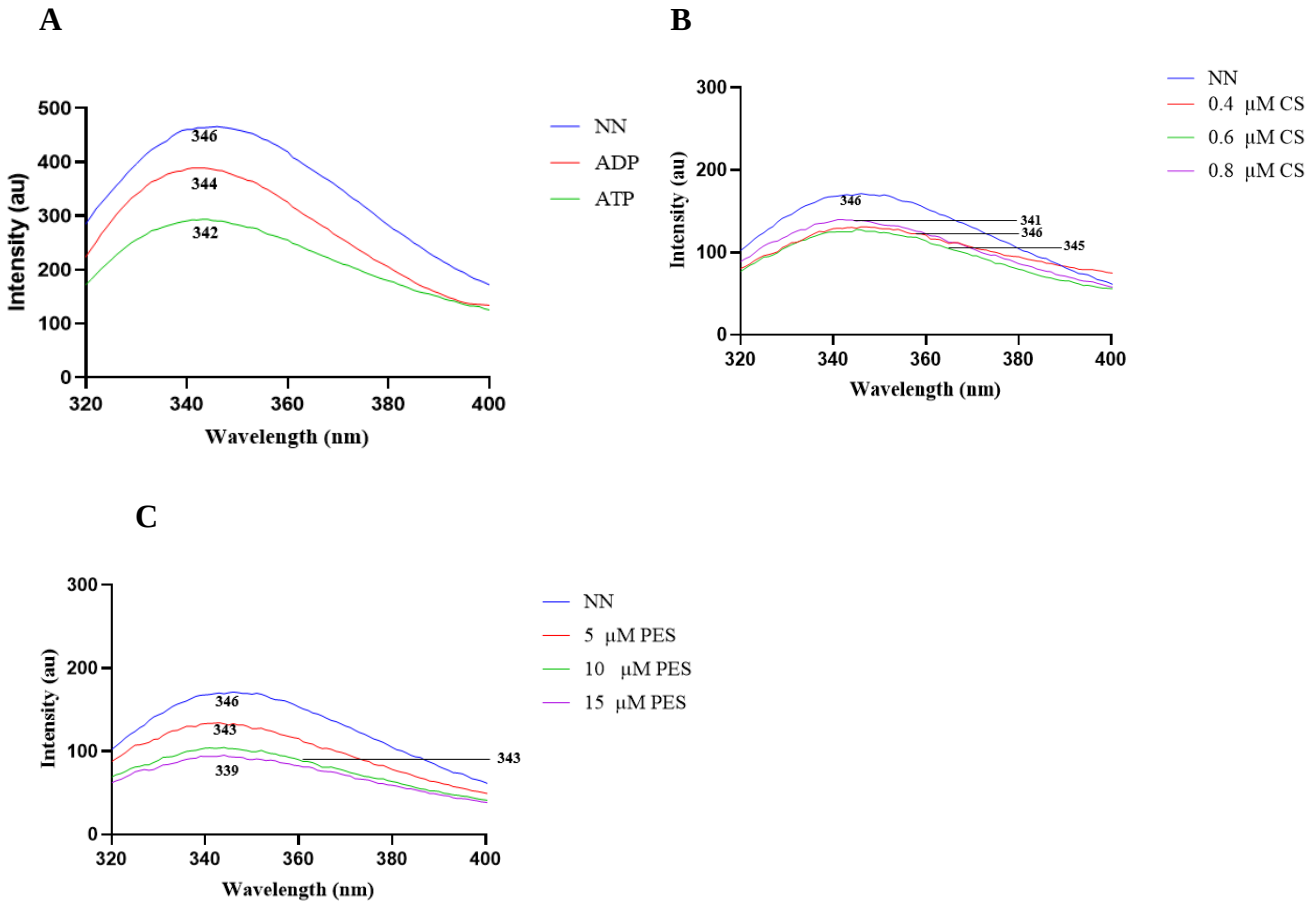

Figure 3.3.3. Determination of the effects of colistin sulfate and pifithrin µ on DnaK tertiary conformation using tryptophan fluorescence (A) Changes in DnaK tryptophan fluorescence emission in response to 5 mM ADP/ATP **(B)** Effects of pifithrin µ (5 µM, 10 µM, 15 µM) on DnaK tryptophan fluorescence and **(C)** Effects of colistin sulfate (0.4 µM, 0.6 µM, 0.8 µM) on DnaK tryptophan fluorescence. The tryptophan residues in protein were excited at 295 nm and emission was recorded between 320 nm to 400 nm.

The background interferences induced by diluting the protein with the buffer, incubating the protein with nucleotides (ADP/ATP), and exposing the protein to inhibitors (colistin sulfate and pifithrin µ) were monitored. Buffer controls were run in parallel. No significant differences in the emission spectra as well as fluorescence intensity were observed. This confirms that the nucleotides and inhibitors were indeed responsible for modulating the protein's tertiary conformation of the proteins.

3.4 Effects of colistin sulfate and pifithrin μ on *E. coli dnaK*756 cells heterologously expressing KPf and DnaK

Tryptophan spectroscopy studies show that colistin sulfate and pifithrin μ perturb the tertiary conformation of PfHsp70-1, DnaK, and KPf. These alterations could potentially lead to the loss of chaperone function by the proteins. A complementation assay was conducted to screen inhibitors targeting DnaK and KPf function to protect thermosensitive *E. coli dnaK756*, BB2362, (*dnaK756 recA::Tc*^{R} *1 pDMI,1)* cells, whose endogenous Hsp70 is functionally compromised (Georgopoulos *et al*., 1979; Tilly *et al*., 1983). Figure 1.7 (section 1.8) schematic diagram represents an overview of the complementation assay. The *E. coli dnaK*756 strain expresses a DnaK mutant protein that is functionally compromised **(**Georgopoulos *et al*., 1979; Tilly *et al*., 1983). *E. coli dnaK*756 cells are unable to grow at temperatures above 40 ℃, hence this explains why this strain was used for this assay. Previous studies have reported on the capability of DnaK and KPf to confer protection to the thermosensitive phenotype of *E. coli dnaK*756 against heat stress (Figure 1.7; Lebepe *et al*., 2020; Makumire *et al*., 2021). Hence, this provides the rationale for leveraging the capability of KPf and DnaK to protect thermosensitive *E. coli dnaK*756 cells to screen possible inhibitors of Hsp70. The main objective of this study was to develop a high throughput complementation assay to identify Hsp70 inhibitors.

It was necessary to first optimize the complementation assay, in this regard, *E. coli dnaK*756 cells were transformed with plasmids encoding DnaK, KPf, KPf-V436F and an empty vector pQE60. Firstly, it was ascertained if the cells heterologously express DnaK, KPf and KPf-V436F. These cells were then grown at a permissive temperature of 35 ℃ and non-permissive temperature of 42 ℃. Cell growth profiles were assessed by taking optical density (OD) readings hourly for 12 hours. The OD readings were then used to plot bar graphs. Cells grown with the empty vector pQE60 and cells expressing the mutant protein KPf-V436F were the negative controls of the experiment. KPf-V436F is a mutant variant of KPf with a mutated hydrophobic pocket (Makhoba *et al*., 2016). While cells heterologously expressing DnaK served as the positive control. In addition, cells heterologously expressing KPf served as the test cells since KPf harbours a substrate binding domain from PfHsp70-1 (Figure 1.5). PfHsp70-1 substrate binding domain is less conserved compared to its human counterpart (Chakafana *et al*., 2019a), hence the reason why KPf was chosen for this experiment. In the

optimization stage, an examination of the cells representing the negative control showed inability to grow at non-permissive temperature of 42 ℃ as expected (Makumire *et al*., 2021; Figure 1.7). Conversely, the cells that heterologously expressed DnaK and KPf survived the thermal stress of 42 ℃ (Makumire *et al*., 2021; Figure 1.7). However, at a permissive temperature of 35 ℃ the cells grown with pQE60 and those heterologously expressing DnaK, KPf, KPf-V436F grew normally as previously observed by (Makhoba *et al*., 2016; Makumire *et al*., 2021, Figure 3.4.1).

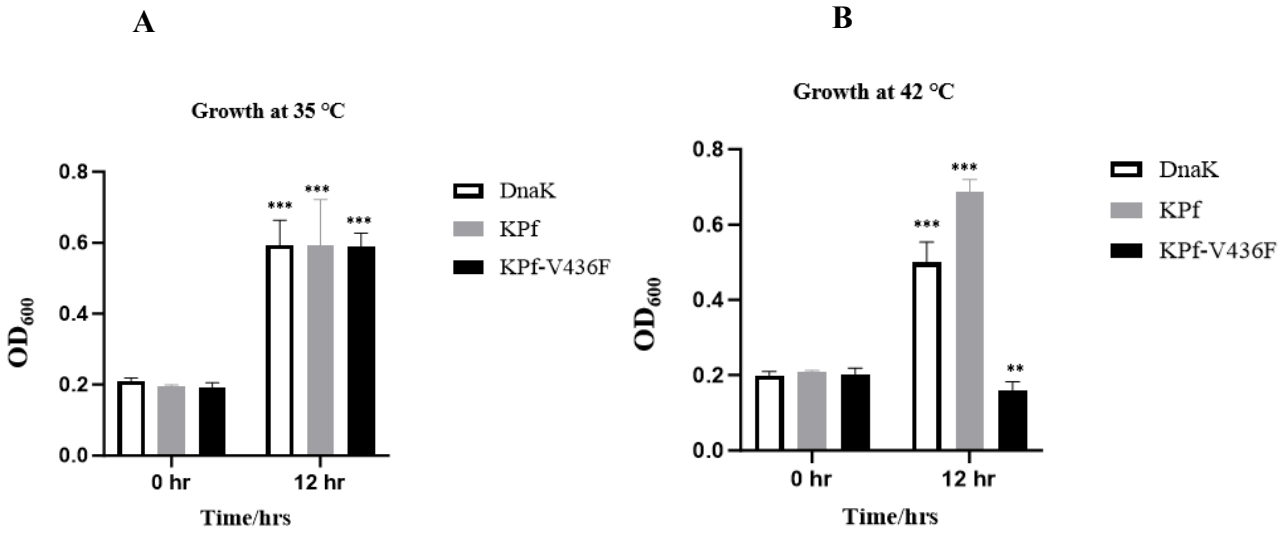

Figure 3.4.1. Cells heterologously expressing DnaK and KPf cytoprotects the thermosensitive mutant phenotype of *E. coli dnaK*756 at elevated temperatures. **(A)** *E. coli dnaK*756 heterologously expressing DnaK, KPf and KPf-V436F were grown at a permissive temperature of 35 ℃. **(B)** *E. coli dnaK*756 cells heterologously expressing DnaK, KPf, KPf-V436F were grown at a non-permissive temperature of 42 ℃. The values on the graphs represent three technical repeats and these are expressed as mean ± SD. Significantly different at $^{*}p < 0.05$, $^{**}p < 0.01$, $^{***}p < 0.0001$.

Following successful optimization (Makhoba *et al*., 2016; Makumire *et al*., 2021), the next step was to develop a high-throughput complementation assay to identify inhibitors of Hsp70. Before the assay was carried out, pilot experiments with various inhibitor concentrations were conducted. Here, inhibitor concentrations that significantly affected growth of cells heterologously expressing DnaK and KPf whilst allowing growth of negative control conditions were opted for. The experimental baseline was *E. coli dnaK*756 cells grown with 0.5 % DMSO, the solvent in which the inhibitors were dissolved in.

DnaK is not essential for *E. coli* growth under permissive conditions, but it is essential for growth during stress (non-permissive temperature) (Bukau and Walker, 1989). Firstly, the growth profile of *E. coli dnaK*756 cells expressing the mutant protein KPf-V436F was explored. KPf-V436F protein is known to be non-functional (Makhoba *et al*., 2016). At a permissive temperature of 35 ℃, cells expressing the mutant protein grew normally, this is observed as an increase in OD readings (Figure 3.4.2). The presence of inhibitors (colistin sulfate and pifithrin μ) did not seem to have adverse effects on the growth of the cells (Figure 3.4.2). However, it should be noted that at concentration of 0.6 μM- 1 μM for colistin sulfate and 15 μM for pifithrin μ, a decline in cell growth was observed. This indicates that at these concentrations, these inhibitors become cytotoxic (Figure 3.4.2). At non-permissive temperature of 42 ℃ the inhibitors (colistin sulfate and pifithrin μ) still did not exert any significant effects on the cells expressing KPf-V436F mutant protein. Cells treated with inhibitors seemed to die at the same rate relative to those grown with 0.5 % DMSO (Figure 3.4.2), suggesting that indeed the inhibitors do not have any significant effects on the mutant protein. The same observations were made for cells grown with the empty vector pQE60 (Appendix C5).

A

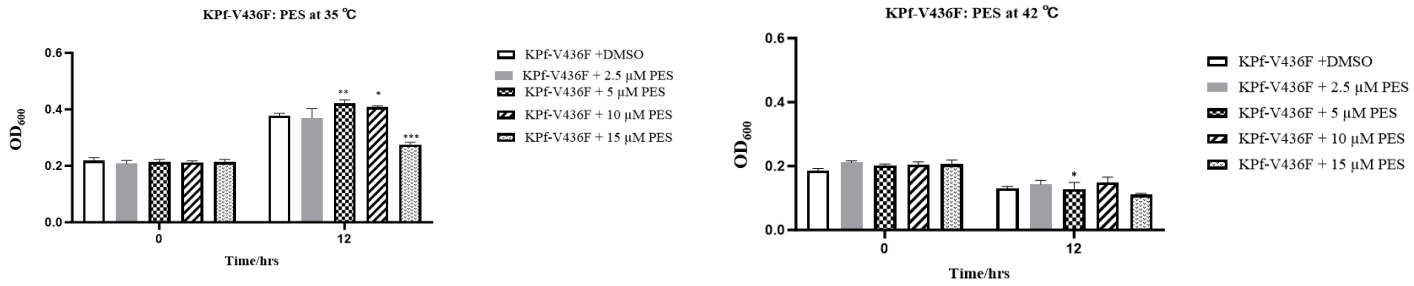

B

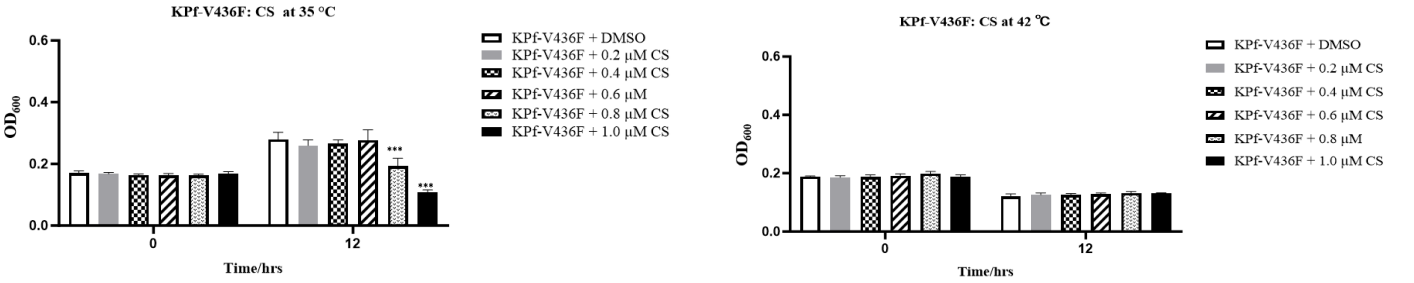

Figure 3.4.2. Pifithrin μ (PES) and colistin sulfate (CS) do not exert any significant effects on KPf-V436F expressed in *E. coli dnaK*756 cells. The figure represents outcome of the complementation assay on *E. coli dnaK*756/KPf-V436F in the presence of pifithrin μ and colistin sulfate. The bar graphs show the growth of cells over a period of 12 hours. The untreated baseline cells receive the same amount of 0.5% DMSO. The growth comparisons are shown as follows; **(A)**; cells grown at a permissive temperature of 35 ℃ and non-permissive temperatures of 42 ℃ in the presence of varying concentrations of pifithrin μ **(B)**; cells grown at a permissive temperature of 35 ℃ and non-permissive temperature of 42 ℃ in the presence of varying concentrations of colistin sulfate. The values on the graphs represent three technical repeats and these are expressed as mean ± SD Significantly different at *p < 0.05, **p < 0.01, ***p < 0.0001. Error bars indicate standard deviation.

Next, the effect of colistin sulfate and pifithrin μ on cells heterologously expressing DnaK and KPf was explored. Cells expressing KPf were the experimental test cells under investigation since the chimeric protein KPf contains a SBD from PfHsp70-1. On the other hand, cells that heterologously expressed DnaK served as the positive control of the experiment. Interestingly, the cells expressing both DnaK and KPf did not show any growth defects at permissive temperature of 35 ℃. This is evidenced by the increased OD readings of the culture compared to initial readings recorded at 0 hour time point (Figure 3.4.3; Figure 3.4.4). DnaK is not essential for *E. coli* growth at permissive temperatures (Walker and Bukau, 1989). Hence, this could explain why the cells grew uninterrupted in the presence of inhibitors at permissive temperature of 35 ℃. This could mean there was no protein to be targeted by the inhibitors. Non-permissive growth conditions at 42 ℃ present stressful conditions to the *E. coli* dnaK756 cells, promoting the expression of Hsp70s. A drastic decrease in cell growth was observed at inhibitor concentrations which allowed cell growth at permissive temperature. Although the inhibitors failed to suppress the growth of cells heterologously expressing DnaK and KPf at permissive temperature, when these cells were exposed to stress conditions (non-permissive temperature of 42 ℃), interesting observations were made. Colistin sulfate at 0.2 μM and pifithrin μ at 2.5 μM, seemed to exert drastic effects on growth cells expressing DnaK and KPf, this is shown by a notable and significant decline in growth by 50-fold (Figure 3.4.3; Figure 3.4.4). The decline in cell growth was noted relative to cells grown with 0.5 % DMSO, which showed normal growth at non-permissive temperature of 42 ℃. In the absence of inhibitor DnaK and KPf were capable of protecting the thermosensitive phenotype of *E. coli dnaK*756 mutant strain. Moreover, it proves that the reduced growth was a result of inhibitor activity against Hsp70s. This therefore suggests that colistin sulfate and pifithrin μ might have compromised the function of DnaK and KPf to confer cytoprotection to *E. coli dnaK*756 cells at elevated temperatures. Moreover, this implies that the observed 50-fold decline in cell growth is a subsequent consequence of the impaired function of DnaK and KPf to rescue the growth of thermosensitive strain. Pifithrin μ has been reported to bind SBD of Hsp70s (Muthelo *et al*., 2022) and colistin sulfate derivative polymyxin B has been reported to bind Hsp70 (Zininga *et al*., 2017a). Introducing inhibitors might have led to disruption of Hsp70 function, subsequently disrupting other cellular functions associated with Hsp70 as well. This highlights the critical role played by Hsp70 in cell survival at elevated temperatures (Walker and Bukau, 1989). Failure by Hsp70 molecular chaperone to carry out it is functions such as interacting with its client proteins, some of which are crucial for processes such as translation and transduction present detrimental effects to the cell (Mogk *et al*., 1999). Also, inhibiting the

chaperone function of Hsp70 promotes aggregation, attributed by the sensitivity of the cells to heat stress. In the context of this experiment, both colistin sulfate and pifithrin μ seemed to have effects on Hsp70s (DnaK and KPf) within a cellular milieu. Also, the findings of this experiment are consistent with those of (Makhoba *et al*., 2016; Lebepe *et al*., 2020; Makumire *et al*., 2021), further supporting the evidence that DnaK and KPf are essential for *E. coli dnaK*756 cell growth at elevated temperatures.

A

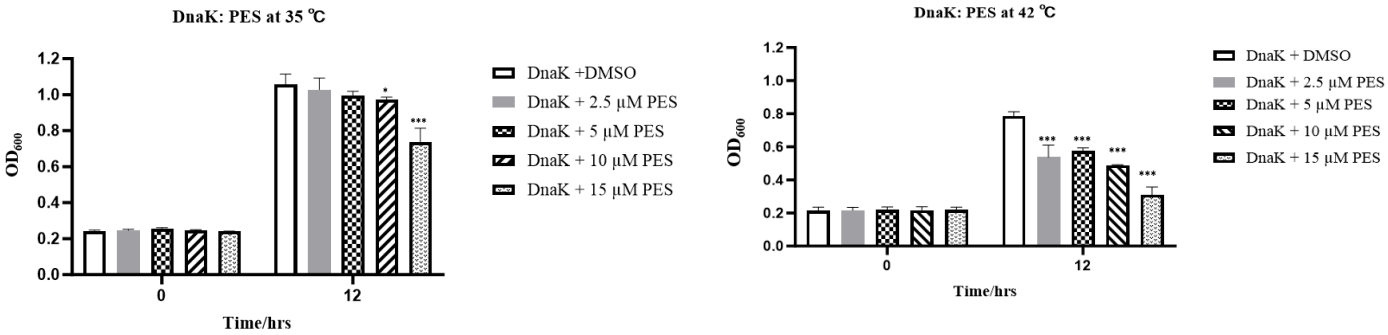

B

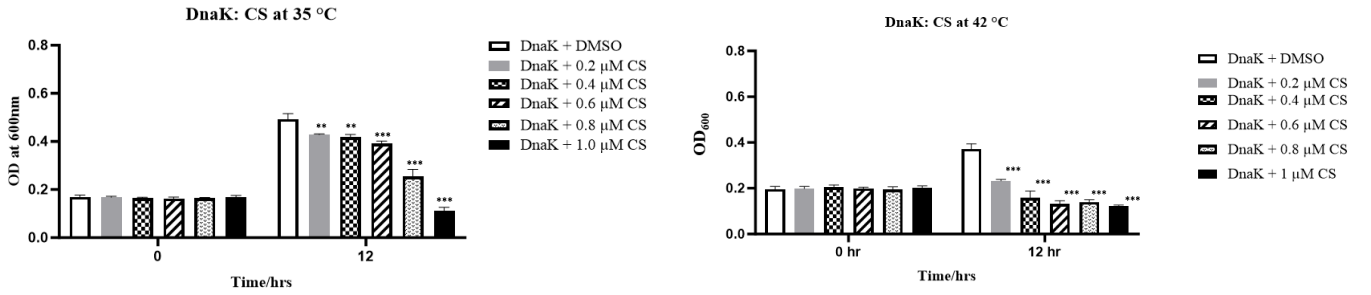

Figure 3.4.3. Pifithrin μ (PES) and colistin sulfate (CS) compromise DnaK function to cytoprotect *E. coli dnaK*756 cells. Assessment of DnaK capability to complement *E. coli dnaK*756 cells in the presence of pifithrin μ and colistin sulfate. The bar graphs represent the evaluation of growth of cells over a 12-hour period. The baseline cells are exposed to same amount of DMSO. The growth assessment encompasses comparisons for **(A)**; cells grown at a permissive temperature of 35 ℃ and non-permissive temperature of 42 ℃, in the presence of varying concentrations of pifithrin μ **(B)**; cells grown at a non-permissive temperature of 35 ℃ and non-permissive temperature of 42 ℃, with variable concentrations colistin sulfate. The values on the graphs represent three technical repeats and these are expressed as mean ± SD. Significant differences denoted by; *$p < 0.05$, **$p < 0.01$, ***$p <$ 0.0001. Error bars on the graphs indicate the standard deviation.

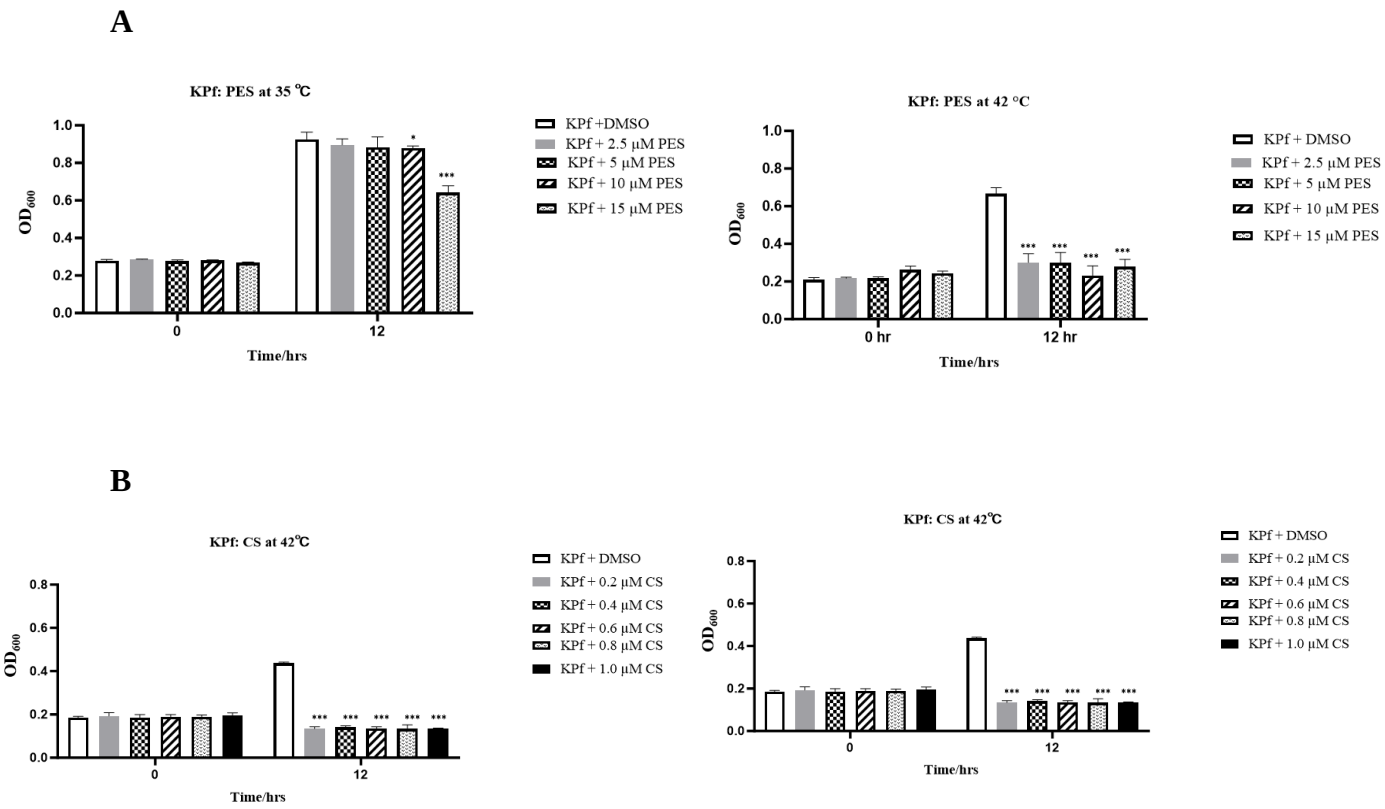

Figure 3.4.4. Pifithrin µ (PES) and colistin sulfate (CS) inhibit KPf chaperone function to cytoprotect *E. coli dnaK*756 cells. The figure represents outcome of the complementation assay on *E. coli dnaK*756/KPf in the presence of pifithrin µ and colistin sulfate. The bar graphs present growth of cells over a period of 12 hours. The baseline cells were exposed to the same amount of 0.5% DMSO. Growth comparison for: **(A)**; cells grown at a permissive temperature of 35 ℃ and non-permissive temperature of 42 ℃, in the presence of varying concentrations of pifithrin µ **(B)**; cells grown at a permissive temperature of 35 ℃ and non-permissive temperature of 42 ℃, with diverse concentrations of colistin sulfate. The values on the graphs represent three technical repeats and these are expressed as mean ± SD. Statistically significant at $^{*}p < 0.05$, $^{**}p < 0.01$, $^{***}p < 0.0001$. Error bars on the graphs signify standard deviation.

The p values obtained by Two-way analysis of variance (ANOVA) using GraphPad Prism software support the validity of this assay. The analysis showed significant differences among the different time points (0-12 hours), validating the assay's ability to track changes in cell growth over time. Furthermore, in the multiple comparison analysis where cells treated with either colistin sulfate or pifithrin µ were compared to cells treated with 0.5% DMSO, mean differences are observed. The analysis clearly underscores the effects of inhibitors on the growth of cells compared to those grown with 0.5 % DMSO. Moreover, the significant differences in the mean averages of treated cells compared to those treated with 0.5 % DMSO, further emphasize the efficacy of colistin sulfate and pifithrin µ against DnaK and KPf at non-permissive conditions. Overall, these statistical findings provide evidence supporting the reliability of the assay for investigating the effects of inhibitors on DnaK and KPf function in protecting *E. coli dnaK*756 cells. It also highlights its potential to be utilized as a screening tool

for small molecule inhibitors targeting Hsp70 function. The development of this assay was a success. This assay has shown that *E. coli* can be used as a model for screening a wide range of inhibitors to help broaden the search for novel antimalarial drugs. Also, this assay can be adapted for other Hsp70s in other diseases such as tuberculosis, and Leishmania since the strain allows the heterologous expression of exogenous Hsp70s.

IC_{50} value represent the quantity of a small molecule inhibitor required to inhibit a biological or biochemical process (Aykul and Martinez-Hackert, 2016). In this study, the IC_{50} values are used as metrics to determine the potency of colistin sulfate and pifithrin μ. These inhibitors are evaluated for their capability to inhibit the function of DnaK and KPf to cytoprotect the thermosensitive *E. coli dnaK*756 mutant phenotype. IC_{50} values are determined to reflect the potency of inhibitors against a target (Neubig *et al*., 2003). In this study, a time point in which the cells are in their logarithmic phase (6^{th} hour) was selected for IC_{50} calculations. Dose-response curves were generated when calculating IC_{50} values using the GraphPad Prism10 software (San Diego, USA). These curves represent percentage inhibition against the concentration of the inhibitor. Colistin sulfate treatment showed remarkable potency, with IC_{50} values of 0.219 μM for DnaK and 0.07 μM for KPf (Table 3.1). Whilst IC_{50} values for PES were found to be 14.48 μM for DnaK and 10.41 μM for KPf. Owing to its lower IC_{50} values, colistin sulfate was found to be more effective. However, both inhibitors are generally desirable compounds since they function in the micromolar range.

3.5 Pifithrin μ and colistin sulfate promote aggregation and reduces chaperone-client interactions in *E. coli dnaK*756 proteome

In cellulo complementation results show the viability of using the assay as a robust tool for screening Hsp70 small molecule inhibitors, which have the potential to compromise their function. However, this approach can be problematic due to the difficulty in linking Hsp70 inhibition to a specific phenotype. Therefore, it was necessary to validate the results through solubility studies, to ascertain whether Hsp70 inhibition indeed led to growth defects observed in (Figure 3.4.4). When proteins are exposed to heat stress, they tend to misfold and aggregate (Morimoto *et al*., 1944, Howrich and Weissman, 1997). To mitigate such damaging effects, molecular chaperones form the central defense system in refolding misfolded proteins, preventing aggregation and mediating degradation of misfolded proteins (Bukau, 1999; Edkins

and Boshoff, 2021). Inhibition of molecular chaperones tends to lead to protein aggregation, particularly during stress. Hence solubility studies were done to evaluate the solubility profiles of *E. coli dnaK*756 proteome following exposure to inhibitors thought to target Hsp70 function and to confirm the aggregation fate of Hsp70 substrates.

Solubility status of *E. coli dnaK*756 proteome was analyzed. Cells heterologously expressing DnaK, KPf and KPf-V436F were subjected to 10 µM pifithrin µ and 0.4 µM colistin sulfate treatment at 42 ℃. After 12 hours, the cell cultures were harvested by centrifugation and the lysates were prepared. The cells were lysed with lysis buffer (100 mM Tris-HCl, pH 7.5, 300 mM NaCl, 10 Mm imidazole, 1 mM EDTA, 1mM PMSF and 1mg/mL lysozyme), and expression was analyzed by SDS-PAGE. Protein expression confirmation was done by employing Western blot analysis. Control cells expressed with DMSO did not exhibit aggregation, suggesting that DnaK and KPf interacted with their client proteins, and carried out their protein folding and refolding duties normally. However, introducing colistin sulfate (0.4 µM) and pifithrin µ (10 µM) seemed to promote aggregation of *E. coli dnaK*756 proteome. This is evidenced by the accumulation of pronounced bands in the pellet fraction (Lane 4; Figure 3.5 A; Figure 3.5 B), suggesting that the presence of inhibitors compromised DnaK and KPf capacity to interact with their substrates and this promoted aggregation. Hsp70 is the central hub of cell proteostasis, and it has an essential role in substrate refolding misfolded and preventing their aggregation (Kohler and Andreasson, 2020). Hsp70 inhibition impairs the propensity of the chaperone to bind its clients, this causes them to misfold and misfolded proteins tend to aggregate (Dugaard *et al*., 2017). Hence this could explain the aggregation observed in (Figure 3.5 A; Figure 3.5 B). Presence of inhibitors promoted aggregation of Hsp70 (DnaK/KPf) substrates, this was observed as accumulation of thick bands in the insoluble cell faction (pellet fraction) (Lane 4; Figure 3.5 A; Figure 3.5 B). Hsp70 chaperone activity requires coordination with proteasome pathways, which is involved in protein turnover and disposal. The pathway prevents accumulation of misfolded and aggregated proteins in the cell and inhibition decreases the cellular proteasome activity, hence accumulation of misfolded proteins (Leu *et al*., 2014). Furthermore, introducing the inhibitor interfered with expression of some proteins in lane 4 and lane 6, this is evidenced by disappearance of some protein bands (Figure 3.5 A; Figure 3.5 B). Reflecting on impairment in cellular proteostasis.

In addition, presence of inhibitors seemed to have an influence on the abundance protein produced, there was a decrease in the amount of KPf protein in the soluble fraction (Lane 6, Figure 3.5 B). KPf might have been complexed with some of its substrates in the pellet fraction hence the absence of the band at around 70 kDa. These findings coincide with those obtained by (Leu *et al*., 2011) where they found that pifithrin μ disrupts interaction of Hsp70 with its substrates and co-chaperones.

Most importantly, these results further confirmed the complementation assay findings observed in (Figure 3.4.3; Figure 3.4.4), further proving that the observed growth defects were attributed to Hsp70 functional compromise and impaired proteostasis. Moreover, these results highlight the important role played by molecular chaperones in protein homeostasis and the consequences of protein inhibition. The cells heterologously expressing the non-functional mutant protein KPf-V436F showed pronounced aggregation during thermal stress, in the presence and absence of inhibitors (Appendix C6). This is attributed to the mutant protein's lack of functionality during stress (non-permissive temperature of 42 ℃) (Makhoba *et al*., 2016), rendering it incapable of suppressing protein aggregation. Hence, the observed aggregation (Appendix C6).

A

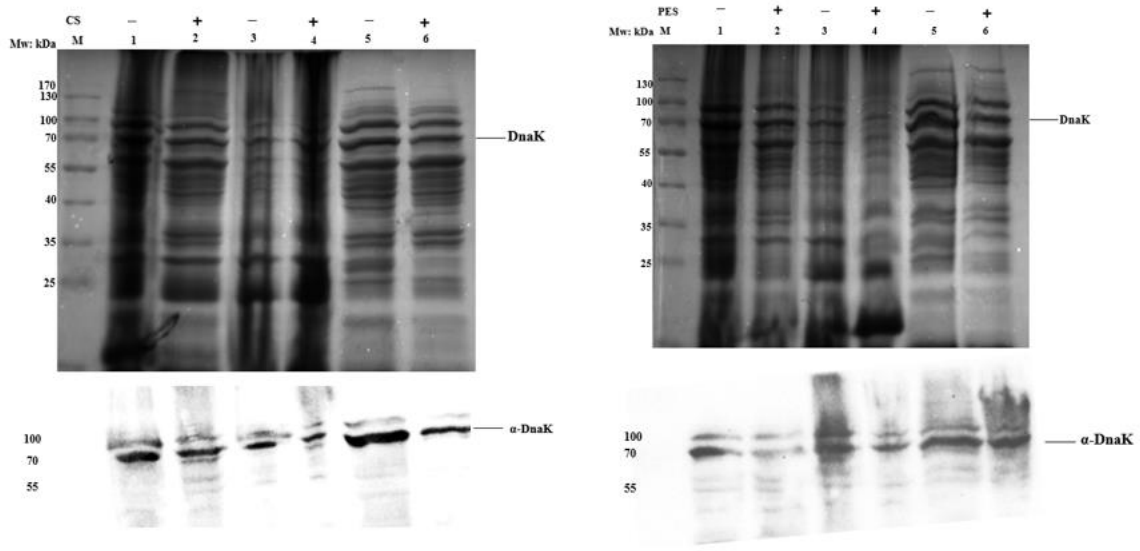

Figure 3.5 A. Fate of *E. coli dnaK*756 proteome. Cells were cultured with indicated doses of pifithrin μ and colistin sulfate. The control cells were grown with DMSO. The cells were grown at 42 ℃ for 12 hours. Protein expression of recombinant proteins was examined using SDS-PAGE and Western blot analysis. M, molecular weight marker in kDa; Lane 1, control whole lysate sample; Lane 2, whole lysate sample treated with either pifithrin μ/colistin sulfate; Lane 3, control pellet fraction; Lane 4, pellet fraction sample treated with pifithrin μ and colistin sulfate; Lane 5, control soluble fraction sample; Lane 6, soluble fraction sample treated with pifithrin μ/ colistin sulfate.

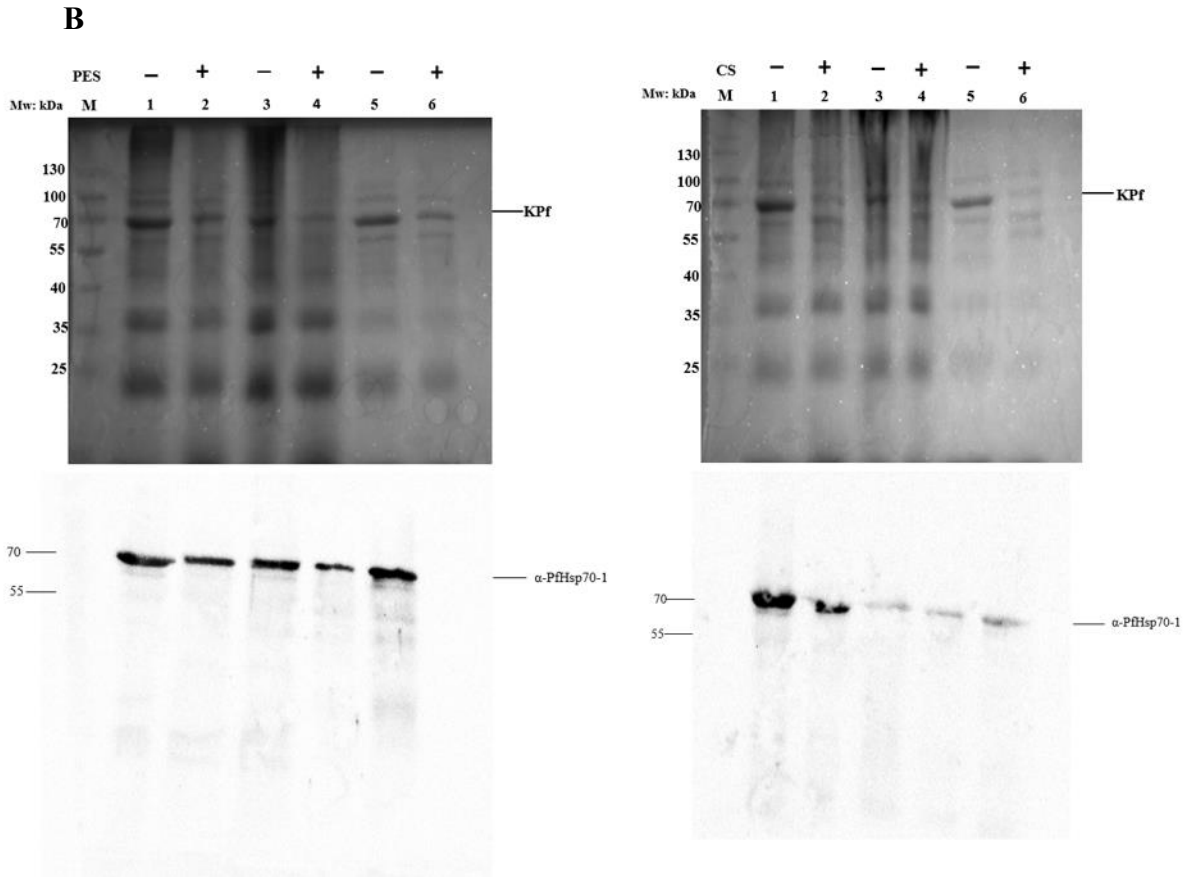

Figure 3.5.B. Fate of *E. coli dnaK*756 proteome. Cells were cultured with indicated doses of pifithrin μ and colistin sulfate. The control cells were grown with DMSO. The cells were grown at 42 ℃ for 12 hours. Protein expression of recombinant proteins was examined using SDS-PAGE and Western blot analysis. M, molecular weight marker in kDa; Lane 1, control whole lysate sample; Lane 2, whole lysate sample treated with either pifithrin μ/colistin sulfate; Lane 3, control pellet fraction; Lane 4, pellet fraction sample treated with pifithrin μ and colistin sulfate; Lane 5, control soluble fraction sample; Lane 6, soluble fraction sample treated with pifithrin μ/ colistin sulfate.

Conclusions and recommendations

PfHsp70-1 has been shown to be essential for parasite survival and development within the human host, targeting its function through inhibition could affect the survival of *P. falciparum*. Findings from this study show the possibility to use an *E. coli*-based complementation assay to screen for PfHsp70-1 inhibitors. Furthermore, this assay offers a simple and cost-effective screening tool for inhibitors with antimalarial activity. Moreover, the *in cellulo* complementation assay offers alternatives to *in vitro* assays for analysing protein function (Slabaugh *et al*., 2014b). The microorganism used for the study *E. coli,* is an extensively studied microorganism that offers several advantages for investigating Hsp70 chaperone function. Its genome is well studied, and it facilitates cost-effective experimentation (Taj *et al*., 2014; Tungekar *et al*., 2021). This assay can be adopted for other disease models such as tuberculosis. However, further in *vitro* and *in vivo* assays in *P. falciparum* itself need to be done to further prove the specificity and efficiency of the identified small molecule inhibitors.

Since KPf looks at the substrate binding domain of PfHsp70-1, future studies should consider replicating the complementation assay using the chimeric protein featuring PfHsp70-1 nucleotide binding domain. Though the nucleotide binding domain of PfHsp70-1 is more conserved, it would be interesting to conduct this assay to check if valuable divergences will be observed.

References

Achan, J., Talisuna, A.O., Erhart, A., Yeka, A., Tibenderana, J.K., Baliraine, F.N., Rosenthal, P.J. and D'Alessandro, U. (2011). Quinine, an old anti-malarial drug in a modern world: role in the treatment of malaria. *Malaria Journal*. **10**: 1-12.

Acharya, P., Kumar, R. and Tatu, U. (2007). Chaperoning a cellular upheaval in malaria: heat shock proteins in *Plasmodium falciparum*. *Molecular and Biochemical Parasitology*. **153**: 85-94.

Akbar, S.M., Sreeramulu, K. and Sharma, H.C. (2016). Tryptophan fluorescence quenching as a binding assay to monitor protein conformation changes in the membrane of intact mitochondria. *Journal of Bioenergetics and Biomembranes*. **48**: 241-247.

Akide-Ndunge, O.B., Tambini, E., Giribaldi, G., McMillan, P.J., Müller, S., Arese, P. and Turrini, F. (2009). Co-ordinated stage-dependent enhancement of *Plasmodium falciparum* antioxidant enzymes and heat shock protein expression in parasites growing in oxidatively stressed or G6PD-deficient red blood cells. *Malaria Journal*. **8**: 1-15.

Alkmim Teixeira, R., Borba, E.F., Pedrosa, A., Nishioka, S., Viana, V.S., Ramires, J.A., Kalil-Filho, R., Bonfá, E. and Martinelli Filho, M. (2014). Evidence for cardiac safety and antiarrhythmic potential of chloroquine in systemic lupus erythematosus. *Europace*.**16**: 887-892.

Amino, R., Thiberge, S., Martin, B., Celli, S., Shorte, S., Frischknecht, F. and Ménard, R. (2006). Quantitative imaging of *Plasmodium* transmission from mosquito to mammal. *Nature Medicine*. **12**: 220-224.

Anas, M., Shukla, A., Tripathi, A., Kumari, V., Prakash, C., Nag, P., Kumar, L.S., Sharma, S.K., Ramachandran, R. and Kumar, N. (2020). Structural–functional diversity of malaria parasite's PfHSP70-1 and PfHSP40 chaperone pair gives an edge over human orthologs in chaperone-assisted protein folding. *Biochemical Journal*. **477**: 3625-3643.

Antony, H.A. and Parija, S.C. (2016). Antimalarial drug resistance: An overview. *Tropical Parasitology*. **6**: 30.

Aykul, S. and Martinez-Hackert, E. (2016). Determination of half-maximal inhibitory concentration using biosensor-based protein interaction analysis. *Analytical Biochemistry*. **508**: 97-103.

Baker, T.A., Grossman, A.D. and Gross, C.A. (1984). A gene regulating the heat shock response in *Escherichia coli* also affects proteolysis. *Proceedings of the National Academy of Sciences*.**21**:6779- 6783.

Bakthisaran, R., Tangirala, R. and Rao, C.M. (2015). Small heat shock proteins: role in cellular functions and pathology. *Biochimicia et Biophysia Acta* (BBA)-*Proteins and Proteomics*. **1854**: 291- 319.

Bailly, C. (2021). Pyronaridine: An update of its pharmacological activities and mechanisms of action. *Biopolymers*, **112**: e23398.

Balaburski, G.M., Leu, J.I.J., Beeharry, N., Hayik, S., Andrake, M.D., Zhang, G., Herlyn, M., Villanueva, J., Dunbrack Jr, R.L., Yen, T. and George, D.L. (2013). A modified HSP70 inhibitor shows broad activity as an anticancer agent. *Molecular Cancer Research*. **11**: 219-229.

Bannister, L.H. and Sherman, I.W. (2009). *Plasmodium*. Encyclopaedia of life sciences (ELS). *Chichester: John Wiley & Sons, Ltd*.

Bao, Y.P., Cook, L.J., O'Donovan, D., Uyama, E. and Rubinsztein, D.C. (2002). Mammalian, yeast, bacterial, and chemical chaperones reduce aggregate formation and death in a cell model of oculopharyngeal muscular dystrophy. *Journal of Biological Chemistry*. **277**: 12263-12269.

Belete, T.M. (2020). Recent progress in the development of new antimalarial drugs with novel targets. *Drug Design, Development and Therapy*. 3875-3889.

Bell, S.L., Chiang, A.N. and Brodsky, J.L. (2011). Expression of a malarial Hsp70 improves defects in chaperone-dependent activities in ssa1 mutant yeast. *PLoS ONE*. **6**: e20047.

Bergen, P.J., Li, J., Rayner, C.R. and Nation, R.L. (2006). Colistin methane sulfonate is an inactive prodrug of colistin against *Pseudomonas Aeruginosa*. *Antimicrobial Agents and Chemotherapy*. **50**: 1953-1958.

Bertelsen, E.B., Chang, L., Gestwicki, J.E. and Zuiderweg, E.R. (2009). Solution conformation of wild-type *E. coli* Hsp70 (DnaK) chaperone complexed with ADP and substrate. *Proceedings of the National Academy of Sciences*. **106**: 8471-8476.

Billker, O., Lindo, V., Panico, M., Etienne, A.E., Paxton, T., Dell, A., Rogers, M., Sinden, R.E. and Morris, H.R. (1998). Identification of xanthurenic acid as the putative inducer of malaria development in the mosquito. *Nature*. **392**: 289-292.

Blaszczak, E., Lazarewicz, N., Sudevan, A., Wysocki, R. and Rabut, G. (2021). Protein-fragment complementation assays for large-scale analysis of protein–protein interactions. *Biochemical Society Transactions*. **49**: 1337-1348.

Botha, M., Chiang, A.N., Needham, P.G., Stephens, L.L., Hoppe, H.C., Külzer, S., Przyborski, J.M., Lingelbach, K., Wipf, P., Brodsky, J.L. and Shonhai, A. (2011). *Plasmodium falciparum* encodes a single cytosolic type I Hsp40 that functionally interacts with Hsp70 and is upregulated by heat shock. *Cell Stress and Chaperones*. **16**: 389-401.

Botha, M., Pesce, E.R. and Blatch, G.L. (2007). The Hsp40 proteins of *Plasmodium falciparum* and other Apicomplexa: regulating chaperone power in the parasite and the host. *The International Journal of Biochemistry & Cell Biology*. **39**: 1781-1803.

Bozdech, Z., Llinás, M., Pulliam, B.L., Wong, E.D., Zhu, J. and DeRisi, J.L. (2003). The transcriptome of the intraerythrocytic developmental cycle of *Plasmodium falciparum*. *PLoS Biology*. **1**: e5.

Bradford, M.M. (1976). A rapid and sensitive method for the quantitation of microgram quantities of protein utilizing the principle of protein-dye binding. *Analytical Biochemistry*.**72**: 248-254.

Brune, M., Hunter, J.L., Corrie, J.E. and Webb, M.R. (1994). Direct, real-time measurement of rapid inorganic phosphate release using a novel fluorescent probe and its application to actomyosin subfragment 1 ATPase. *Biochemistry*. **33**: 8262-8271.

Buchberger, A., Gässler, C.S., Büttner, M., McMacken, R. and Bukau, B. (1999). Functional Defects of the DnaK756 Mutant Chaperone of *Escherichia coli* Indicate Distinct Roles for Amino-and Carboxyl-terminal Residues in Substrate and Co-chaperone Interaction and Interdomain Communication. *Journal of Biological Chemistry*. **274**: 38017-38026.

Buchner, J. and Li, J. (2013). Structure, function and regulation of the Hsp90 machinery. *Biomedical Journal*. **36**: 106.

Bullock, W. (1987). XL1-blue: a high efficiency plasmid transforming recA *Escherichia coli* strain with beta-ga-galactosidase selection. *BioTechniques*. **5**: 376.

Burkholder, W.F., Panagiotidis, C.A., Silverstein, S.J., Cegielska, A., Gottesman, M.E. and Gaitanaris, G.A. (1994). Isolation and characterization of an *Escherichia coli* DnaK mutant with impaired ATPase activity. *Journal of Molecular Biology*. **242**: 364-377.

Bukau, B., Deuerling, E., Pfund, C. and Craig, E.A. (2000). Getting newly synthesized proteins into shape. *Cell*. **101**: 119-122.

Bakau, B. (1999). *Molecular Chaperones and Folding Catalysts: Regulation, Cellular Functions and Mechanisms*. CRC Press.

Bukau, B. and Walker, G.C. (1989). Cellular defects caused by deletion of the *Escherichia coli dnaK* gene indicate roles for heat shock protein in normal metabolism. *Journal of Bacteriology*. **171**: 2337-2346.

Calabrese, V., Cornelius, C., Cuzzocrea, S., Iavicoli, I., Rizzarelli, E. and Calabrese, E.J. (2011). Hormesis, cellular stress response and vitagenes as critical determinants in aging and longevity. *Molecular Aspects of Medicine*. **32**: 279-304.

Calabrese, V., Cornelius, C., Dinkova-Kostova, A.T., Calabrese, E.J. and Mattson, M.P. (2010). Cellular stress responses, the hormesis paradigm, and vitagenes: novel targets for therapeutic intervention in neurodegenerative disorders. *Antioxidants & Redox Signalling*. **13**: 1763-1811.

Centres for Disease Control and Prevention. Malaria transmission. https://www.cdc.gov/malaria/about/us/_transmission. Accessed 19/04/2024.

Chakafana, G., Zininga, T. and Shonhai, A. (2019a). Comparative structure-function features of Hsp70s of *Plasmodium falciparum* and human origins. *Biophysical reviews*. **11**: 591-602.

Chakafana, G., Zininga, T. and Shonhai, A. (2019b) The link that binds: the linker of Hsp70 as a helm of the protein's function. *Biomolecules.* **9***:* 543.

Charnaud, S.C., Dixon, M.W., Nie, C.Q., Chappell, L., Sanders, P.R., Nebl, T., Hanssen, E., Berriman, M., Chan, J.A., Blanch, A.J. and Beeson, J.G. (2017). The exported chaperone

Hsp70-x supports virulence functions for *Plasmodium falciparum* blood stage parasites. *PloS One*. **12**: e0181656.

Chatterjee, N. and Walker, G.C. (2017). Mechanisms of DNA damage, repair, and mutagenesis. *Environmental and Molecular Mutagenesis*. **5**: 235-263.

Chen, Y., Murillo-Solano, C., Kirkpatrick, M.G., Antoshchenko, T., Park, H.W. and Pizarro, J.C. (2018). Repurposing drugs to target the malaria parasite unfolding protein response. *Scientific Reports*. **8**: 10333.

Chen, J., Ren, J., Gu, G., Wang, G., Wu, X., Yan, D., Liu, S. and Li, J. (2013). Crohn's disease and polymorphism of heat shock protein gene HSP 70-2 in the Chinese population. *Journal of Gastroenterology and Hepatology*. **28**: 814-818.

Chora, Â.F., Mota, M.M. and Prudêncio, M. (2022). The reciprocal influence of the liver and blood stages of the malaria parasite's life cycle. *International Journal for Parasitology*. **52**: 711-715.

Christensen, S., Rämisch, S. and André, I. (2022). DnaK response to expression of protein mutants is dependent on translation rate and stability. *Communications Biology*. **5**: 597.

Clark, M.S. and Peck, L.S. (2009). Triggers of the HSP70 stress response: environmental responses and laboratory manipulation in an Antarctic marine invertebrate (Nacella concinna). *Cell Stress and Chaperones*. **6**: 649-660

Cobb, D.W., Florentin, A., Fierro, M.A., Krakowiak, M., Moore, J.M. and Muralidharan, V. (2017). The exported chaperone PfHsp70x is dispensable for the *Plasmodium falciparum* intraerythrocytic life cycle. *MSphere*. **2**: 10-1128.

Cockburn, I.L., Boshoff, A., Pesce, E.R. and Blatch, G.L. (2014). Selective modulation of plasmodial Hsp70s by small molecules with antimalarial activity. *Biological Chemistry*. **395**: 1353-1362.

Cockburn, I.L., Pesce, E.R., Pryzborski, J.M., Davies-Coleman, M.T., Clark, P.G., Keyzers, R.A., Stephens, L.L. and Blatch, G.L. (2011). Screening for small molecule modulators of Hsp70 chaperone activity using protein aggregation suppression assays: inhibition of the plasmodial chaperone PfHsp70-1. *Biological Chemistry*. **392**: 431- 438.

Conrad, M.D. and Rosenthal, P.J. (2019). Antimalarial drug resistance in Africa: the calm before the storm? *The Lancet Infectious Diseases*. **19**: e338-e351.

Cowman, A.F., Healer, J., Marapana, D. and Marsh, K. (2016). Malaria: biology and disease. *Cell*. **167**: 610-624.

Cowman, A.F., Galatis, D. and Thompson, J.K. (1994). Selection for mefloquine resistance in *Plasmodium falciparum* is linked to amplification of the *pfmdr*1 gene and cross-resistance to halofantrine and quinine. *Proceedings of the National Academy of Sciences*. **91**: 1143-1147.

Craig, E.A., Gambill, B.D. and Nelson, R.J. (1993). Heat shock proteins: molecular chaperones of protein biogenesis. *Microbiological Reviews*. **2**: 402- 414

Cunico, W., Carvalho, S.A., Gomes, C.R. and Marques, G.H. (2008). Antimalarial drugs - history and perspectives. *Brazilian Journal of Pharmacy*. **89**: 49-55.

Curtis, C.F., Maxwell, C.A., Magesa, S.M., Rwegoshora, R.T. and Wilkes, T.J. (2006). Insecticide-treated bed-nets for malaria mosquito control. *Journal of the American Mosquito Control Association*. **22**: 501-506.

Cyr, D.M. and Ramos, C.H. (2015). Specification of Hsp70 function by type I and type II Hsp40. In the networking of chaperones by co-chaperones: Control of cellular protein homeostasis; Blatch, G.L., Edkins, A.L., Eds; Springer: Switzerland, pp 99-102.

Dagen, M. (2020). History of malaria and its treatment. In Antimalarial agents; Graham, P.L; Eds; Elsevier, pp. 1-48.

Daniyan, M.O. and Blatch, G.L. (2017). Plasmodial Hsp40s: new avenues for antimalarial drug discovery. *Current Pharmaceutical Design*. **23**: 4555-4570.

Daniyan, M.O., Przyborski, J.M. and Shonhai, A. (2019). Partners in mischief: functional networks of heat shock proteins of *Plasmodium falciparum* and their influence on parasite virulence. *Biomolecules*. **9**: 295.

Daugaard, M., Rohde, M. and Jäättelä, M. (2007). The heat shock protein 70 family: Highly homologous proteins with overlapping and distinct functions. *FEBS letters*. **581**: 3702-3710.

De Maio, A., Santoro, M.G., Tanguay, R.M. and Hightower, L.E. (2012). Ferruccio Ritossa's scientific legacy 50 years after his discovery of the heat shock response: a new view of biology, a new society, and a new journal. *Cell Stress and Chaperones*. **17**: 139-143.

Dhingra, S.K., Redhi, D., Combrinck, J.M., Yeo, T., Okombo, J., Henrich, P.P., Cowell, A.N., Gupta, P., Stegman, M.L., Hoke, J.M. and Cooper, R.A. (2017). A variant PfCRT isoform can contribute to *Plasmodium falciparum* resistance to the first-line partner drug piperaquine. *MBio*. **8**: 10-1128.

Dhingra, S.K., Small-Saunders, J.L., Ménard, D. and Fidock, D.A. (2019). *Plasmodium falciparum* resistance to piperaquine driven by PfCRT. *The Lancet Infectious Diseases*. **19**: 1168-1169.

Djimde, A.A., Doumbo, O.K., Traore, O., Guindo, A.B., Kayentao, K., Diourte, Y., Niare-Doumbo, S., Coulibaly, D., Kone, A.K., Cissoko, Y. and Tekete, M. (2003). Clearance of drug-resistant parasites as a model for protective immunity in *Plasmodium falciparum* malaria. *American Journal of Tropical Medicine and Hygiene*. **69**:558.

Dongola, T.H. (2022). *In cellulo* biophysical exploration of the role of GGMP residues in Hsp70. MSc Thesis, University of Venda.

Dutta, T., Pesce, E.R., Maier, A.G. and Blatch, G.L. (2021a). Role of the J Domain Protein Family in the Survival and Pathogenesis of *Plasmodium falciparum*. In Heat Shock Proteins of Malaria; Shonhai, A., Picard, D., Blatch, G., Eds.; Springer: Switzerland, pp 97- 123.

Dutta, T., Singh, H., Gestwicki, J.E. and Blatch, G.L. (2021b). Exported plasmodial J domain protein, PFE0055c, and PfHsp70-x form a specific co-chaperone-chaperone partnership. *Cell Stress and Chaperones*. **26**: 355-366.

Easton, D.P., Kaneko, Y. and Subjeck, J.R. (2000). The Hsp110 and Grp170 stress proteins: newly recognized relatives of the Hsp70s. *Cell Stress & Chaperones*. **5**: 276.

Ecker, A., Lehane, A.M., Clain, J. and Fidock, D.A. (2012). PfCRT and its role in antimalarial drug resistance. *Trends in Parasitology*. **28**: 504-514.

Edkins, A.L. and Boshoff, A. (2021). General structural and functional features of molecular chaperones. In Heat Shock Proteins of Malaria; Shonhai, In Heat Shock Proteins of Malaria; Shonhai, A., Picard, D., Blatch, G.L., Eds, Springer: Switzerland, pp 11-73.

Falagas, M.E., Kasiakou, S.K. and Saravolatz, L.D. (2005). Colistin: the revival of polymyxins for the management of multidrug-resistant gram-negative bacterial infections. *Clinical Infectious Diseases*. **40**: 1333-1341.

Fan, C.Y., Lee, S., Ren, H.Y. and Cyr, D.M. (2004). Exchangeable chaperone modules contribute to specification of type I and type II Hsp40 cellular function. *Molecular Biology of the Cell*. **15**: 761-773.

Fenton, W.A., Kashi, Y., Furtak, K. and Norwich, A.L. (1994). Residues in chaperonin GroEL required for polypeptide binding and release. *Nature*. **371**: 614-619.

Fidock, D.A., Nomura, T., Talley, A.K., Cooper, R.A., Dzekunov, S.M., Ferdig, M.T., Ursos, L.M., Naudé, B., Deitsch, K.W., Su, X.Z. and Wootton, J.C. (2000). Mutations in the *P. falciparum* digestive vacuole transmembrane protein PfCRT and evidence for their role in chloroquine resistance. *Molecular Cell*. **6**: 861-871.

Fitch, C.D. (2004). Ferriprotoporphyrin IX, phospholipids, and the antimalarial actions of quinoline drugs. *Life Sciences*. **74**: 1957-1972.

Flaherty, K.M., DeLuca-Flaherty, C. and McKay, D.B. (1990). Three-dimensional structure of the ATPase fragment of a 70K heat-shock cognate protein. *Nature*. **346**: 623-628.

Gallardo-Godoy, A., Muldoon, C., Becker, B., Elliott, A.G., Lash, L.H., Huang, J.X., Butler, M.S., Pelingon, R., Kavanagh, A.M., Ramu, S. and Phetsang, W. (2016). Activity and predicted nephrotoxicity of synthetic antibiotics based on polymyxin B. *Journal of Medicinal Chemistry*. **59**: 1068-1077.

Garrido, C., Gurbuxani, S., Ravagnan, L. and Kroemer, G. (2001). Heat shock proteins: endogenous modulators of apoptotic cell death. *Biochemical and Biophysical Research Communications*. **286**: 433-442.

Genevaux, P., Wawrzynow, A., Zylicz, M., Georgopoulos, C. and Kelley, W.L. (2001). DjlA is a third DnaK co-chaperone of Escherichia coli, and DjlA-mediated induction of colanic acid capsule requires DjlA-DnaK interaction. *Journal of Biological Chemistry*. **276**: 7906-7912.

Georgopoulos, C.P., Lam, B., Lundquist-Heil, A., Rudolph, C.F., Yochem, J. and Feiss, M. (1979). Identification of the *E. coli dnaK* (groPC756) gene product. *Molecular and General Genetics MGG*. **172**: 143-149.

Ghisaidoobe, A.B. and Chung, S.J. (2014). Intrinsic tryptophan fluorescence in the detection and analysis of proteins: a focus on Förster resonance energy transfer techniques. *International journal of molecular sciences*. **15**: 22518-22538.

Greenwood, B.M., Fidock, D.A., Kyle, D.E., Kappe, S.H., Alonso, P.L., Collins, F.H. and Duffy, P.E. (2008). Malaria: progress, perils, and prospects for eradication. *The Journal of Clinical Investigation*. **118**: 1266-1276.

Gupta, B.D. and Sharma, A.K. (2005). Sensitivity evaluation of a multi-layered surface plasmon resonance-based fiber optic sensor: a theoretical study. *Sensors and Actuators B: Chemical*. **107**: 40-46.

Gusev, N.B., Bogatcheva, N.V. and Marston, S.B. (2002). Structure and properties of small heat shock proteins (sHsp) and their interaction with cytoskeleton proteins. *Biochemistry (Moscow)*. **67**: 511-519.

Haldar, K., Murphy, S.C., Milner Jr, D.A. and Taylor, T.E. (2007). Malaria: mechanisms of erythrocytic infection and pathological correlates of severe disease. *Annual Review of Pathology: Mechanisms of Disease.* **2**: 217-249.

Hartl, F.U. (1996). Molecular chaperones in cellular protein folding. *Nature*. **381**: 571-580.

Hartl, F.U. and Hayer-Hartl, M. (2002). Molecular chaperones in the cytosol: from nascent chain to folded protein. *Science*. **295**: 1852-1858.

Hartl, F.U. and Hayer-Hartl, M. (2009). Converging concepts of protein folding *in vitro* and *in vivo*. *Nature Structural & Molecular Biology*.**6**: 574-581.

Hartl, F.U., Bracher, A. and Hayer-Hartl, M. (2011). Molecular chaperones in protein folding and proteostasis. *Nature*.**7356**: 324-332.

Haslbeck, M. and Vierling, E. (2015). A first line of stress defense: small heat shock proteins and their function in protein homeostasis. *Journal of Molecular Biology*. **427**: 1537-1548.

Hatherley, R., Blatch, G.L. and Bishop, Ö.T. (2014). *Plasmodium falciparum* Hsp70-x: a heat shock protein at the host–parasite interface. *Journal of Biomolecular Structure and Dynamics*. **32**: 1766-1779.

Hayes, S.A. and Dice, J.F. (1996). Roles of molecular chaperones in protein degradation. *The Journal of Cell Biology*. **3**: 255-258.

Hellmann, N. and Schneider, D. (2019). Hands on: Using tryptophan fluorescence spectroscopy to study protein structure. In Protein Supersecondary Structures: Methods in Molecular Biology; Kister, A., Eds; Humana Press, New York, USA, pp.379-401.

Hennessy, F., Boshoff, A. and Blatch, G.L. (2005). Rational mutagenesis of a 40 kDa heat shock protein from *Agrobacterium tumefaciens* identifies amino acid residues critical to its *in vivo* function. *The International Journal of Biochemistry & Cell Biology*. **37**: 177-191.

Horwich, A.L. and Weissman, J.S. (1997). Deadly conformations—protein misfolding in prion disease. *Cell*. **89**: 499-510.

Hu, C., Yang, J., Qi, Z., Wu, H., Wang, B., Zou, F., Mei, H., Liu, J., Wang, W. and Liu, Q. (2022). Heat shock proteins: Biological functions, pathological roles, and therapeutic opportunities. *MedComm*. **3**: e161.

Johnston, D.M., Miot, M., Hoskins, J.R., Wickner, S. and Doyle, S.M. (2017). Substrate discrimination by ClpB and Hsp104. *Frontiers in Molecular Biosciences*. **4**: 36.

Kampinga, H.H., Andreasson, C., Barducci, A., Cheetham, M.E., Cyr, D., Emanuelsson, C., Genevaux, P., Gestwicki, J.E., Goloubinoff, P., Huerta-Cepas, J. and Kirstein, J. (2019). Function, evolution, and structure of J-domain proteins. *Cell Stress and Chaperones*. **24**: 7-15.

Kampinga, H.H. and Craig, E.A., (2010). The HSP70 chaperone machinery: J proteins as drivers of functional specificity. *Nature reviews Molecular cell biology*. **11**: 579-592.

Kayamba, F., Malimabe, T., Ademola, I.K., Pooe, O.J., Kushwaha, N.D., Mahlalela, M., van Zyl, R.L., Gordon, M., Mudau, P.T., Zininga, T. and Shonhai, A. (2021). Design and synthesis of quinoline-pyrimidine inspired hybrids as potential plasmodial inhibitors. *European Journal of Medicinal Chemistry*. **217**: 113330.

Kayentao, K., Garner, P., van Eijk, A.M., Naidoo, I., Roper, C., Mulokozi, A., MacArthur, J.R., Luntamo, M., Ashorn, P., Doumbo, O.K. and ter Kuile, F.O. (2013). Intermittent preventive

therapy for malaria during pregnancy using 2 vs 3 or more doses of sulfadoxine-pyrimethamine and risk of low birth weight in Africa: systematic review and meta-analysis. *Jama*. **309**: 594-604.

Kiaco, K., Teixeira, J., Machado, M., Do Rosário, V. and Lopes, D. (2015). Evaluation of artemether-lumefantrine efficacy in the treatment of uncomplicated malaria and its association with *pfmdr1*, pfatpase6, and K13-propeller polymorphisms in Luanda, Angola. *Malaria Journal*. **14**: 1-10.

Kityk, R. and Mayer, M.P. (2018). Hsp70-substrate interactions. In Heat shock proteins in the Immune System; Binder, R., Srivastava, P., Eds; Springer, Cham, pp.3-20.

Kublin, J.G., Cortese, J.F., Njunju, E.M., G. Mukadam, R.A., Wirima, J.J., Kazembe, P.N., Djimdé, A.A., Kouriba, B., Taylor, T.E. and Plowe, C.V. (2003). Reemergence of chloroquine-sensitive *Plasmodium falciparum* malaria after cessation of chloroquine use in Malawi. *The Journal of Infectious Diseases*. **187**: 1870-1875.

Kumar, S., Bhardwaj, T.R., Prasad, D.N. and Singh, R.K. (2018). Drug targets for resistant malaria: historic to future perspectives. *Biomedicine & Pharmacotherapy*. **104**: 8-27.

Külzer, S., Charnaud, S., Dagan, T., Riedel, J., Mandal, P., Pesce, E.R., Blatch, G.L., Crabb, B.S., Gilson, P.R. and Przyborski, J.M. (2012). *Plasmodium falciparum*-encoded exported hsp70/hsp40 chaperone/co-chaperone complexes within the host erythrocyte. *Cellular Microbiology*. **14**: 1784-1795.

Kohler, V. and Andréasson, C. (2020). Hsp70-mediated quality control: should I stay or should I go?. *Biological Chemistry*. **401**: 1233-1248.

Komura, S. and Kurahashi, K. (1979). Partial purification and properties of L-2, 4-aminobutyric acid activating enzyme from a polymyxin E producing organism. *The Journal of Biochemistry*. **86**: 1013-1021.

Kudyba, H.M., Cobb, D.W., Fierro, M.A., Florentin, A., Ljolje, D., Singh, B., Lucchi, N.W. and Muralidharan, V. (2019). The endoplasmic reticulum chaperone PfGRP170 is essential for asexual development and is linked to stress response in malaria parasites. *Cellular Microbiology*. **21**: e13042.

Külzer, S., Charnaud, S., Dagan, T., Riedel, J., Mandal, P., Pesce, E.R., Blatch, G.L., Crabb, B.S., Gilson, P.R. and Przyborski, J.M. (2012). *Plasmodium falciparum*-encoded exported hsp70/hsp40 chaperone/co-chaperone complexes within the host erythrocyte. *Cellular Microbiology*. **14**: 1784-1795.

Kumar, D.P., Vorvis, C., Sarbeng, E.B., Ledesma, V.C.C., Willis, J.E. and Liu, Q. (2011). The four hydrophobic residues on the Hsp70 inter-domain linker have two distinct roles. *Journal of Molecular Biology*. **411**: 1099-1113.

Kumar, S., Bhardwaj, T.R., Prasad, D.N. and Singh, R.K. (2018). Drug targets for resistant malaria: historic to future perspectives. *Biomedicine & Pharmacotherapy*. **104**: 8-27.

Lackowicz, J.R. (2006). Principles of Fluorescence Spectroscopy. *Springer Science & Business Media.* **13**: 978-980.

Lakowicz, J.R., Maliwal, B., Cherek, H. and Balter, A. (1983). Rotational freedom of tryptophan residues in proteins and peptides. *Biochemistry*. **22**: 1741-1752.

Langer, T., Lu, C., Echols, H., Flanagan, J., Hayer, M.K. and Hartl, F.U. (1992). Successive action of DnaK, DnaJ and GroEL along the pathway of chaperone-mediated protein folding. *Nature*. **356**: 683-689.

Lebepe, C.M., Matambanadzo, P.R., Makhoba, X.H., Achilonu, I., Zininga, T. and Shonhai, A. (2020). Comparative characterization of *Plasmodium falciparum* Hsp70-1 relative to *E. coli* DnaK reveals the functional specificity of the parasite chaperone. *Biomolecules*. **10**: 856.

Lee-Yoon, D., Easton, D., Murawski, M., Burd, R. and Subjeck, J.R. (1995). Identification of a major subfamily of large hsp70-like proteins through the cloning of the mammalian 110-kDa heat shock protein. *Journal of Biological Chemistry*. **270**: 15725-15733.

Leite, F.H.A., Fonseca, A., Nunes, R.R., Júnior, M.C., Varotti, F.P. and Taranto, A.G. (2013). Malaria: from old drugs to new molecular targets. *BBR*. **2**: 59-76.

Leu, J.J., Pimkina, J., Frank, A., Murphy, M.E. and George, D.L. (2009). A small molecule inhibitor of inducible heat shock protein 70. *Molecular cell*. **36**: 15-27.

Leu, J.I.J., Pimkina, J., Pandey, P., Murphy, M.E. and George, D.L. (2011). HSP70 inhibition by the small-molecule 2-phenylethynesulfonamide impairs protein clearance pathways in tumor cells. *Molecular Cancer Research*. **9**: 936-947.

Leu, J.I.J., Zhang, P., Murphy, M.E., Marmorstein, R. and George, D.L. (2014). Structural basis for the inhibition of HSP70 and DnaK chaperones by small-molecule targeting of a C-terminal allosteric pocket. *ACS Chemical Biology*. **9**:2508-2516.

Liberek, K., Marszalek, J., Ang, D., Georgopoulos, C. and Zylicz, M. (1991). *Escherichia coli* DnaJ and GrpE heat shock proteins jointly stimulate ATPase activity of DnaK. *Proceedings of the National Academy of Sciences*. **88**: 2874-2878.

Mabate, B., Zininga, T., Ramatsui, L., Makumire, S., Achilonu, I., Dirr, H.W. and Shonhai, A., (2018). Structural and biochemical characterization of Plasmodium falciparum Hsp70-x reveals functional versatility of its C-terminal EEVN motif. *Proteins: Structure, Function, and Bioinformatics*. **86**: 1189-1201.

Macošek, J., Mas, G. and Hiller, S. (2021). Redefining molecular chaperones as chaotropes. *Frontiers in Molecular Biosciences*. **8**: 683132.

Maier, A.G., Rug, M., O'Neill, M.T., Brown, M., Chakravorty, S., Szestak, T., Chesson, J., Wu, Y., Hughes, K., Coppel, R.L. and Newbold, C. (2008). Exported proteins required for virulence and rigidity of *Plasmodium falciparum*-infected human erythrocytes. *Cell*. **134**: 48-61.

Makhoba, X.H., Burger, A., Coertzen, D., Zininga, T., Birkholtz, L.M. and Shonhai, A. (2016). Use of a chimeric Hsp70 to enhance the quality of recombinant *Plasmodium falciparum* s-adenosylmethionine decarboxylase protein produced in *Escherichia coli*. *PLoS One*. **11**: e0152626.

Makumire, S., Revaprasadu, N. and Shonhai, A. (2015). DnaK protein alleviates toxicity induced by citrate-coated gold nanoparticles in *Escherichia coli*. *PLoS One*. **10**: e0121243.

Makumire, S., Dongola, T.H., Chakafana, G., Tshikonwane, L., Chauke, C.T., Maharaj, T., Zininga, T. and Shonhai, A. (2021). Mutation of GGMP repeat segments of *Plasmodium falciparum* Hsp70-1 compromises chaperone function and Hop co-chaperone binding. *International Journal of Molecular Sciences*. **22**: 2226.

Martin, R.E. and Kirk, K. (2004). The malaria parasite's chloroquine resistance transporter is a member of the drug/metabolite transporter superfamily. *Molecular Biology and Evolution*. **10**: 1938-1949.

Matambo, T.S., Odunuga, O.O., Boshoff, A. and Blatch, G.L. (2004). Overproduction, purification, and characterization of the *Plasmodium falciparum* heat shock protein 70. *Protein Expression and Purification*. **33**: 214-222.

Mayer, M.P. (2013). Hsp70 chaperone dynamics and molecular mechanism. *Trends in Biochemical Sciences*. **38**: 507-514.

Mayer, M.P. and Kityk, R. (2015). Insights into the molecular mechanism of allostery in Hsp70s. *Frontiers in Molecular Biosciences*. **2**: 58.

Mayer, M.P., Laufen, T., Paal, K., McCarty, J.S. and Bukau, B. (1999). Investigation of the interaction between DnaK and DnaJ by surface plasmon resonance spectroscopy. *Journal of Molecular Biology*. **289**: 1131-1144.

Mayer, M.P., Schröder, H., Rüdiger, S., Paal, K., Laufen, T. and Bukau, B. (2000). Multistep mechanism of substrate binding determines chaperone activity of Hsp70. *Nature Structural Biology*. **7**: 586-593.

Mayer, M.P. and Bukau, B. (2005). Hsp70 chaperones: cellular functions and molecular mechanism. *Cellular and Molecular Life Sciences*. **62**: 670-684.

Mayer, M.P. and Gierasch, L.M. (2020). Correction: Recent advances in the structural and mechanistic aspects of Hsp70 molecular chaperones. *Journal of Biological Chemistry*. **295**: 288.

Mayer, M.P. (2021). The Hsp70-chaperone machines in bacteria. *Frontiers in Molecular Biosciences*. **8**: 694012.

McGready, R., Lee, S.J., Wiladphaingern, J., Ashley, E.A., Rijken, M.J., Boel, M., Simpson, J.A., Paw, M.K., Pimanpanarak, M., Mu, O. and Singhasivanon, P. (2012). Adverse effects of *falciparum* and *vivax* malaria and the safety of antimalarial treatment in early pregnancy: a population-based study. *The Lancet Infectious Diseases*. **12**: 388-396.

Melnikov, S.V., van den Elzen, A., Stevens, D.L., Thoreen, C.C. and Söll, D. (2018). Loss of protein synthesis quality control in host-restricted organisms. *Proceedings of the National Academy of Sciences*. **115**: E11505-E11512.

Meshnick, S.R. and Dobson, M.J. (2001). The history of antimalarial drugs. In Antimalarial Chemotherapy: Mechanisms of Action, Resistance, and New Directions in Drug Discovery; Rosenthal, P.J.; Ed; Springer Science + Business Media, New York, USA. pp. 15-25

Milner Jr, D.A., Lee, J.J., Frantzreb, C., Whitten, R.O., Kamiza, S., Carr, R.A., Pradham, A., Factor, R.E., Playforth, K., Liomba, G. and Dzamalala, C. (2015). Quantitative assessment of multiorgan sequestration of parasites in fatal paediatric cerebral malaria. *The Journal of Infectious Diseases*. **212**: 1317-1321.

Minagawa, S., Kondoh, Y., Sueoka, K., Osada, H. and Nakamoto, H. (2011). Cyclic lipopeptide antibiotics bind to the N-terminal domain of the prokaryotic Hsp90 to inhibit the chaperone activity. *Biochemical Journal*. **435**: 237-246.

Misra, G. and Ramachandran, R. (2009). Hsp70-1 from *Plasmodium falciparum*: protein stability, domain analysis and chaperone activity. *Biophysical Chemistry*. **142**: 55-64.

Mogk, A., Kummer, E. and Bukau, B. (2015). Cooperation of Hsp70 and Hsp100 chaperone machines in protein disaggregation. *Frontiers in Molecular Biosciences*. **2**: 22.

Mogk, A., Tomoyasu, T., Goloubinoff, P., Rüdiger, S., Röder, D., Langen, H. and Bukau, B. (1999). Identification of thermolabile *Escherichia coli* proteins: prevention and reversion of aggregation by DnaK and ClpB. *The EMBO Journal*. **18**: 6934-6949.

Mogk, A., Kummer, E. and Bukau, B. (2015). Cooperation of Hsp70 and Hsp100 chaperone machines in protein disaggregation. *Frontiers in Molecular Biosciences*. **2**: 22.

Mok, S., Ashley, E.A., Ferreira, P.E., Zhu, L., Lin, Z., Yeo, T., Chotivanich, K., Imwong, M., Pukrittayakamee, S., Dhorda, M. and Nguon, C. (2015). Population transcriptomics of human malaria parasites reveals the mechanism of artemisinin resistance. *Science*. **347**: 431-435.

Morimoto, R.I. (1994). Progress and perspectives on the biology of heat shock proteins and molecular chaperones. *The Biology of Heat Shock Proteins and Molecular Chaperones*. 1-30.

Monroe, A., Williams, N.A., Ogoma, S., Karema, C. and Okumu, F. (2022). Reflections on the 2021 World Malaria Report and the future of malaria control. *Malaria Journal*. **21**: 154.

Mudau, P.T. (2021). Characterization of *Plasmodium falciparum* PFF1010c and screening of pyrimidine-quinoline hybrids as inhibitors of Hsp70-Hsp40 functional partnerships of the malaria parasite. MSc Thesis, University of Venda.

Munishkina, L.A. and Fink, A.L. (2007). Fluorescence as a method to reveal structures and membrane-interactions of amyloidogenic proteins. *Biochimica et Biophysica Acta (BBA)-Biomembranes*. **1768**: 1862-1885.

Muralidharan, V., Oksman, A., Pal, P., Lindquist, S. and Goldberg, D.E. (2012). *Plasmodium falciparum* heat shock protein 110 stabilizes the asparagine repeat-rich parasite proteome during malarial fevers. *Nature Communications*. **3**: 1310.

Muthelo, T., Mulaudzi, V., Netshishivhe, M., Dongola, T.H., Kok, M., Makumire, S., de Villiers, M., Burger, A., Zininga, T. and Shonhai, A. (2022). Inhibition of *Plasmodium falciparum* Hsp70-Hop partnership by 2-phenylthynesulfonamide. *Frontiers in Molecular Biosciences*. **9**: 947203.

Nation, R.L. and Li, J. (2009). Colistin in the 21st century. *Current Opinion in Infectious Diseases*. **22**: 535.

Ncube, H.R., Dali, U., Dongola, T.H. and Shonhai, A. (2024). Author Spotlight: Exploring Heat Shock Proteins in Malaria and Tuberculosis Infections. *JoVE (Journal of Visualized Experiments)*. **205**: e66515.

Neubig, R.R., Spedding, M., Kenakin, T. and Christopoulos, A. (2003). International Union of Pharmacology Committee on Receptor Nomenclature and Drug Classification. XXXVIII. Update on terms and symbols in quantitative pharmacology. *Pharmacological Reviews*. **55**: 597-606.

Nicoll, W.S., Botha, M., McNamara, C., Schlange, M., Pesce, E.R., Boshoff, A., Ludewig, M.H., Zimmermann, R., Cheetham, M.E., Chapple, J.P. and Blatch, G.L. (2007). Cytosolic and ER J-domains of mammalian and parasitic origin can functionally interact with DnaK. *The International Journal of Biochemistry & Cell Biology*. **39**: 736-751.

Njunge, M., Ludewig, J. H., Boshoff, A., Pesce, E.R. and Blatch, G. L. (2013). Hsp70s and J proteins of *Plasmodium* parasites infecting rodents and primates: structure, function, clinical relevance, and drug targets. *Current Pharmaceutical Design*. **19**: 387-403.

Nyakundi, D.O., Vuko, L.A., Bentley, S.J., Hoppe, H., Blatch, G.L. and Boshoff, A. (2016). *Plasmodium falciparum* Hep1 is required to prevent the self-aggregation of PfHsp70-3. *PLoS One*. **11**: 0156446.

Nguyen, T.D., Gao, B., Amaratunga, C., Dhorda, M., Tran, T.N.A., White, N.J., Dondorp, A.M., Boni, M.F. and Aguas, R. (2023). Preventing antimalarial drug resistance with triple artemisinin-based combination therapies. *Nature Communications*. **14**: 4568.

Pallavi, R., Acharya, P., Chandran, S., Daily, J.P. and Tatu, U. (2010a). Chaperone expression profiles correlate with distinct physiological states of *Plasmodium falciparum* in malaria patients. *Malaria Journal*. **9**:1-12.

Padma Priya, P., Grover, M., Tatu, U.S. and Natarajan, V. (2015). Characterization of precursor PfHsp60 in *Plasmodium falciparum* cytosol during its asexual development in human erythrocytes. *PloS One*. **10**: 0136401.

Pesce, E.R. and Blatch, G.L. (2014). Plasmodial Hsp40 and Hsp70 chaperones: current and future perspectives. *Parasitology*. **141**: 1167-1176.

Pesce, E.R., Acharya, P., Tatu, U., Nicoll, W.S., Shonhai, A., Hoppe, H.C. and Blatch, G.L. (2008). The *Plasmodium falciparum* heat shock protein 40, Pfj4, associates with heat shock protein 70 and shows similar heat induction and localisation patterns. *The International Journal of Biochemistry & Cell Biology*. **40**: 2914-2926.

Przyborski, J.M., Diehl, M. and Blatch, G.L. (2015). Plasmodial HSP70s are functionally adapted to the malaria parasite life cycle. *Frontiers in Molecular Biosciences*. **2**: 34.

Ritossa, F. (1963). A new puffing pattern induced by temperature shock and DNP in Drosophila. *Experientia*. **12**: 571-573.

Ritossa, F.M. and Von Borstel, R.C. (1964). Chromosome puffs in Drosophila induced by ribonuclease. *Science*. **3631**:513-514.

Rule, C.S., Patrick, M. and Sandkvist, M. (2016). Measuring in vitro ATPase activity for enzymatic characterization. *JoVE (Journal of Visualized Experiments)*. **114**: e54305.

Sargeant, T.J., Marti, M., Caler, E., Carlton, J.M., Simpson, K., Speed, T.P. and Cowman, A.F. (2006). Lineage-specific expansion of proteins exported to erythrocytes in malaria parasites. *Genome Biology*. **7**: 1-22.

Salomane, N., Pooe, O.J. and Simelane, M.B. (2021). Iso-mukaadial acetate and ursolic acid acetate inhibit the chaperone activity of *Plasmodium falciparum* heat shock protein 70-1. *Cell Stress and Chaperones*. **26**: 685-693.

Sato, S. and Wilson, R.I. (2005). Organelle-specific cochaperonins in apicomplexan parasites. *Molecular and Biochemical Parasitology*. **141**: 133-143.

Seraphim, T.V., Chakafana, G., Shonhai, A. and Houry, W.A. (2019). *Plasmodium falciparum* R2TP complex: driver of parasite Hsp90 function. *Biophysical Reviews*. **11**: 1007-1015.

Sidhu, A.B.S., Valderramos, S.G. and Fidock, D.A. (2005). *pfmdr1* mutations contribute to quinine resistance and enhance mefloquine and artemisinin sensitivity in *Plasmodium falciparum*. *Molecular Microbiology*. **4**: 913-926.

Sharma, D. and Masison, D.C. (2009). Hsp70 structure, function, regulation and influence on yeast prions. *Protein and Peptide Letters*. **16**: 571-581.

Shonhai, A. (2010). Plasmodial heat shock proteins: targets for chemotherapy. *FEMS Immunology & Medical Microbiology*. **58**: 61-74.

Shonhai, A., G Maier, A., M Przyborski, J. and L Blatch, G. (2011). Intracellular protozoan parasites of humans: the role of molecular chaperones in development and pathogenesis. *Protein and Peptide Letters*. **18**: 143-157.

Shonhai, A. (2021). The Role of Hsp70s in the Development and Pathogenicity of *Plasmodium falciparum*. In Heat Shock Proteins of Malaria; Shonhai, A., Picard, D., Blatch, G.L., Eds, Springer: Switzerland, pp.75-95.

Shonhai, A., Boshoff, A. and Blatch, G.L. (2005). *Plasmodium falciparum* heat shock protein 70 is able to suppress the thermosensitivity of an *Escherichia coli* DnaK mutant strain. *Molecular Genetics and Genomics*. **274**: 70-78.

Shonhai, A., Boshoff, A. and Blatch, G.L. (2007). The structural and functional diversity of Hsp70 proteins from *Plasmodium falciparum*. *Protein Science*. **16**: 1803-1818.

Shonhai, A., Botha, M., de Beer, T.A., Boshoff, A. and Blatch, G.L. (2008). Structure-function study of a *Plasmodium falciparum* Hsp70 using three-dimensional modelling and in vitro analyses. *Protein and Peptide Letters*. **15**: 1117-1125.

Silva, M.D., Cooke, B.M., Guillotte, M., Buckingham, D.W., Sauzet, J.P., Scanf, C.L., Contamin, H., David, P., Mercereau-Puijalon, O. and Bonnefoy, S. (2005). A role for the *Plasmodium falciparum* RESA protein in resistance against heat shock demonstrated using gene disruption. *Molecular Microbiology*. **56**: 990-1003.

Sidhu, A.B.S., Valderramos, S.G. and Fidock, D.A. (2005). *pfmdr*1 mutations contribute to quinine resistance and enhance mefloquine and artemisinin sensitivity in *Plasmodium falciparum*. *Molecular Microbiology*. **4**: 913-926.

Siracusa, R., Scuto, M., Fusco, R., Trovato, A., Ontario, M.L., Crea, R., Di Paola, R., Cuzzocrea, S. and Calabrese, V. (2020). Anti-inflammatory and antioxidant activity of Hidrox® in rotenone-induced Parkinson's disease in mice. *Antioxidants*. **9**: 824.

Slabaugh, E., Sethaphong, L., Xiao, C., Amick, J., Anderson, C.T., Haigler, C.H. and Yingling, Y.G. (2014b). Computational and genetic evidence that different structural conformations of a non-catalytic region affect the function of plant cellulose synthase. *Journal of Experimental Botany*. **65**: 6645-6653.

Spence, J., Cegielska, A. and Georgopoulos, C. (1990). Role of *Escherichia coli* heat shock proteins DnaK and HtpG (C62.5) in response to nutritional deprivation. *Journal of Bacteriology*. **172**: 7157-7166.

Strom, E., Sathe, S., Komarov, P.G., Chernova, O.B., Pavlovska, I., Shyshynova, I., Bosykh, D.A., Burdelya, L.G., Macklis, R.M., Skaliter, R. and Komarova, E.A. (2006). Small-molecule inhibitor of p53 binding to mitochondria protects mice from gamma radiation. *Nature Chemical Biology*. **2**: 474- 479.

Summers, D.W., Douglas, P.M., Ramos, C.H. and Cyr, D.M. (2009a). Polypeptide transfer from Hsp40 to Hsp70 molecular chaperones. *Trends in Biochemical Sciences*. **34**: 230-233.

Suppini, J.P., Amor, M., Alix, J.H. and Ladjimi, M.M. (2004). Complementation of an *Escherichia coli* DnaK defect by Hsc70-DnaK chimeric proteins. *Journal of Bacteriology*. **186**: 6248-6253.

Taj, M.K., Samreen, Z., Ling, J.X., Taj, I., Hassan, T.M. and Yunlin, W. (2014). *Escherichia coli* as a model organism. *International Journal of Engineering Research and Science and Technology*. **3**: 1-8.

Teale, F.W.J. and Weber, G. (1957). Ultraviolet fluorescence of the aromatic amino acids. *Biochemical Journal*. **65**: 476.

Teixeira, C., Vale, N., Perez, B., Gomes, A., Gomes, J.R. and Gomes, P. (2014). "Recycling" classical drugs for malaria. *Chemical Reviews*. **114**: 11164-11220.

Tilly, K., McKittrick, N., Zylicz, M. and Georgopoulos, C., 1983. The dnaK protein modulates the heat-shock response of *Escherichia coli*. *Cell*. **34**: 641-646.

Tran, C.V. and Saier, M.J. (2004). The principal chloroquine resistance protein of *Plasmodium falciparum* is a member of the drug/metabolite transporter superfamily. *Society for General Microbiology*. 1-3.

Tu, Y., Ni, M., Zhong, Y., Li, L., Gui, S., Zhang, M. and Liang, X. (2015). Studies on the constituents of Artemisia annua L. *Acta Pharmaceutica Sinica*. 366-70.

Tungekar, A.A., Castillo-Corujo, A. and Ruddock, L.W. (2021). So you want to express your protein in *Escherichia coli*?. *Essays in Biochemistry*. **65**: 247-260.

Vaughan, A.M., Aly, A.S. and Kappe, S.H. (2008). Malaria parasite pre-erythrocytic stage infection: gliding and hiding. *Cell host & Microbe*. **4**: 209-218.

Velavan, T.P., Pallerla, S.R., Rüter, J., Augustin, Y., Kremsner, P.G., Krishna, S. and Meyer, C.G. (2021). Host genetic factors determining COVID-19 susceptibility and severity. *EBioMedicine*. *72*.

Veiga, M.I., Dhingra, S.K., Henrich, P.P., Straimer, J., Gnädig, N., Uhlemann, A.C., Martin, R.E., Lehane, A.M. and Fidock, D.A. (2016). Globally prevalent PfMDR1 mutations modulate *Plasmodium falciparum* susceptibility to artemisinin-based combination therapies. *Nature Communications*. **7**: 11553.

Veinger, L., Diamant, S., Buchner, J. and Goloubinoff, P. (1998). The small heat-shock protein IbpB from *Escherichia coli* stabilizes stress-denatured proteins for subsequent refolding by a multichaperone network. *Journal of Biological Chemistry*. **273**: 11032-11037.

Vivian, J.T. and Callis, P.R. (2001). Mechanisms of tryptophan fluorescence shifts in proteins. *Biophysical Journal*. **80**: 2093- 2109.

Wall, D., Zylicz, M. and Georgopoulos, C. (1994). The NH2-terminal 108 amino acids of the *Escherichia coli* DnaJ protein stimulate the ATPase activity of DnaK and are sufficient for lambda replication. *Journal of Biological Chemistry*. **269**: 5446-5451.

Walsh, P., Bursać, D., Law, Y.C., Cyr, D. and Lithgow, T. (2004). The J-protein family: modulating protein assembly, disassembly and translocation. *EMBO reports*. **5**: 567-571.

Wellems, T.E. and Plowe, C.V. (2001). Chloroquine-resistant malaria. *The Journal of Infectious Diseases*. **184**: 770-776.

White, N.J. (1992). Antimalarial pharmacokinetics and treatment regimens. *British Journal of Clinical Pharmacology*. **34**: 1.

White, N.J. (2012). Counter perspective: artemisinin resistance: facts, fears, and fables. *The American Journal of Tropical Medicine and Hygiene*. **87**: 785.

Willmund, F., del Alamo, M., Pechmann, S., Chen, T., Albanèse, V., Dammer, E.B., Peng, J. and Frydman, J. (2013). The cotranslational function of ribosome-associated Hsp70 in eukaryotic protein homeostasis. *Cell*. **152**: 196-209.

World Health Organization. (2021). *World malaria report 2021*. World Health Organization.

World Health Organization. (2022). *World malaria report 2022*. World Health Organization.

World Health Organization. (2023). *World malaria report 2023*. World Health Organization.

Zhang, M., Wang, C., Otto, T.D., Oberstaller, J., Liao, X., Adapa, S.R., Udenze, K., Bronner, I.F., Casandra, D., Mayho, M. and Brown, J. (2018). Uncovering the essential genes of the human malaria parasite *Plasmodium falciparum* by saturation mutagenesis. *Science*. **360**: 7847.

Zhang, M., Wang, C., Otto, T.D., Oberstaller, J., Liao, X., Adapa, S.R., Udenze, K., Bronner, I.F., Casandra, D., Mayho, M. and Brown, J. (2018). Uncovering the essential genes of the human malaria parasite *Plasmodium falciparum* by saturation mutagenesis. *Science*. **360**: eaap7847.

Zheng, X.Y., Xia, Y., Gao, F.H. and Chen, C. (1979). Synthesis of 7351, a new antimalarial drug (author's transl). *Yao xue xue bao= Acta pharmaceutica Sinica*. **14**: 736-737.

Zhu, X., Zhao, X., Burkholder, W.F., Gragerov, A., Ogata, C.M., Gottesman, M.E. and Hendrickson, W.A. (1996). Structural analysis of substrate binding by the molecular chaperone DnaK. *Science*. **272**: 1606-1614.

Zininga, T., Achilonu, I., Hoppe, H., Prinsloo, E., Dirr, H.W. and Shonhai, A. (2016). *Plasmodium falciparum* Hsp70-z, an Hsp110 homologue, exhibits independent chaperone activity and interacts with Hsp70-1 in a nucleotide-dependent fashion. *Cell Stress and Chaperones*. **21**: 499-513.

Zininga, T., Achilonu, I., Hoppe, H., Prinsloo, E., Dirr, H.W. and Shonhai, A. (2015a). Overexpression, purification and characterisation of the *Plasmodium falciparum* Hsp70-z (PfHsp70-z) protein. *PLoS One*. **10**: e0129445.

Zininga, T., Makumire, S., Gitau, G.W., Njunge, J.M., Pooe, O.J., Klimek, H., Scheurr, R., Raifer, H., Prinsloo, E., Przyborski, J.M. and Hoppe, H. (2015b). *Plasmodium falciparum* Hop (PfHop) interacts with the Hsp70 chaperone in a nucleotide-dependent fashion and exhibits ligand selectivity. *PLoS One*. **10**: e0135326.

Zininga, T., Pooe, O.J., Makhado, P.B., Ramatsui, L., Prinsloo, E., Achilonu, I., Dirr, H. and Shonhai, A. (2017a). Polymyxin B inhibits the chaperone activity of *Plasmodium falciparum* Hsp70. *Cell Stress and Chaperones*. **22**: 707-715.

Zininga, T., Ramatsui, L., Makhado, P.B., Makumire, S., Achilinou, I., Hoppe, H., Dirr, H. and Shonhai, A. (2017b). (−)-Epigallocatechin-3-gallate inhibits the chaperone activity of *Plasmodium falciparum* Hsp70 chaperones and abrogates their association with functional partners. *Molecules*. **22**: 2139.

Zininga, T., Anokwuru, C.P., Sigidi, M.T., Tshisikhawe, M.P., Ramaite, I.I., Traoré, A.N., Hoppe, H., Shonhai, A. and Potgieter, N. (2017c). Extracts obtained from Pterocarpus

angolensis DC and Ziziphus mucronata exhibit antiplasmodial activity and inhibit heat shock protein 70 (Hsp70) function. *Molecules*. **22**: 1224.

Zininga, T. and Shonhai, A. (2019). Small molecule inhibitors targeting the heat shock protein system of human obligate protozoan parasites. *International Journal of Molecular Sciences*. **20**: 5930.

Appendices

Appendix A: Additional materials

A1: Table A1. List of reagents

Acetic acid	Merck, Germany
Adenosine triphosphate	Sigma-Aldrich, USA
Agarose	Merck, Germany
Ammonium persulfate	Sigma-Aldrich, USA
Ampicillin	Melford, UK
Bovine serum albumin	Melford, UK
Bromophenol blue	Merck, Germany
Calcium chloride	Merck, Germany
Chemiluminescence Western Blotting kit	Amersham, USA
Nitrocellulose membrane	Thermo Scientific, USA
Immobilon-P transfer membrane	Merck, Germany
Coomassie Brilliant blue R250	Merck, Germany
Ethidium bromide	Merck, Germany
Glacial acetic acid	Merck, Germany
Glycerol	Merck, Germany
Glycine	Merck, Germany
Imidazole	Merck, Germany
Isopropyl-β-D-1-thiogalactopyranoside	Merck, Germany
GeneRuler 1kb DNA ladder	Thermo Scientific, USA
Lysozyme	Merck, Germany
Magnesium chloride	Merck, Germany
Methanol	Merck, Germany
Phenylmethylsulphonyl fluoride	Merck, Germany
Amicin® Ultra-15 10K centrifuge filter device	Merck, Germany
Sodium chloride	Merck, Germany
Sodium dodecyl sulphate	Merck, Germany
TEMED	VWR International, USA
Tris-HCl	VWR International, USA
Tryptone	Merck, Germany
Tween20	Merck, Germany
Yeast extract	Merck, Germany
Page ruler prestained protein ladder	Thermo Scientific, USA
α-DnaK antibody	Inqaba, South Africa
α-Rabbit antibody	Thermofischer scientific
Tetracycline	Duchefa Biochemies, Germany
Nutrient agar	Merck, Germany

Appendix A: Additional materials

Appendix B: Methodology

B1: Preparation of *E. coli* JM109, XL1 Blue and *E. coli dnaK*756 competent cells

A single colony of *E. coli* JM109, XL1 Blue and *E. coli dnaK*756 was picked and inoculated into 5 mL of 2 x YT [1.6 % tryptone (w/v), 1 % yeast extract (w/v), 0.5 % NaCl (w/v)] broth. An aliquot of 100 µg/mL of ampicillin was added to the control broth for *E. coli* JM109 and XL1 Blue. This was followed by incubation overnight (17 hours) at 37℃ while shaking at 250 rpm. To the broth where *E. coli dnaK*756 was inoculated, 50 µg/mL of kanamycin and 10 µg/mL of tetracycline was added. The control was supplemented with 100 µg/mL of ampicillin, 50 µg/mL kanamycin and 10 µg/mL of tetracycline. The broth was incubated at 35 ℃ overnight (17 hours) while shaking at 150 rpm. The following morning the overnight culture was transferred into 45 mL of 2 x YT broth and grown till OD_{600} = 0.4- 0.6. The control flasks with ampicillin should not exhibit any growth. Once the cells had reached their mid-log phase, the cell culture was harvested by centrifuging at 5000 x g for 10 minutes at 4 ℃. The supernatant was discarded, and the resultant pellet resuspended with 5 mL of 0.1 M $MgCl_2$ and stored on ice for 30 minutes. The cell + $MgCl_2$ suspension was centrifuged at 5000 x g for 10 minutes, the supernatant was discarded, and the remaining pellet was resuspended in 5 mL of 0.1 M $CaCl_2$. This was followed by storing on ice for 5 hours. The suspension was then centrifuged at 5000 x g for 10 minutes at 4 ℃. The supernatant was discarded, afterwards the pellet was resuspended in 2 mL of 0.1 M $CaCl_2$ and 2 mL of 30 % glycerol and incubated on ice for 20 minutes. Following incubation, the competent cells were aliquoted into 1.5 mL sterile pre-chilled Eppendorf tubes. The cells were then stored at -80℃.

B2: Transformation of plasmid DNA

Chemically competent *E. coli* JM109 cells were transformed with the following constructs: pQE30/DnaK, pQE60/DnaK, pQE30/KPf, pQE60/KPf, pQE60/KPf-V436F, pQE30/PfHsp70-1 towards the extraction of DNA. The constructs pQE30/DnaK, pQE30/KPf and pQE30/PfHsp70-1 were transformed in *E. coli* XL1 Blue cells to produce the respective recombinant proteins. On the other hand, the plasmids pQE60/DnaK, pQE60/KPf and pQE60/KPf-V436F were transformed with *E. coli dnaK*756 cells for the complementation assay. An aliquot of 2 µL of the plasmid DNA (50-100 ng) was into a 1.5 mL Eppendorf tube containing 50 uL of chemically competent cells. The DNA + competent cell mix was stored on ice for 30 minutes. After incubation on ice, the Eppendorf tube with the competent cells and

DNA was heat shocked at 42 ℃ for 45 seconds and returned on ice for an additional 10 minutes. Freshly prepared 2x YT broth (950 µL) was added to the Eppendorf tube, followed by incubating in shaking incubator for an hour. After growing the cells, an aliquot of 100 µl was streaked onto agar [1.6 % tryptone (w/v), 1 % yeast extract (w/v), 0.5 % NaCl (w/v), 1.5 % (w/v) agar] plates containing the respective antibiotics for each strain. The agar plates were incubated overnight at 37 ℃ for *E. coli* JM109/XL1 Blue and at 35 ℃ for *E. coli dnaK*756 strain.

B3: DNA extraction

Single colonies of pQE30/DnaK, pQE60/DnaK, pQE30/KPf, pQE60/KPf, pQE60/KPf-V436F, pQE30/PfHsp70-1plasmids were transformed with competent *E. coli* JM109 were inoculated 2x YT [1.6 % tryptone (w/v), 1% yeast extract (w/v), 0.5 % NaCl (w/v)] broth containing 100 µg/mL ampicillin. The broth was incubated at 37 ℃ in a shaking incubator overnight (17 hours). Plasmid DNA extraction and purification was carried out using the GeneJet Plasmid Miniprep kit from ThermoScientific. The manufacturers protocol was followed in carrying out all the steps.

Table B1: Restriction digest reaction mixture

Components	**Tube 1 Uncut**	**Tube 2 *Bam*HI**	**Tube 3 *Hind*III**	**Tube 4 *Bam*HI+ *Hind*III**
Deionised water	16	15	14	13
10 x fast digest green buffer	2	2	2	2
DNA	2	2	2	2
Fast digest enzymes		1	2	3
Total volume (µL)	20	20	20	20

B4: Agarose gel electrophoresis

Agarose gel was utilized to verify if the restriction digest was successful. The agarose gel was prepared by dissolving 0.8 % of agarose in TAE (400 mM Tris, 0.1 % acetic acid, 10 mM EDTA pH 7.4). The agarose mixture was heated in a microwave for 2 minutes to ensure complete dissolution. The agarose solution was then cooled at room temperature, 10 % of ethidium bromide was added followed by mixing. The gel was transferred into a casting tray, the combs were placed immediately. The gel was allowed to solidify at room temperature. Before loading the restriction digest samples onto the gel, the combs were removed and the casting tray with the set gel was placed in a buffer tank (electrophoresis chamber). Electrophoresis was carried out at 100 V for 1 hour. The gel was then visualized using the ChemiDoc Imaging System (Bio-Rad, USA).

B5: SDS-PAGE analysis of proteins

Protein expression and purification were analyzed using SDS-PAGE. The expression and purification samples were prepared with SDS LAEMLLI sample buffer (0.25 % Coomassie Brilliant blue (R250), 2 % SDS, 10 % glycerol, 100 mM Tris, 1 % β-mercaptoethanol) in a ratio 4:1. The samples were boiled for 5 minutes at 100 ℃ and were resolved by 12 % acrylamide resolving gel. Before loading the samples (20 uL), the prestained protein marker (2uL) (Thermofischer Scientific, USA) was loaded first. The gel was run at 120 V for 1 hour 20 minutes using the Bio-Rad Mini electrophoresis system (Bio-Rad, USA). Table B2 and B3 show constituents of the running and stacking gel.

Table B2: 12 % SDS-PAGE running gel (X2)

Reagents	**X2**
Bis acrylamide (mL)	4.16
1.5 M Tris pH 8.8 (mL)	2.5
10 % SDS (mL)	0.1
H_2O (mL)	3.16
APS (mL)	0.050
TEMED (mL)	0.02

Table B3: 12 % SDS-PAGE stacking gel (X2)

Reagents	X2
Bis (mL)	0.47
0.5 M Tris pH 8.8 (mL)	0.875
10 % SDS (mL)	0.035
H_2O (mL)	2.1
APS (mL)	0.017
TEMED (mL)	0.02

B6: Western blot analysis of proteins

Western blot analysis was used to confirm the expression and purification of all proteins analyzed by SDS-PAGE. After electrophoresis, the gels were removed from the glasses and immersed in Western (pH 7.4 25 mM Tris, 198 mM glycine, 20 % (v/v) methanol) buffer to equilibrate at 8 °C for 15- 20 minutes. Also, immerse two filter papers, nitrocellulose membrane and skotch brite fibre pads in Western transfer buffer. Prepare the gel transfer as follows: place filter paper on skotch brite pad, followed by the gel (the gel was placed on a cathode). The nitrocellulose membrane was placed on top of the gel using a sterile tweezer. The filter paper was then placed on top of the nitrocellulose membrane followed by the skotch brite pad. The electrophoretic transfer was performed using the Western (pH 7.4 25 mM Tris, 198 mM glycine, 20 % (v/v) methanol) transfer buffer and run at 100 V for 10 minutes. The nitrocellulose membrane was removed from the tank and rinsed in transfer buffer ensuring no gel was left adhered to it. The membrane was blocked with blocking buffer (5 % non-fat milk pH 7.4, 50 mM Tris, 150 mM NaCl) for 1 hour while shaking. Afterward the membrane was rinsed with wash buffer (pH 7.4, 50 mM Tris, 150 mM NaCl, 1 % (v/v) Tween) for 15 minutes. Then the membrane was incubated with primary antibody while shaking for 1 hour, followed by washing for 15 minutes to ensure unbound antibody was removed. The membrane was incubated in secondary antibody while shaking for 1 hour, followed by washing for 15 minutes with wash buffer. The membrane was visualized using enhanced Chemiluminescence (ECL) following the manufacturer's instructions and subsequently viewed by ChemiDoc Imaging system (Bio-Rad, USA).

B7: Quantification of proteins using Bradford's assay

Protein concentration was quantified using the Bradford's assay (1976). The Bradford's assay is a colorimetric technique based on absorbance shift of the dye Coomassie Brilliant blue (G-250). When the dye is bound to protein being assayed, it turns blue. If the protein is absent the solution will remain brown (Bradford, 1976). Standard solutions were prepared as follows: BSA concentrations ranging from 0- 100 µg/mL were pipetted into a 96-well plate and 0.15 M NaCl was also added. An aliquot of 200 µL of Bradford's reagent was added to the BSA + 0.15 M NaCl in the plate. The protein to be assayed was also prepared by pipetting 10 µL of the protein, 0.15 M NaCl and Bradford's reagent. The reaction mixture was incubated at room temperature conditions for 10 minutes. Absorbance at 595 nm was measured using SpectraMax iD3 (Molecular Devices, USA). Triplicate samples were assayed, and their average was determined. The unknown protein concentration was determined using the standard curve.

Appendix C: Supplementary data

C1. Confirmation of pQE60 plasmid vector.

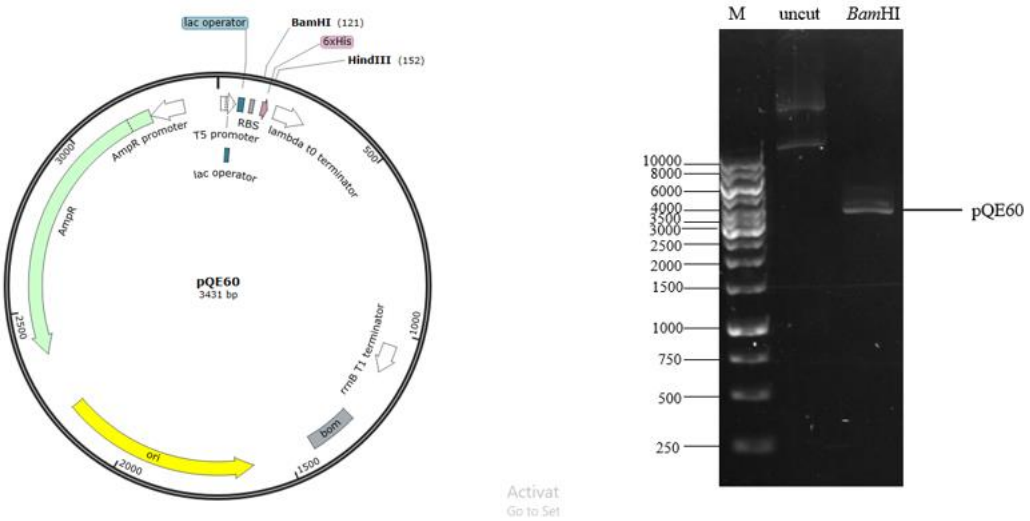

Figure C1. Restriction analysis of pQE60.

(A) Restriction map of pQE60 showing *Bam*HI; *Hind*III restriction sites. **(B)** Agarose gel electrophoresis of pQE60, various lanes representing plasmid DNA, uncut and treated enzymatically are shown as follows; lane M, DNA molecular marker in bp; lane 1, uncut plasmid; lane 2, restricted with *Bam*HI

C2. Confirmation of pQE60/DnaK plasmid DNA

A **B**

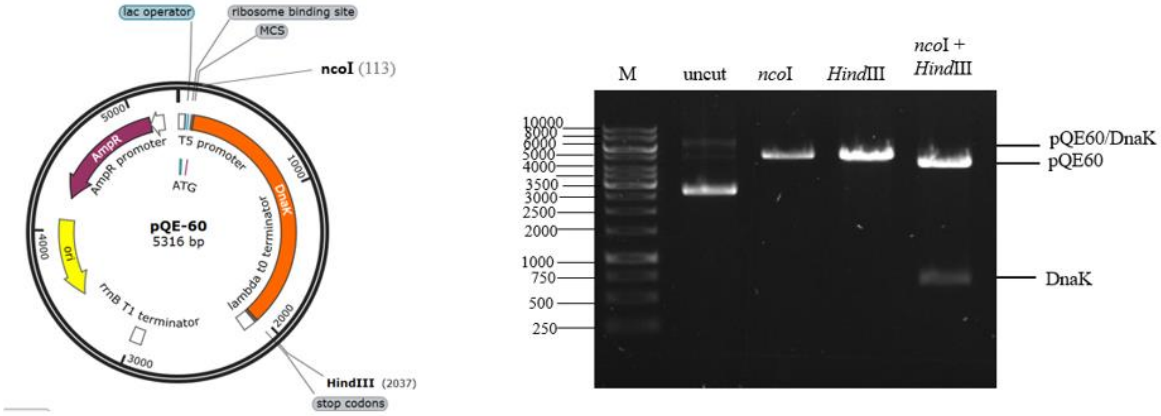

Figure C2. Restriction analysis of pQE60/DnaK plasmid DNA.

(A) Restriction map of pQE60/DnaK showing the *nco*I and *Hind*III restriction sites. **(B)** Agarose gel electrophoresis of pQE60/DnaK, with various lanes representing plasmid DNA, uncut and treated enzymatically are shown as follows; lane M, molecular weight marker in bp; lane1, uncut; lane 2, restricted with *nco*I; lane3, restricted with *Hind*III; lane 4, double restriction with *nco*I and *Hind*III.

C3. Confirmation of pQE60/KIF1 plasmid DNA

A **B**

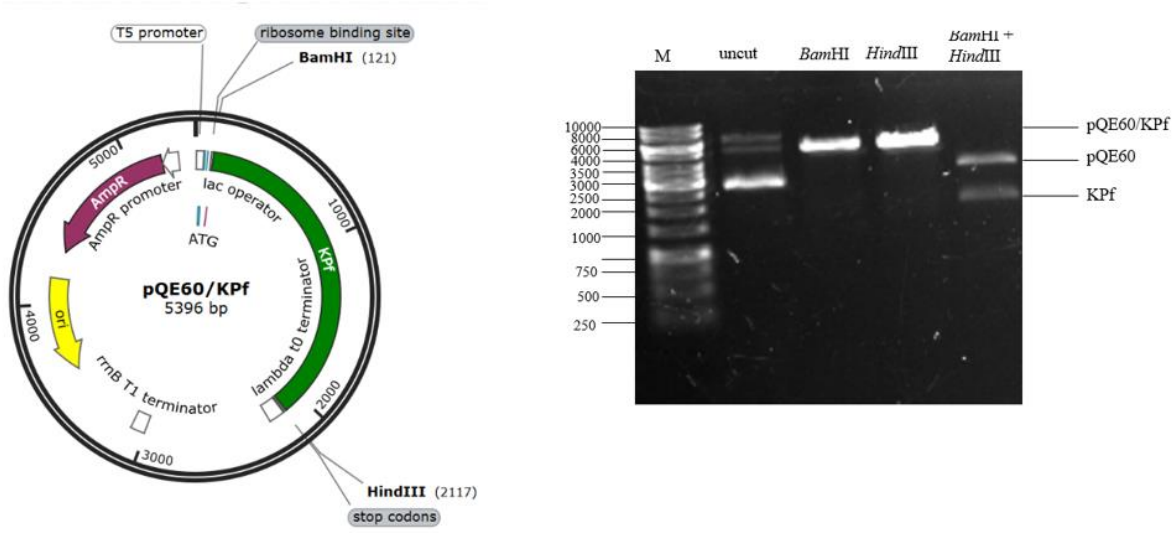

Figure C3. Restriction analysis of pQE60/KPf plasmid DNA.

(A) Restriction map of pQE60/KPf showing the *Bam*HI and *Hind*III restriction sites. **(B)** Agarose gel electrophoresis of pQE60/KPf, with various lanes representing plasmid DNA, uncut and treated enzymatically are shown as follows; lane M, molecular weight marker in bp; lane1, uncut; lane 2, restricted with *Bam*HI; lane3, restricted with *Hind*III; lane 4, double restriction with *Bam*HI and *Hind*III.

C4. Confirmation of KPf-V436F plasmid DNA

A **B**

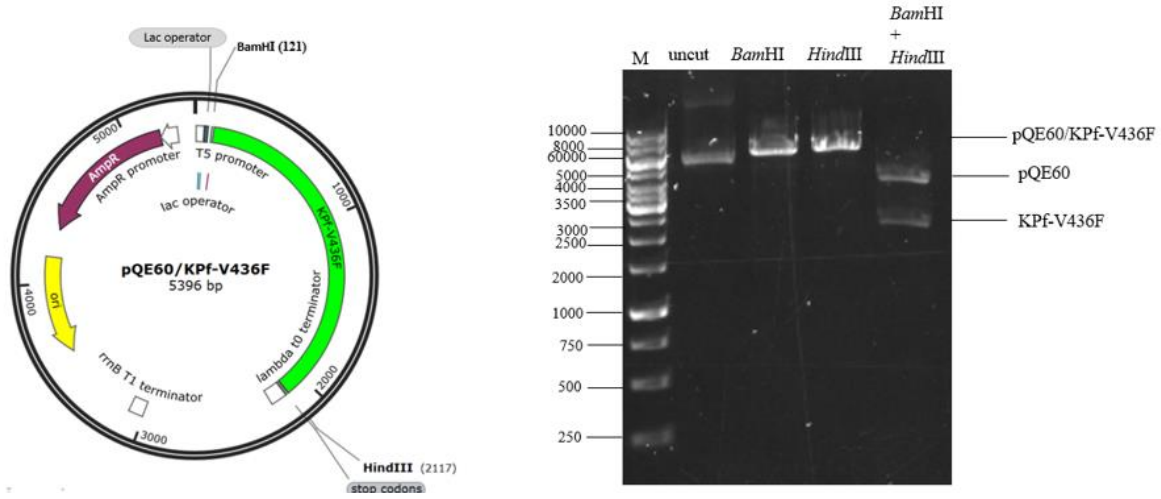

Figure C3. Restriction analysis of pQE60/KPf plasmid DNA.

(A) Restriction map of pQE60/KPf-V436F showing the *Bam*HI and *Hind*III restriction sites. **(B)** Agarose gel electrophoresis of pQE60/KPf, with various lanes representing plasmid DNA, uncut and treated enzymatically are shown as follows; lane M, molecular weight marker in bp; lane1, uncut; lane 2, restricted with *Bam*HI; lane3, restricted with *Hind*III; lane 4, double restriction with *Bam*HI and *Hind*III.

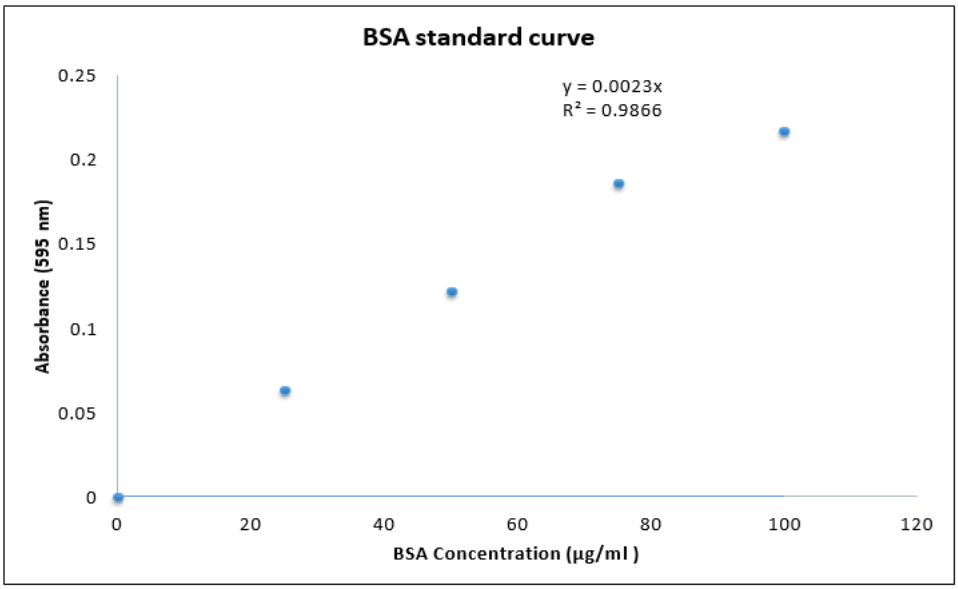

Figure C4. BSA standard curve for protein determination. Protein's (PfHsp70-1, DnaK, KPf) concentrations were determined using Bradford's reagents. The equation Y= 0.0023x ;R^2 = 0.9866 was used to calculate protein concentration in mg/ml.

C5. Cell growth analysis of *E. coli dnaK*756 cells transformed with pQE60 plasmid vector.

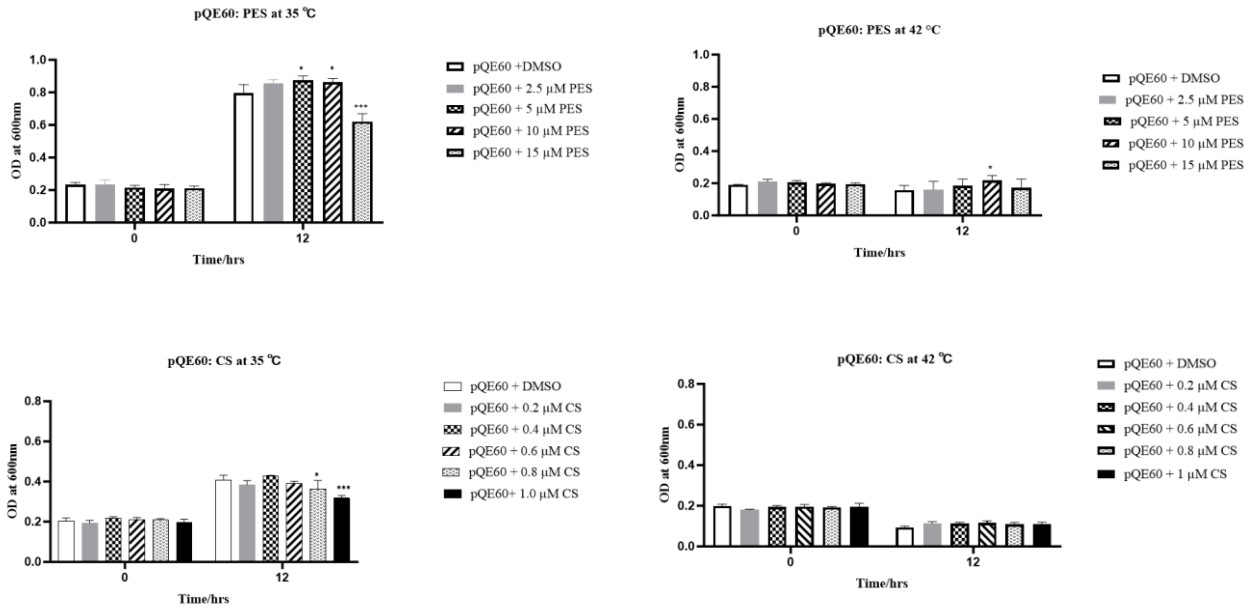

Figure C5. Pifithrin µ (PES) and colistin sulfate (CS) does not exert any effects on *E. coli dnaK*756 cells transformed with the plasmid vector pQE60. The figure represents outcome of the complementation assay on *E. coli dnaK*756/pQE60 in the presence of pifithrin µ and colistin sulfate. The bar graphs present growth of cells over a period of 12 hours. The baseline cells were exposed to the same amount of 0.5% DMSO. Growth comparison for: **(A)**; cells grown at a permissive temperature of 35 °C and non-permissive temperature of 42 °C, in the presence of varying concentrations of pifithrin µ **(B)**; cells grown at a permissive temperature of 35 °C and non-permissive temperature of 42 °C, with diverse concentrations of colistin sulfate. The values on the graphs represent three technical repeats and these are expressed as mean ± SD. Statistically significant at *$p < 0.05$, **$p < 0.01$, ***$p < 0.0001$. Error bars on the graphs signify standard deviation.

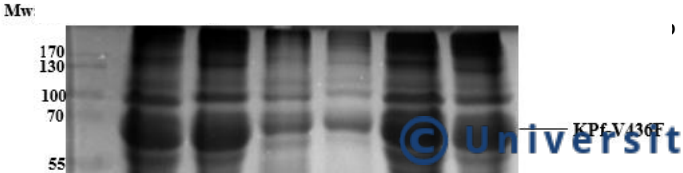

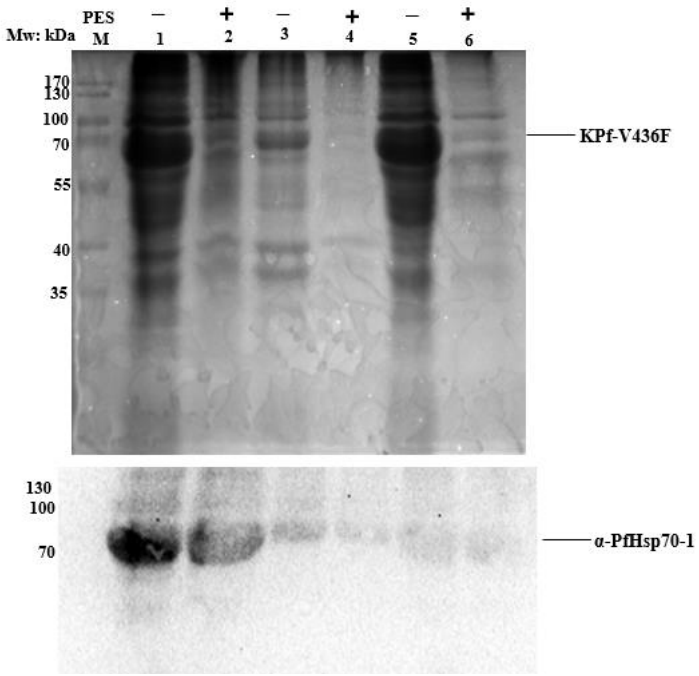

Figure C6. Fate of *E. coli dnaK*756 proteome. Cells were cultured with indicated doses of pifithrin μ and colistin sulfate. The control cells were grown with DMSO. The cells were grown at 42 ℃ for 12 hours. Protein expression of recombinant proteins was examined using SDS-PAGE and Western blot analysis. M, molecular weight marker in kDa; Lane 1, control whole lysate sample; Lane 2, whole lysate sample treated with either pifithrin μ/colistin sulfate; Lane 3, control pellet fraction; Lane 4, pellet fraction sample treated with pifithrin μ and colistin sulfate; Lane 5, control soluble fraction sample; Lane 6, soluble fraction sample treated with pifithrin μ/ colistin sulfate.